

การวิเคราะห์ลักษณะการแสดงออกของยีนและการถ่ายภาพรังสีด้วยไมโครคอมพิวเตอร์โทโมกราฟี
ในกระดุกปลุกถ่ายไร่โปรตีนจากวัวและกระดุกแช่แข็งจากมนุษย์



บทคัดย่อและแฟ้มข้อมูลฉบับเต็มของวิทยานิพนธ์ตั้งแต่ปีการศึกษา 2554 ที่ให้บริการในคลังปัญญาจุฬาฯ (CUIR)
เป็นแฟ้มข้อมูลของนิสิตเจ้าของวิทยานิพนธ์ ที่ส่งผ่านทางบัณฑิตวิทยาลัย

The abstract and full text of theses from the academic year 2011 in Chulalongkorn University Intellectual Repository (CUIR)
are the thesis authors' files submitted through the University Graduate School.

วิทยานิพนธ์นี้เป็นส่วนหนึ่งของการศึกษาตามหลักสูตรปริญญาวิทยาศาสตรมหาบัณฑิต

สาขาวิชาพันธุกรรมประดิมศาสตร์ ภาควิชาพันธุกรรมประดิมศาสตร์

คณะทันตแพทยศาสตร์ จุฬาลงกรณ์มหาวิทยาลัย

ปีการศึกษา 2558

ลิขสิทธิ์ของจุฬาลงกรณ์มหาวิทยาลัย

GENE EXPRESSION AND MICRO-COMPUTED TOMOGRAPHY ANALYSIS OF GRAFTED
BONE USING DEPROTEINIZED BOVINE BONE AND FREEZE-DRIED HUMAN BONE

Miss Thanyaporn Kangwannarongkul



A Thesis Submitted in Partial Fulfillment of the Requirements
for the Degree of Master of Science Program in Prosthodontics

Department of Prosthodontics

Faculty of Dentistry

Chulalongkorn University

Academic Year 2015

Copyright of Chulalongkorn University

ธันยาพร กังวานณรงค์กุล : การวิเคราะห์ลักษณะการแสดงออกของยีนและการถ่ายภาพรังสีด้วยไมโครคอมพิวเตอร์โทโมกราฟีในกระดูกปลูกถ่ายไร้โปรตีนจากวัวและกระดูกแช่แข็งจากมนุษย์ (GENE EXPRESSION AND MICRO-COMPUTED TOMOGRAPHY ANALYSIS OF GRAFTED BONE USING DEPROTEINIZED BOVINE BONE AND FREEZE-DRIED HUMAN BONE) อ.ที่ปรึกษาวิทยานิพนธ์หลัก: อ. ทญ. ดร. ใจแจ่ม สุวรรณเวลา, 95 หน้า.

วัตถุประสงค์ การทำศัลยกรรมปลูกกระดูกเป็นขั้นตอนหนึ่งที่มีความสำคัญในทันตกรรมรากเทียมในปัจจุบันมีกระดูกปลูกถ่ายหลายชนิดที่นำมาใช้ในทางทันตกรรม การศึกษาที่ใช้กระดูกปลูกถ่าย 2 ชนิด ได้แก่ กระดูกปลูกถ่ายไร้โปรตีนจากวัว (Bio-Oss®) และ กระดูกแช่แข็งจากมนุษย์ (DFDBA) ซึ่งให้ผลการรักษาที่ดีในทางคลินิกมาเป็นระยะเวลาอันยาวนาน อย่างไรก็ตามการศึกษาในสิ่งมีชีวิตถึงกระบวนการซ่อมสร้างของกระดูกในระดับโมเลกุลยังคงมีอยู่น้อย ในการศึกษาที่มีวัตถุประสงค์คือศึกษาลักษณะการสร้างกระดูกขึ้นใหม่และการแสดงออกของยีนในกะโหลกศีรษะของหนูด้วยกระดูกปลูกถ่าย 2 ชนิด คือ Bio-Oss® และ DFDBA เปรียบเทียบกับลักษณะการหายของกระดูกปกติ ที่ระยะเวลา 1 และ 3 เดือน

วิธีการทดลอง หนู C57BL/6 จำนวน 36 ตัว แบ่งออกเป็น 3 กลุ่ม คือ กลุ่มที่ 1 กลุ่มควบคุม หนูไม่มีการใส่กระดูกปลูกถ่าย กลุ่มที่ 2 หนูใส่กระดูกปลูกถ่าย Bio-Oss® และ กลุ่มที่ 3 หนูใส่กระดูกปลูกถ่าย DFDBA กระดูกปลูกถ่ายถูกใส่บนช่องว่างบนกะโหลกศีรษะพาริเยทอลขนาด 3 มิลลิเมตร ทั้งด้านซ้ายและด้านขวา ก่อนนำมาประเมินการสร้างกระดูกขึ้นใหม่ด้วยไมโครซีทีและการแสดงออกของยีนด้วยเทคนิคเรียลไทม์ พีซีอาร์ที่ระยะเวลา 1 และ 3 เดือน

ผลการทดลอง จากการวิเคราะห์การสร้างกระดูกด้วยไมโครซีทีที่หนูที่มีการปลูกถ่ายกระดูกด้วย Bio-Oss® บริเวณกะโหลกศีรษะพาริเยทอลมีปริมาตรกระดูกมากกว่ากลุ่มที่ปลูกถ่ายด้วย DFDBA และ กลุ่มควบคุม ทั้งในระยะเวลา 1 และ 3 เดือนอย่างมีนัยสำคัญทางสถิติ ด้านการแสดงออกของยีนพบว่าทั้ง Bio-Oss® และ DFDBA มีระดับการแสดงออกของยีนที่เกี่ยวข้องกับการสร้างกระดูกมากกว่ากลุ่มควบคุมในระยะเวลา 3 เดือน การแสดงออกของยีน Runx2 และ Osx ในกลุ่ม Bio-Oss® และ DFDBA มีระดับการแสดงออกที่มากกว่ากลุ่มควบคุม อย่างมีนัยสำคัญทางสถิติอีกด้วย

สรุปผล ผลการทดลองแสดงให้เห็นว่ากระดูกปลูกถ่ายช่วยส่งเสริมการสร้างกระดูกขึ้นใหม่และกระดูกปลูกถ่าย Bio-Oss® มีคุณสมบัติออสทิโอคอนดักชันสูง

ภาควิชา ทันตกรรมประดิษฐ์

ลายมือชื่อนิสิต

สาขาวิชา ทันตกรรมประดิษฐ์

ลายมือชื่อ อ.ที่ปรึกษาหลัก

ปีการศึกษา 2558

5575809732 : MAJOR PROSTHODONTICS

KEYWORDS: REAL-TIME PCR / DFDBA / CALVARIAL DEFECT / MICE / MICRO-CT / BIO-OSS

THANYAPORN KANGWANNARONGKUL: GENE EXPRESSION AND MICRO-COMPUTED TOMOGRAPHY ANALYSIS OF GRAFTED BONE USING DEPROTEINIZED BOVINE BONE AND FREEZE-DRIED HUMAN BONE. ADVISOR: JAIJAM SUWANWELA, D.D.S., Ph.D., 95 pp.

Objectives: Bio-Oss[®] and DFDBA are two commercial bone grafts that have been associated with clinical success for many years. However, there are few *in vivo* studies regarding their healing mechanism. The purpose of this study was to investigate bone forming characteristics and gene expression in mouse calvarium at 1 and 3 months after bone grafting with deproteinized bovine bone and freeze-dried human bone, and compare them to natural bone healing.

Methods: Thirty-six mice were divided into three groups (n = 6/group) according to the type of bone graft used: group 1 (control) -an empty defect without bone graft, group 2 - treatment with deproteinized bovine xenograft (Bio-Oss[®]) and group 3 - treatment with freeze-dried bone allograft (DFDBA). The bone graft was inserted into two 3-mm calvarium defects created on both sides of the parietal bone. At 1 and 3 months, the mice were dissected, and bone volume was evaluated using micro-CT and gene expression analysis.

Results: Micro-CT analysis demonstrated that the parietal bone of mice grafted with Bio-Oss[®] had significantly greater bone volume than both the DFDBA and control groups at both 1 and 3 months. The bone marker genes were increased in both Bio-Oss[®] and DFDBA groups at 3 months. Runx2 and Osx had significantly higher expression in the Bio-Oss[®] and DFDBA group compared to the control at 3 months.

Conclusion: These results showed that both bone graft materials promoted bone regeneration. Bio-Oss[®] demonstrated high osteoconductive properties.

Department: Prosthodontics

Student's Signature

Field of Study: Prosthodontics

Advisor's Signature

Academic Year: 2015

ACKNOWLEDGEMENTS

I would like to express my gratitude to my thesis advisor Dr.Jaijam Suwanwela for her invaluable advice and support throughout this research study. Furthermore, I would like to thank Dr.Philaiporn Vivatbutsiri for her all her suggestions and teachings on operating on mice. I would also like to extend thanks to my thesis committee; Assistant Professor Dr. Keskanya Subbalekha and Dr. Pisaisit Chaijareenont for their encouragement and insightful comments.

Additionally, I would like to acknowledge the service from the Biomaterial testing center of Chulalongkorn University for their help in taking care of the animals.



CONTENTS

	Page
THAI ABSTRACT	iv
ENGLISH ABSTRACT	v
ACKNOWLEDGEMENTS.....	vi
CONTENTS.....	vii
LIST OF TABLES.....	ix
LIST OF FIGURES	x
CHAPTER I INTRODUCTION	1
CHAPTER II REVIEW OF LITERATURE.....	2
Type of bone graft.....	2
The socket bone healing process	5
The calvarial defect model.....	7
Micro-computed tomography or micro-CT	8
Quantitative Real-time polymerase chain reaction (qRT- PCR)	9
CHAPTER III RESEARCH METHODOLOGY	12
Animals.....	12
Surgical procedure	12
Micro-computed tomography (Micro-CT) imaging.....	15
Data analysis	15
RNA extraction and Real-time polymerase chain reaction	16
Data analysis	22
CHAPTER IV RESULTS	23
Micro-CT imaging of bone regeneration.....	23

	Page
Gene expression of bone markers	25
CHAPTER V DISCUSSION	28
CHAPTER VI CONCLUSION	31
REFERENCES	32
APPENDIX	39
Nucleic acid concentration and purity	39
Average C_t value in qRT-PCR	40
Statistics test	41
Animal care	93
VITA	95



LIST OF TABLES

Table 1 Showed the filling of bone grafts into the cavariae. C = control, B = Bio-Oss [®] D = DFDBA.....	14
Table 2 Reverse-transcription reaction components	19
Table 3 The specific primers for Real-time PCR.....	20
Table 4 KAPA SYBR [®] FAST qPCR Master Mix	20
Table 5 qPCR protocol.....	21



LIST OF FIGURES

Figure 1 Anatomical landmarks of mouse caviarium	12
Figure 2 Location of created the defect.....	13
Figure 3 Showed bone grafts filled into the calvariae Bio-Oss [®] on the left side and DFDBA on the right side.....	13
Figure 4 SCANCO Medical AG, uCT 35	15
Figure 5 Location of collected sample bone	16
Figure 6 Bone sample and storage.....	16
Figure 7 The homogenization tube with metal beads (left) and homogenization (right) .	17
Figure 8 Three-dimensional micro-CT images of defects with (a) control (b) Bio-Oss [®] and (c) DFDBA 1 month after implantation.....	24
Figure 9 Three-dimensional micro-CT images of defects with (a) control (b) Bio-Oss [®] and (c) DFDBA 3 months after implantation.....	24
Figure 10 The mean bone formation (mm ³) of bone grafts at 1 and 3 months. (* indicated significant difference in bone volume at p<0.05)	24
Figure 11 The expression of bone markers gene among groups. Value present by means ± SD.	26
Figure 12 The expression of bone markers gene between 1 and 3 months. Value present by means ± SD. (** Indicated significant difference in relative gene expression at p< 0.05)	27
Figure 13 Regulation of gene expression in osteoblasts.....	30

CHAPTER I INTRODUCTION

Nowadays, the combination of the conventional prosthesis and implant placement is considered one of the first choice prosthodontic treatments in edentulous patients. However, the main problem for patients with long-term tooth loss is a lack of bone quality and quantity. Dimensional changes of the residual ridge also occur, especially during the first 6 months after tooth extraction [1-3]. Without ridge preservation, the extraction site may lose up to 50% of its width within the first year [4]. As a result, many grafting materials have been used both in oral and maxillofacial surgery including autograft, allograft, xenograft and alloplast. Autografts are well known as the “gold standard” of grafting materials due to its osteoconductive, osteoinductive, osteogenic properties, and its non-immunological response [5]. However, it comes in limited quantity, requires a secondary surgical site, prolongs operation time, and may cause higher risk of donor site morbidity [6, 7]. Therefore, the use of alternative bone materials such as allograft and xenograft have increased [8, 9].

Clinically, the different healing patterns of natural bone and bone grafts can be distinguished by radiographic examination. However, there is still a lack of research on the possible role of gene expression in the different radiographic patterns. Therefore, this study aims to investigate bone regeneration in an animal model after placing two types of commonly used bone grafts, namely xenograft (Bio-oss[®]) and human allograft (Oragraft[®]), and compare them to the healing of normal bone. Bio-oss[®] is a deproteinized bovine bone composed of calcium and phosphate in a ratio of approximately 2:1; whereas Oragraft[®] is a freeze-dried human bone allograft without inorganic component.

CHAPTER II REVIEW OF LITERATURE

Review literature

Bone grafting is an important procedure performed prior to pre-prosthetic or implant placement. It is done for patients who lack bone quality and quantity after tooth extraction. It is known that the alveolar ridge dramatically resorbs during the first 6 months post-extraction and continues to resorb for up to 2 years [2, 10, 11]. Tallgren 1972 found that patients who wore complete dentures for 15 and 25 years had four times more resorption at the lower anterior edentulous ridge than the upper edentulous ridge [3]. Pietrokovski 1967 used study casts to demonstrate that buccal bone had greater bone loss compared to the palatal and lingual bone [12]. As the alveolar ridge becomes shorter and thinner it increases the difficulty in reconstruction; thus bone grafting is one commonly used solution for this problem [13].

Type of bone graft

- Autograft or autogenous bone graft
- Allograft or allogenic bone graft
- Xenograft or xenogenic bone graft
- Alloplast or alloplastic bone graft

Autograft or autogenous bone graft

Autograft is a bone graft that is harvested from another site, either intra- or extraoral, in the same host. At present, autograft remains the gold standard as it is the only bone graft that has osteogenic properties [6,9,14,15]. Hydroxyapatite and collagen, from the graft, acts as a framework for osteoblast cells and growth factors (ie. BMP, TGF- β) in bone formation.

The advantages of this graft are that it provides osteoprogenitor cells, does not induce an immune response or transmit disease. However, only few cells survive as there are merely 300 microns of blood vessels during the first 2 weeks. The cells that lack nutrition die and provide osteoconduction. Osteoclasts degrade the dead cells and slowly replace them with new bone. This process is known as “creeping substitution”.

The disadvantages of autogenous bone grafts are the need for a second operative site, risk of morbidity, limited host bone, and the unpredictable resorption rate of the bone graft. Therefore, it is preferable in cases of large defects to combine autografts with other bone grafts [6, 7].

Allograft or allogenic bone graft

Allograft is a human bone graft that is harvested from another person in the same species. The freeze-dried process is done to preserve its contents and sterilize the material. This graft can be divided into 3 subtypes according to the manufacturing process.

- **Fresh frozen allograft** is bone that is collected from a host and kept in temperatures below -60°C to prevent enzyme degradation and maintain biological and physiological properties before use. This type of bone graft is rarely used because of the increased risk of infection and graft rejection.
- **Freeze-dried bone allograft (FDBA)** is a bone graft that is dehydrated, frozen, sterilized, and then kept it in a vacuum. This process does not change cell components. It has been suggested that this type of allograft still has osteoinductive properties.
- **Demineralized freeze-dried bone allograft (DFDBA)** is a bone graft that is immersed in 0.6 molar hydrochloric acid for 6 to 16 hours before frozen,

resulting in complete removal of inorganic contents. Bone morphogenic proteins (BMPs) do not dissolve in acid and provide the osteoinductive properties in this graft. Urist et al. 1960 claimed that DFDBA possessed osteoinductive properties different from FDBA [16]. This contradicted a study in 1996, in which no osteoinductive properties were found from both grafts [17]. Histological analysis by Wood and Mealey [18] revealed that bone grafted with DFDBA showed significantly greater new bone formation and lower amounts of residual bone graft than FDBA after grafting in human for 19 weeks. Presently, the osteoinductive properties of FDBA and DFDBA are still unclear.

The advantages of allograft are that it is available in large quantity and it reduces the number of surgeries. However, there have been 2 case reports of HIV infection from patients who received fresh frozen grafts.

Xenograft or xenogenic bone graft

Xenograft is bone graft taken from another species ie. bovine or pig [19]. It undergoes a heating process under 300°C to remove cells and organic contents [20]. Only osteoconductive properties are found in this bone graft. One product readily available in the market is Bio-Oss[®]. It comes from bovine bone, has a porous structure similar to human bone, and can resist compressive forces of up to 35 mega pascals. Moreover, it does not induce a host response. Bio-Oss[®] was widely used for its high osteoconductive properties, slow resorption rate, and biocompatibility. Bio-Oss[®] can be used in patients with oral maxillofacial defects and in dental implants, especially in maxillary sinus floor augmentation [21-24].

The advantages of this graft are its capacity for maintaining load-bearing bone volume, biocompatibility, and reduced complication. This material is considered as the material of choice for maxillary sinus floor augmentation [22, 25].

Alloplast or alloplastic bone graft

Alloplast is a synthetic material. There are many kinds available in various density, porosity, and shapes. It is compatible with soft tissue. Alloplasts are often used in combination with other bone grafts and are thus called “composite graft”. They serve to increase bone volume and improve bone density. Examples of materials used in clinic are hydroxyapatite etc.

In this study, we selected 2 commercial bone grafts, Bio-Oss[®], Oragraft[®], as they are often used at Faculty of Dentistry, Chulalongkorn University. We hope that this study will be beneficial to the organization.

The socket bone healing process

Following tooth extraction, the socket immediately fills with blood and blood clot formation begins. This is the primary step of the bone healing process. The blood clot carries growth factors to the wound site and then gradually resorbs. Within a few days, it is replaced by granulation tissue. After 1 week, soft tissue remodeling and bone remineralization begins. After 2-4 weeks, the socket is filled with granulation tissue (rich in newly formed blood vessels) and a provisional matrix (collagen fibers and mesenchymal stem cells). During 6-8 weeks, the granulation tissue is replaced by matrix and woven bone. The immature woven bone continues to dominate till the late stages of healing. After 24 weeks, bone organization and architecture is still incomplete [26]. Although there are numerous studies concerning socket healing [11,19, 26], to date we still face problems with the loss of alveolar bone. For many years, clinicians have found good clinical results in using bone graft materials for the restoration of function and esthetics. In this study, micro-computed tomography and realtime PCR were performed

to study bone microarchitecture and molecular characterization in grafted bone and compare it to natural bone healing using a mouse model.

Furthermore, in terms of gene expression, medical research has found that, after babies are born, the bones still have mesenchymal stem cells. These cells can differentiate into specific cells if they are stimulated or in the appropriate environment. An in vitro study and animal experimental study found that the differentiation of mesenchymal stem cells into osteoblast cells can be divided into 3 stages (Stage 1 Cell proliferation, Stage 2 Matrix maturation, Stage 3 Matrix mineralization). Gene expression in each stage is different. The specific genes for osteoblasts include alkaline phosphatase (ALP), osteopontin (OPN), osteocalcin (OCN) and bone sialoprotein (BSP) etc [27]. There are high expressions of ALP in the early stages of matrix maturation and its levels decrease in the late stages. OPN has increased expression during cell proliferation and matrix maturation, before the expression of BSP and OCN. BSP has short expression in early stages of matrix maturation and is expressed again in mature osteoblasts. The expression of OCN can be found in the late stages of matrix maturation [28]. The complete regulation of osteoblast differentiation requires transcription factors. The transcription factors important for osteoblast differentiation are Runt related transcription factor 2 (Runx2) and Osterix (Osx).

Runx2 or Cbfa1 (Core binding factor-1) is a transcription factor in the Runt domain family. It plays an important role in controlling mesenchymal stem cell differentiation into osteoblasts and chondroblasts. All Runx2 deficient mice died after birth due to a complete lack of osteoblast cells, intramembranous ossification, and endochondral ossification. In embryos, Runx2 expression in mesenchymal stem cells causes transformation into osteoblasts. It can be said that Runx2 is the first transcription factor in osteoblast differentiation [29, 30]. It was found that the specific gene markers to

osteoblasts, such as Collagen type I, OPN, and OCN, have a promoter region for Runx2 adhesion. In addition, the increased expression of Runx2 in other cells can induce these cells to transform into osteoblasts themselves. The number of Runx2 genes are decreased in mature osteoblasts [31, 32].

Osterix (Osx) is a zinc finger-containing protein that is also essential in osteoblast differentiation and is more specific to osteoblast cells than Runx2 [33, 34]. Osx deficient mice lack bone formation by both endochondral and intramembranous ossification and have no expression specific gene markers like collagen type I, BSP, OPN and OCN. In mice, if there is no detection of Runx2, there is no expression of Osx. However, if there is no detection of Osx, Runx2 is still expressed normally. Hence, Osx acts downstream to Runx2. It is said that Osx directly affects regulation of preosteoblasts into fully functional osteoblasts.

In 2009, Sollazzo et al. studied the *in vitro* effect of Bio-oss[®] in mesenchymal stem cells using realtime PCR technique [35]. They found that on day 7 Bio-Oss[®] induced increased expression of Runx2 and OPN while decreasing the expression of Osx, OCN, ALP and collagen type I. This explained the decreased Osx, as its effects occur in the late stages of differentiation. In 2012, Shahram Vaziri et al. found that DFDBA induced expression of OPN and OCN in human osteoblast-like cell line. The analysis of gene expression helps to indicate the stage of bone formation [36-38].

The calvarial defect model

In vivo studies often use animal models to evaluate the bone regeneration process, bone substitute interaction, and physiological or pathological pathway [39-41]. O'Loughlin *et al.* reviewed the use of animal models in bone research over the course of 10 years and found that the most commonly used animal models were rats (38%), rabbits (19%), mice (13%), sheep (11%), dogs(9%), goats(4%) and others(4%) [42]. The

rodent models (rats and mice) were commonly used due to their low cost, high reproducibility, and easy handling and maintenance. In consideration of the implantation site, the calvarial defect serves as a model of intramembranous ossification [43]. This provides several advantages as it is reproducible, does not require internal or external fixation (support is provided by dura mater and skin for implant material), and provides for easy evaluation by radiography and histology.

To use the calvarial model, the defect size must be considered while planning the experiment [44, 45]. Schmitz described the calvarial critical size defect as the smallest wound established intraosseously in a particular bone, which does not report spontaneous healing during the lifetime of the animal. The mouse calvarial critical size defect is greater or equal 5 mm. Aalami *et al* compared bone healing between juvenile (6 day-old) and adult (60 day-old) mice with calvarial bone defect sizes 3, 4 and 5 mm. After 8 weeks of bone healing, it was concluded that all defect sizes were critical to adult mice [46]. Therefore, in this study two size 3-mm calvarial defects per mouse was selected. This ultimately decreased the amount of mice required to complete this study.

Moreover, the resulting medical trials are uniform as mice are identical to humans in genetics. In other words, their genetic, biological and behavioral characteristics resemble those of human [47].

Micro-computed tomography or micro-CT

Micro-CT is a highly powerful technique that can be described as a miniaturized form of CT scanning with a high spatial resolution range of 5 to 50 μm . It was developed in the early 1980s. In the past, dental hard tissue development and composition was studied through histology. However, histology required sample destruction and an extended period of time. Micro-CT is increasingly being used in dental research as it is faster, provides greater accuracy, and does not damage the specimen. It allows for 3-dimensional imaging of small dental hard tissues. The technique also discriminates change in dental hard tissue volumes. It is used for evaluation of volume, mineral density, and level of mineralization in hard tissue development [48].

Micro-CT is more efficient in terms of material science and biology such as in animal bones, tooth, medical equipment or electronic devices. Presently, micro-CT is the standard technique used in bone research [43, 49].

Quantitative Real-time polymerase chain reaction (qRT- PCR)

Quantitative Real-time polymerase chain reaction (qRT- PCR) is the most commonly used method for studying quantitative gene expression. It can accurately detect low mRNAs expression level. This assay is based on the detection fluorescent signal, which corresponds with the amount of DNA produced in the reaction. The qRT-PCR provides data in the form of cycle thresholds (C_t). If the messenger RNA (mRNA) of the target gene is high, the C_t value will be low. The process of qRT- PCR is divided into 2 steps: 1) Reverse transcriptase conversion of RNA to cDNA as RNA is less stable compared to DNA. 2) The quantification of amplified products by PCR. The fluorescent detection by fluorescent molecules (ie. dyes) that bind to the double-stranded DNA (non-specific detection) or specific probes (specific detection). The non-specific detection is the most simple and cheapest method in realtime PCR. The most widely used fluorescent molecule is SYBR Green, which is a fluorochrome that binds to the minor grooves of the DNA double helix. The fluorescence increase as the product accumulates in each cycle of amplification. The reaction stops when there are no more products for amplification. The realtime PCR assay is fast and efficient. It does not require post-PCR process and is a reproducible method for quantifying gene expression [50, 51].

In this study, we used qRT-PCR method to evaluate the 5 specific genes (Alkaline phosphatase (ALP), Osteopontin (OPN), Osteocalcin (OCN), Runt related transcription factor 2 (Runx-2) and Osterix (Osx)) after bone graft placement using either deproteinized bovine bone and freeze-dried human bone.

Research question:

Are there any differences in bone forming characteristics or gene expression between deproteinized bovine bone and freeze-dried human bone, compared to natural bone healing?

Research objective:

1. To investigate the bone forming characteristics of deproteinized bovine bone and freeze-dried human bone, and compare them to natural bone healing using micro-CT.
2. To study the expression of 5 marker genes, ALP, OPN, OCN, Runx-2, and Osx, after bone graft placement and compare them to natural bone healing.

Hypothesis

H_0 : No difference in bone forming characteristics between the 2 different bone grafts was found from micro-CT.

H_A : At least one difference in bone forming characteristics between the 2 different bone grafts was found from micro-CT.

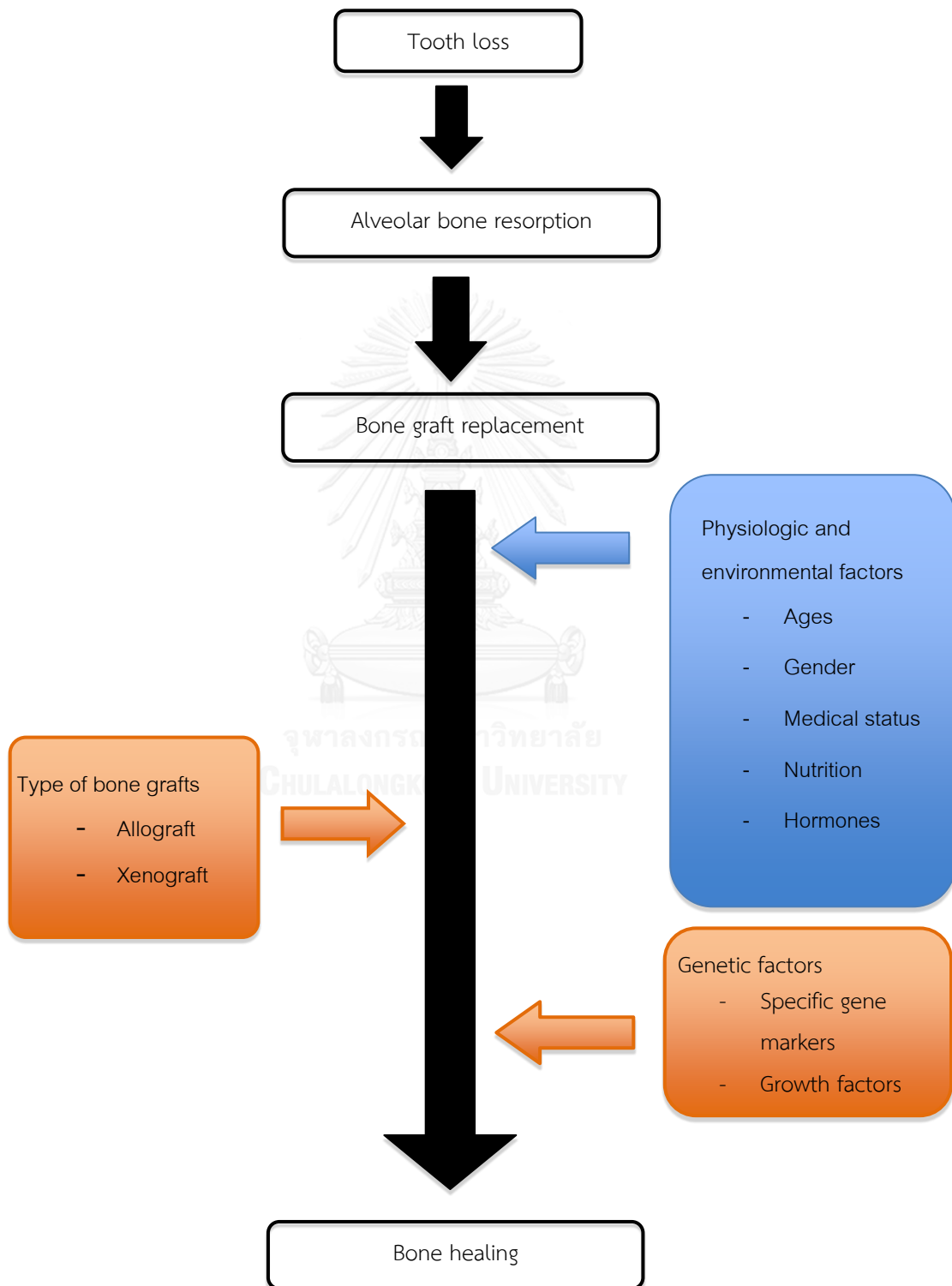
H_{01} : No difference in gene expression of ALP, OPN, OCN, Runx2 and Osx between the 2 different bone grafts was found.

H_{A1} : At least one difference in gene expression of ALP, OPN, OCN, Runx2 and Osx between the 2 different bone grafts was found.

Expected benefit

This study will provide information regarding genetics and bone characteristics after bone grafting that could help in making the pre-prosthesis treatment plan.

Conceptual framework



CHAPTER III RESEARCH METHODOLOGY

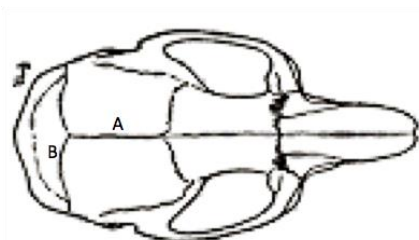
Animals

Thirty-six 8 -week old C57BL/6MLac mice weighing 25-30 g were used in this study. The experiment was approved by the Animal Care and Use Committee of Chulalongkorn University. The mice were housed in light and temperature controlled facilities and given food and water *ad libitum*.

Surgical procedure

The sedative, Nembutal[®] (Pentobarbital), was diluted with a phosphate buffered saline in a ratio of 1:10 and a concentration of 4 mg/kg [or 8 μ L of dilution/wt (g)] was used [52]. After the sedative was injected into the peritoneum layer, the mice's hair was removed with a blade, and the scalp cleaned with alcohol and povidone iodine. Next, 0.2 ml of 1% lidocaine with 1:100,000 epinephrine was injected into the subcutaneous tissue of the skull. The scalpel then provided an incision of 1.5 mm length to visualize the parietal bone. A cavity of 3-mm diameter was created on both the right and left sides of parietal bone using a hand drill and trephine burs with normal saline coolant. The procedure had to be performed gently in order to avoid dura mater injury. The bone graft was then inserted into the skull cavity and stitched up with nylon 3-0.

To create the cavities on mice cavarium, some anatomical landmarks were located. (Figure 1)



A = sagittal suture

B = lambdoid suture

Figure 1 Anatomical landmarks of mouse cavarium

The 3-mm cavities created on each side of the parietal bone were located 1.5 mm away from the sagittal suture and 3 mm from the lambdoid suture.

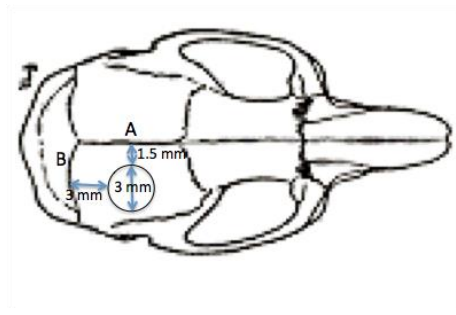


Figure 2 Location of created the defect

The mice were divided into 3 groups according to the type of graft;

Group 1: bare defect as control

Group 2: deproteinized bovine bone [Bio-oss[®]; Geistlich Pharma AG, Wolhusen, Switzerland]

Group 3: demineralized freeze-dried human bone [OraGraft[®]; LifeNet, Virginia, USA]

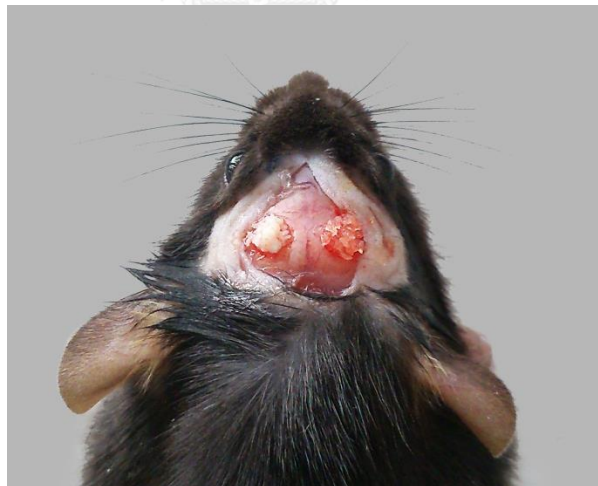


Figure 3 Showed bone grafts filled into the calvariae Bio-Oss[®] on the left side and DFDBA on the right side.

Bone formation and gene expression were determined at 4 and 12 weeks. Thirty-six mice were used for each examination period (eighteen for micro-CT analysis and the others for PCR) as shown in the below table. (Table 1)










Mice No.	Left defect		Right defect
1, 10, 19, 28	C1, C7		B1, B7
2, 11, 20, 29	C2, C8		D1, D7
3, 12, 21, 30	B2, B8		D2, D8
4, 13, 22, 31	B3, B9		D3, D9
5, 14, 23, 32	C3, C9		C4, C10
6, 15, 24, 33	C5, C11		B4, B10
7, 16, 25, 34	C6, C12		D4, D10
8, 17, 26, 35	B5, B11		D5, D11
9, 18, 27, 36	B6, B12		D6, D12

Table 1 Showed the filling of bone grafts into the cavariae. C = control, B = Bio-Oss[®] D = DFDBA

Micro-computed tomography (Micro-CT) imaging

Four and twelve weeks after surgery, the animals were dissected. Their calvariae were removed and immediately immersed in 10% formalin overnight (n=6/groups). They were then rinsed with PBS before being analyzed with micro-CT (SCANCO Medical AG, uCT 35, Switzerland (Figure 4)) in a standard resolution scanning mode. To position the calvariae, a holder of 20-mm width and 75-mm height was used. The following micro-CT settings were used: 70 kVp, 114 μ A, 8 W, voxel size 20 μ m. A threshold of 212 was used for analysis of mineralization. A reference line was created to determine the analyzed area from the upper border of calvariae to the lower border that covered all of defect by picture of scout view. The mineral deposition in skull cavity and transform this data into bone volume. The morphology was observed and bone volume was also calculated into mean \pm S.D. (mm^3).

Data analysis

The bone volume was analyzed using SPSS version 17.0 (SPSS Inc, Chicago, Illinois, USA). The difference of bone volume among groups was evaluated using a one-way analysis of variance (ANOVA), followed by Post hoc Tukey's Honestly Significance Difference with a significant level of 5%.



Figure 4 SCANCO Medical AG, uCT 35

RNA extraction and Real-time polymerase chain reaction

1. Bone samples adjacent to the parietal and coronal suture were collected using a 5-mm diameter trephine bur (Figure 5), and stored in a cryotube that was submerged in liquid nitrogen immediately prior to RNA extraction. (Figure 6)

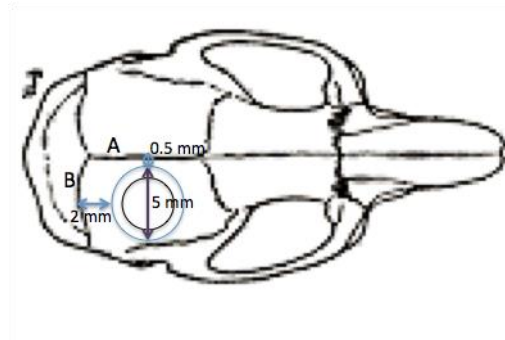


Figure 5 Location of collected sample bone



Figure 6 Bone sample and storage

2. Total RNA isolation was done using Qiazol[®] reagent (Qiagen, Inc., USA). 500 μ L were added to the cryotube and then transferred into a homogenization tube, which was prechilled in liquid nitrogen. The bone sample was homogenized using a homogenizer speed 3,500 RPM for 30 seconds [53]. (Figure 7)



Figure 7 The homogenization tube with metal beads (left) and homogenization (right)

3. After homogenization, RNA was extracted using spin-column based method with PureLink[®] RNA Mini Kit, Life Technologies, Inc., USA. This was performed according to the manufacturer instructions, which is stated as followed.

3.1 Transfer the lysate into a clean RNase-free tube, add 200 μ l chloroform vortex for 15 seconds, incubate 2-3 minutes in room temperature, then centrifuge at 12,000 g for 15 minutes in 4 °C

3.2 Lysate is separated into 2 layers. Pipette transparent layer 150 μ l into a new tube, beware of the turbid layer attached, and add 70% alcohol equal volume of cell homogenate. Vortex 10 seconds for a thorough mix.

3.3 Transfer the entire sample to the spin cartridge and then centrifuge at 12,000g for 15 seconds. RNA will be bound to the membrane, discard the flow-through and repeat this step 3-4 times.

3.4 Add 700 μ l of Wash Buffer I to the spin cartridge and centrifuge at 12,000g for 15 seconds. Discard the flow-through and put the spin cartridge into a new collection tube.

3.5 Add 500 μ l of Wash Buffer II with ethanol to the spin cartridge and centrifuge at 12,000g for 15 seconds. Discard the flow-through and repeat this step once more.

3.6 Centrifuge spin cartridge at 12,000g for 1-2 minutes to dry the membrane with bound RNA and then place the spin cartridge into the new recovery tube.

3.7 Add 80 µl of RNase-free water into the spin cartridge, incubate at room temperature for 1 minute, and then centrifuge at 12,000g for 2 minute. The RNA was eluted from the membrane into the recovery tube.

3.8 Keep the RNA on ice for immediate use or -80°C for long-term storage.

4. Assessment of RNA purity by Nanodrop spectrophotometer (NanoDrop 2000, Thermo Fisher Scientific, Inc., USA), the spectrophotometer was set to absorb the wave length of interest within the sample. Nucleic acids and proteins have absorbance at a range of 260 and 280 nm. The ratio of these wavelengths were used to determine RNA purity. The A260/280 ratio ~2.0 is accepted as pure for RNA.

Real-time polymerase chain reaction

Two-step RT-qPCR was used in this study. Reverse transcription converted RNA to cDNA, which was followed by PCR. The two-step protocol is more sensitive than the one-step protocol. However, this technique offers more control and flexibility. It is considered when amplification of multiple targets from one RNA sample is required.

Step 1 Reverse transcription

The Sensiscript RT kit (Sensiscript[®], Qiagen, Inc., USA) was used per the manufacturer's instruction. The following protocol is used when < 50 ng RNA.

1. Thaw template RNA on ice. Thaw 10x Buffer RT, dNTP mix, Oligo DT primer and RNase-free water at room temperature and put on ice immediately after thawing.

2. Prepare the master mix according to Table 2. Mix and vortex gently, centrifuge briefly. Keep tube on ice.
3. Add the template RNA for the final components to the master mix. Mix and vortex gently, centrifuge briefly.
4. Incubate for 60 minute at 37° C
5. Keep the reverse-transcription reactions on ice and continue process with PCR or store at -20°C for long-term storage.

Table 2 Reverse-transcription reaction components

Component	Volume/reaction	Final concentration
10x Buffer RT	2.0 µl	1x
dNTP Mix (5mM each dNTP)	2.0 µl	0.5mM each dNTP
Oligo-dT primer (10 µM)	2.0 µl	1 µM
Sensiscript Reverse Transcriptase	1.0 µl	
RNase-free water	Variable	-
Template RNA	Variable	<50 ng (per reaction)
Total volume	20.0 µl	-

Step 2 Polymerase chain reactions

1. Primer design and preparation

Primer3 and blast was used for designing primers. (<http://www.ncbi.nlm.nih.gov/tools/primer-blast/>) the primer sequences are shown in Table 3. 18s rRNA was used as a housekeeping gene to normalize the expression data [54]. Primers were shipped in dry form. Dissolve the primers with RNase free water to stock at 100µM

concentration. Keep the stocked primers in -20°C. The stocked primers were diluted in 10 µM concentration for use in PCR reaction.

Table 3 The specific primers for Real-time PCR

Gene	Forward primer (5'-3')	Reverse primer (5'-3')
Runx2	TCC TTC ACT CCA AGA CCC TA	TCA GAT ACC ATG GGT GCT TC
Osx	GAT TCC TGG GGT ATG TAG GA	TGG GAA ACA GGA ATA TGG GC
ALP	GGC TCT CTT CAC TCC AAG AT	GAA GGA AGC TAC CAA CTG CT
OCN	TGG GAA ACA GGA ATA TGG GC	GCA GAT TGT GAG ACC TTC AG
OPN	TGA AAG TGA CTG ATT CTG GC	CCT TTT CTT CAG AGG ACA CA
18S rRNA	GTG ATG CCC TTA GAT GTC C	CCA TCC AAT CGG TAG TAG C

2. Set up and run the qPCR reaction

KAPA SYBR[®] FAST qPCR Kits (Kapa Biosystems, Inc., USA) was used with Bio-Rad CFX96[™] real time RT-PCR system (Bio-Rad laboratories, Inc., USA).

2.1 Prepare the PCR master mix as per Table 4.

Table 4 KAPA SYBR[®] FAST qPCR Master Mix

Component	Volume/reaction	Final concentration
PCR-grade water	3.6 µl	N/A
KAPA SYBR [®] FAST qPCR	5 µl	1x
Master Mix Universal		
10 µM Forward Primer	0.2 µl	200 nM
10 µM Reverse Primer	0.2 µl	200 nM
Template DNA	1.0 µl	<20 ng
Total volume	10 µl	-

2.2 Mix PCR master mix gently, centrifuge briefly. Set up the plate reaction.

2.3 Run the qPCR reaction following parameters in Table 5.

Table 5 qPCR protocol

Step	Temperature	Duration	Cycles
Enzyme activation	95°C	3 min	Hold
Denature	95°C	1-3 sec	40
Anneal/extend	60°C	≥ 20 sec+ Plate Read	
Dissociation (Melt curve)	60.0-95.0 °C,	5 sec + Plate Read	increment 0.5 °C until reach 95.0 °C

For each gene, all samples were amplified in duplicate in one run. Negative control reactions with no sample (RNase free water) were included in each run. Analysis of relative gene expression was performed using the $2^{-\Delta\Delta C_t}$ method. This method compared each target gene to a reference gene (housekeeping gene). The mean C_t values from each gene were provided by Bio-Rad CFX96™. The ΔC_t for each gene was calculated by subtracting the C_t of the target from the control sample.

The $2^{-\Delta\Delta C_t}$ method is described in Applied Biosystems User Bulletin No.2 (P/N 4303859).

$$\text{The relative gene expression} = 2^{-\Delta\Delta C_t}$$

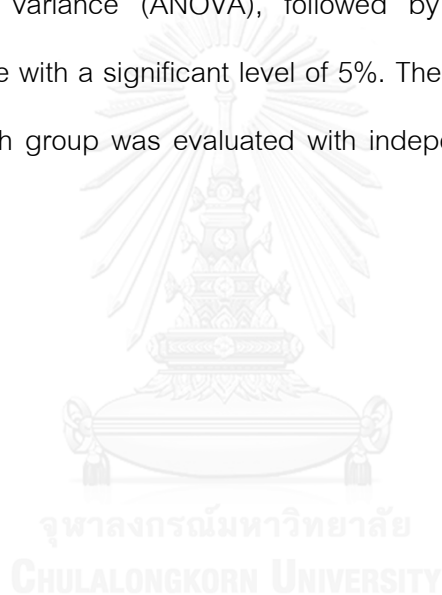
$$\text{Whereas } \Delta\Delta C_t = \Delta C_{t \text{ target}} - \Delta C_{t \text{ control}}$$

$$= (C_{t \text{ target}} - C_{t \text{ 18S}})_{\text{treatment}} - (C_{t \text{ target}} - C_{t \text{ 18S}})_{\text{untreatment}}$$

The threshold cycle (C_T) is the fractional cycle number at which the amount of amplified target reaches a fixed threshold. The analyzed data using this equation presented as the fold change in gene expression normalized to an endogenous reference gene and relative to the untreated control [55-57].

Data analysis

The data was analyzed using SPSS version 17.0 (SPSS Inc, Chicago, Illinois, USA). The difference of the relative gene expression among groups was evaluated with one-way analysis of variance (ANOVA), followed by Post hoc Tukey's Honestly Significance Difference with a significant level of 5%. The difference of the relative gene expression within each group was evaluated with independent t-test with a significant level of 5%.



CHAPTER IV RESULTS

One of thirty-six mice treated with Bio-Oss[®] and DFDBA was lost during the operation period. Micro-CT analysis of calvarial defects was performed and the analysis showed new bone formation in all groups.

Micro-CT imaging of bone regeneration

Three-dimensional micro-CT images from the 1-month group showed new bone formation in all groups at the defect margins. The Bio-Oss[®] grafts had more remaining particles within the defect compared to the DFDBA grafts (Figure 8). In the 3-month group, bone formation from defect margins were increased in all groups compared to the 1-month group. However, the residual grafts in the defects were markedly decreased, especially in DFDBA group (Figure 9).

At 1 month, mean bone formation was $0.25 \pm 0.08 \text{ mm}^3$ (1.5% bone volume (BV) of the total volume (TV)) in the control group followed by $0.5 \pm 0.12 \text{ mm}^3$ (3.14% BV/TV) in DFDBA and $2.0 \pm 0.45 \text{ mm}^3$ (12.64% BV/TV) in the Bio-Oss[®] group. At 3 months, the results were similar to the first month. Mean bone formation was $0.33 \pm 0.13 \text{ mm}^3$ (1.95% BV/TV) in the control group, $0.48 \pm 0.2 \text{ mm}^3$ (2.47% BV/TV) in DFDBA and $1.06 \pm 0.7 \text{ mm}^3$ (6.26% BV/TV) in Bio-Oss[®] (Figure 10).

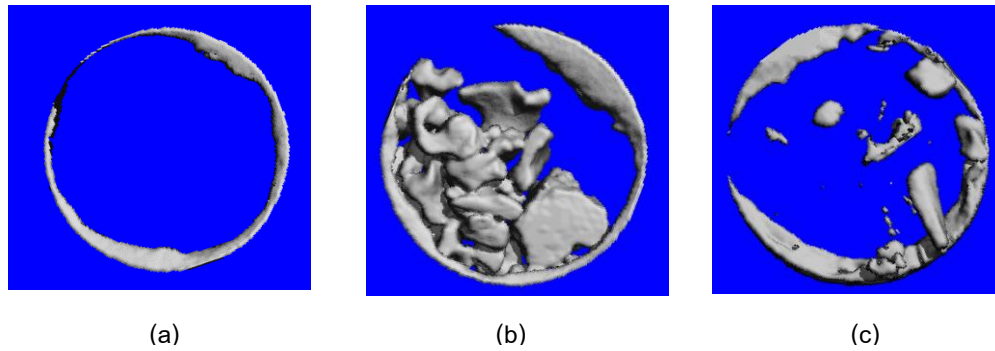


Figure 8 Three-dimensional micro-CT images of defects with (a) control (b) Bio-Oss[®] and (c) DFDBA 1 month after implantation.

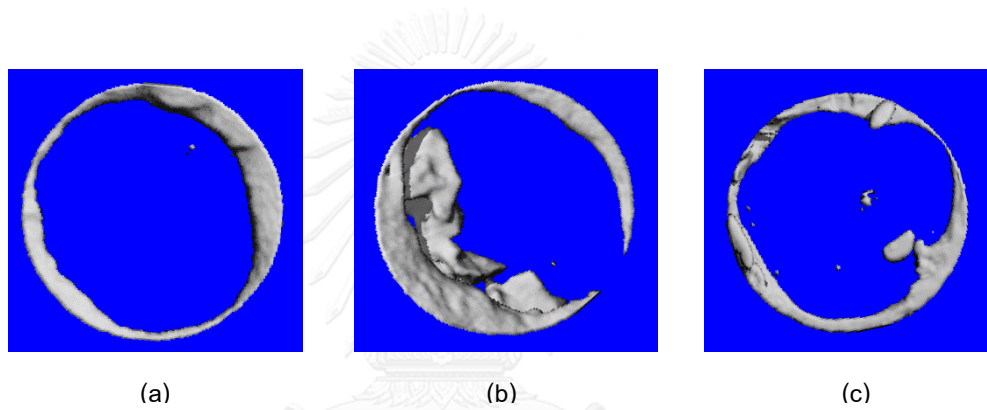


Figure 9 Three-dimensional micro-CT images of defects with (a) control (b) Bio-Oss[®] and (c) DFDBA 3 months after implantation.

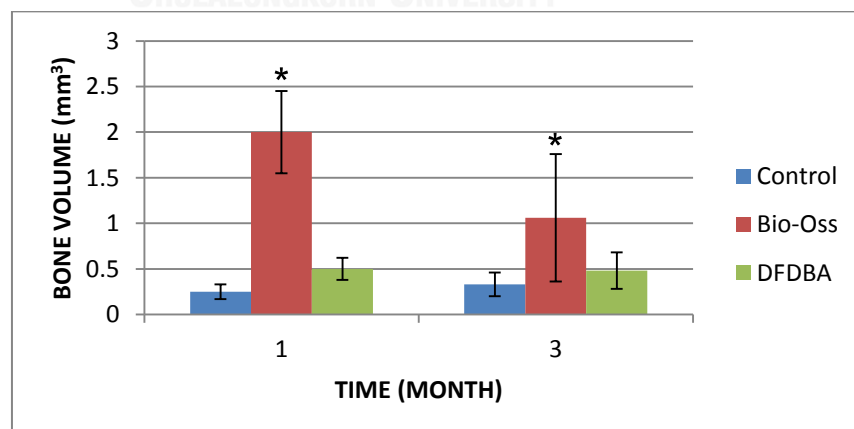


Figure 10 The mean bone formation (mm³) of bone grafts at 1 and 3 months. (* indicated significant difference in bone volume at $p < 0.05$)

Gene expression of bone markers

The evaluation of gene expression in grafted bone was performed. Figure 11 shows the relative mRNA levels of bone marker genes (ALP, OPN, OCN, Runx2 and Osx). At 1 month, no difference in bone marker gene expression was found, both in Bio-Oss[®] and DFDBA compared to the control. At 3 months, Bio-Oss[®] had up-regulation of Runx2, Osx and ALP compared to the control and also had significantly increased Runx2 expression compared to DFDBA. DFDBA had up-regulated Osx, ALP and OPN compared to the control. The expression of OPN was significantly up-regulated in the DFDBA group. No difference was observed for OCN in both materials.

Gene expression within each group was evaluated at 1 and 3 months. In the control group, all genes except OPN decreased in 3 months with statistically significant difference in Runx2 and Osx. Bio-Oss[®] up-regulated ALP and OPN significantly in the 3 months group, whereas DFBA up-regulated Osx and OPN significantly in the 3 months group. (Figure 12)

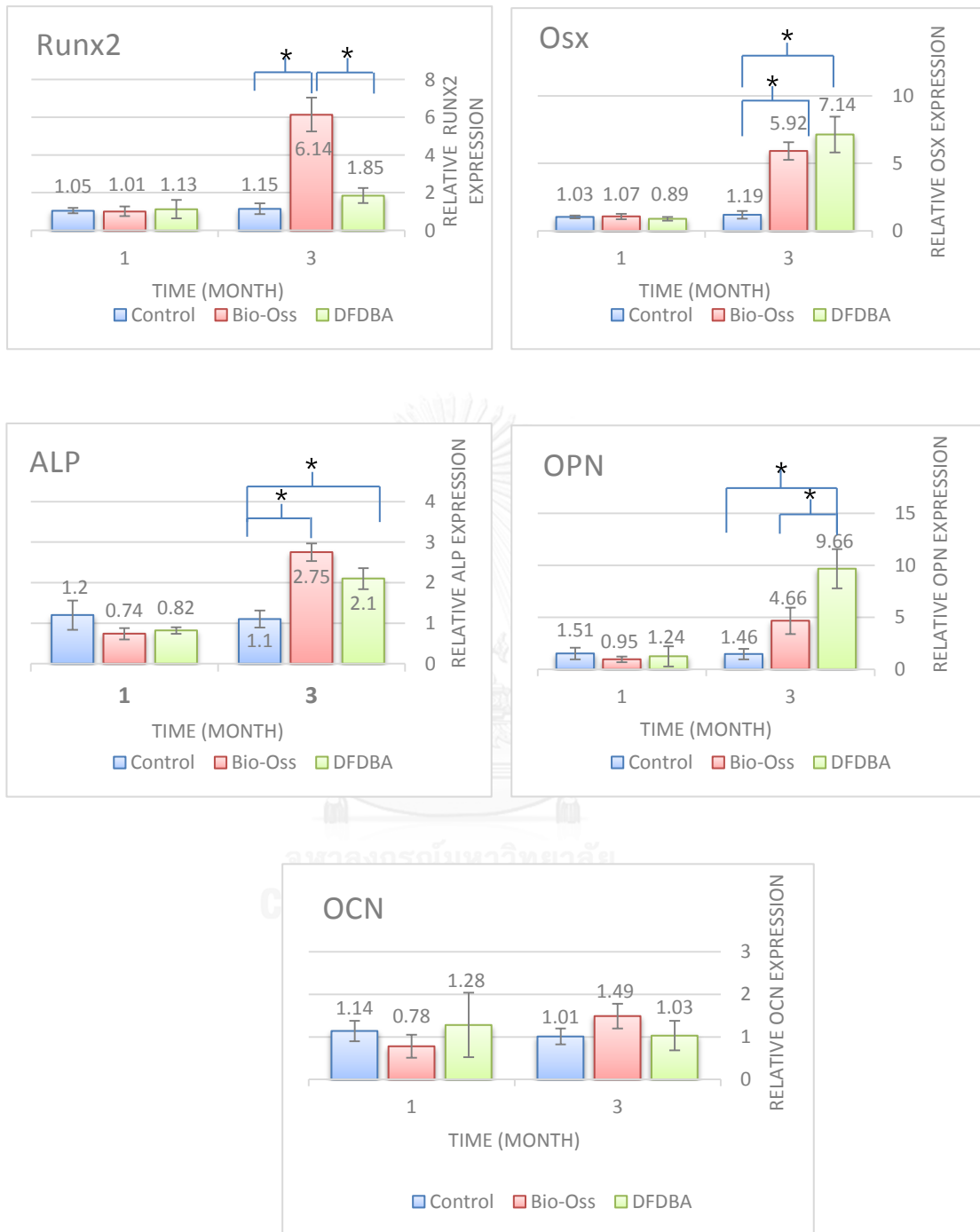


Figure 11 The expression of bone markers gene among groups. Value present by means ± SD.

(* Indicated significant difference in relative gene expression at p < 0.05)

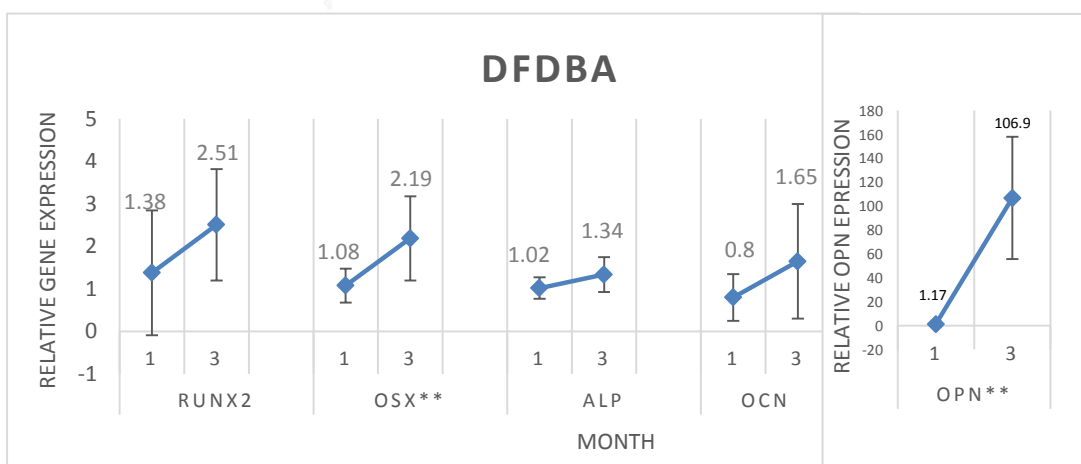
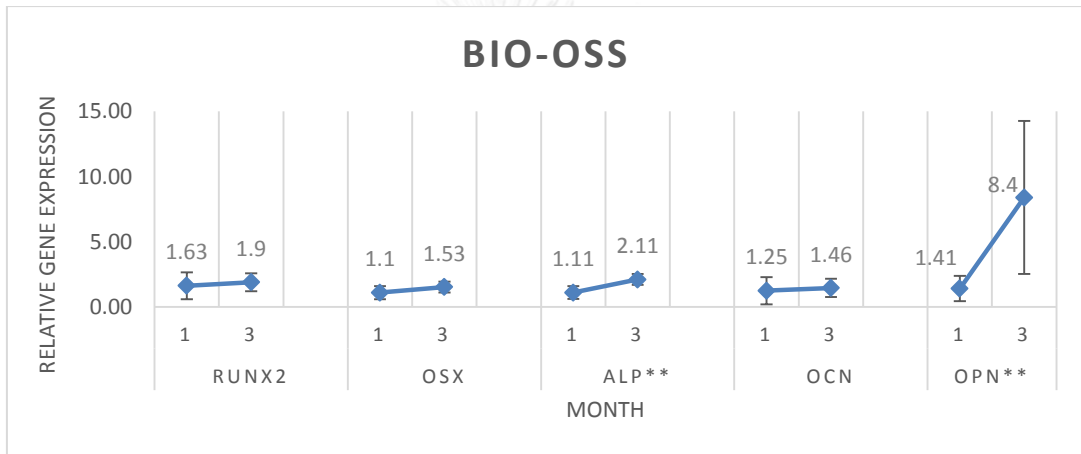
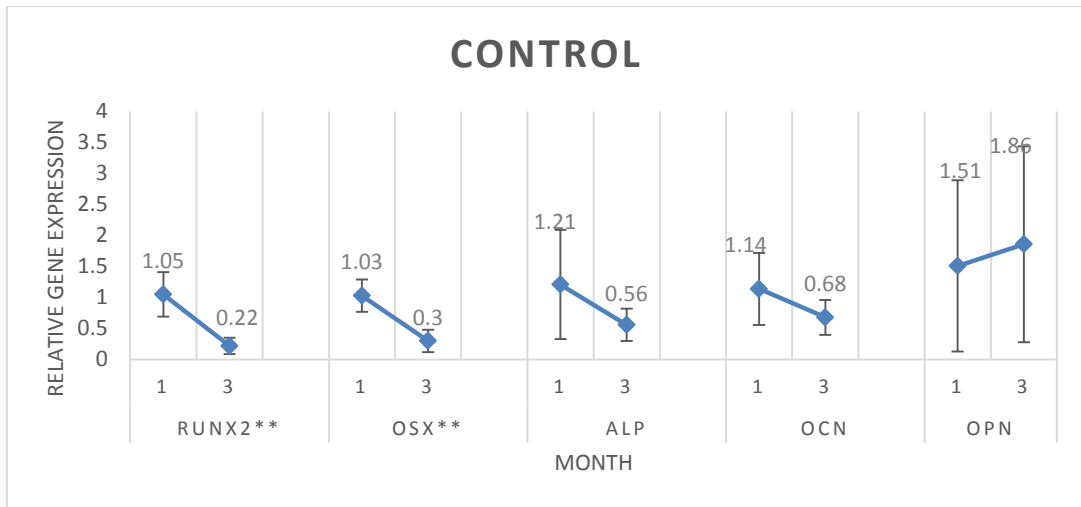


Figure 12 The expression of bone markers gene between 1 and 3 months. Value present by means \pm SD. (** Indicated significant difference in relative gene expression at $p < 0.05$)

CHAPTER V DISCUSSION

Many bone grafting materials are available in the market today. For grafting procedures, Bio-Oss[®] and DFDBA have been widely used for many years, as they have history of good clinical outcome. Therefore, Bio-Oss[®] and DFDBA were chosen as representative for xenograft and allograft, respectively, and compared in efficiency in bone formation [7,18, 58-60].

From the micro-CT analysis, it was found that new bone formation in all groups started from the defect margins, leaving bone grafting material encapsulated within the new bone. At the end of the experiment, no defect was completely filled with new bone. Bio-oss[®] had the highest percentage of bone volume at both 1 and 3 months. The results of DFDBA were better than those of the control groups at both 1 and 3 months; however, it was not statistically significant. This may be due to the faster resorption of DFDBA particles (3.14% of BV/TV) compared to Bio-Oss[®] (12.64% of BV/TV) at 1 month. At 3 months, Bio-oss[®] had increased resorption (6.26% of BV/TV) compared to 1 month, while DFDBA showed no significant reduction in bone volume (2.47% of BV/TV).

We found that Bio-Oss[®] had greater bone volume than DFDBA at both 1 and 3 months. This corresponds with a previous study in that Bio-Oss[®] showed osteoconductive properties and good biocompatibility with intra-oral tissue. Histomorphometric study of sinus grafting with Bio-Oss[®] in chimpanzees demonstrated that organic bovine bone was resorbed and replaced with new bone within 1.5 years [58]. Some studies reported that organic bovine bone still remains after 44 months in humans [61, 62]. From this study, it was found that, though there was reduction of Bio-Oss[®] graft particles within the first month, new vital host bone gradually occupied this space. However, at 3 months period, Bio-oss[®] particles still remained in the defect sites. The period of time required for the graft to be completely replaced by new bone cannot be predicted due to the time constraints of this study.

The micro-CT results showed that DFDBA particles were rapidly resorbed. Whether the remaining graft residuals stimulate new bone formation or delay normal

bone formation is still a topic of controversy. This suggests that this material might have a resorption rate that coincides with the remodeling rate of new bone.

Our further question was whether the grafting materials interfere with or influence the bone healing process. Previous studies have found the relationship between physiological and genetic data to be unclear. This *in vivo* study placed focus on specific genes related in bone formation using a mouse model. We found that Bio-Oss[®] and DFDBA had up-regulated ALP in the 3 month group compared to control. ALP was detected in the initial stage of bone formation. Thus, both materials can help promote cell proliferation. Furthermore, Runx2 was significantly up-regulated in the 3 month Bio-Oss[®] group. Runx2 is essential for osteoblast differentiation from mesenchymal stem cells to premature osteoblasts, but inhibits osteoblast maturation [31]. The level of expression of Osx had significant up-regulation at 3 months both in Bio-Oss[®] and DFDBA. Osx is a downstream gene to Runx2 that is required for the differentiation of premature osteoblasts into mature osteoblasts [33]. Runx2 interact with Osx and can upregulate the expression of OCN, a specific bone marker found at the late stage of cell maturation [30]. Monjo 2013 revealed that OCN is the best predictive marker for osseointegration of titanium implants in the animal model [63]. According to our study, Runx2 and Osx had increased expression while no difference in OCN expression was found at 3 months. This may have been due to the short time period of this study.

Another investigated gene, OPN, was significantly increased in the 3 months DFDBA group. The OPN gene is produced by osteoblasts but yields resorptive activity by osteoclasts [64]. This may have caused the high resorption rate of DFDBA particles as shown in microCT. Additionally, it functions to inhibit crystal growth and turn into more mature bone. From these findings, it can be concluded that both Bio-Oss[®] and DFDBA can promote osteoblast differentiation (Figure 13).

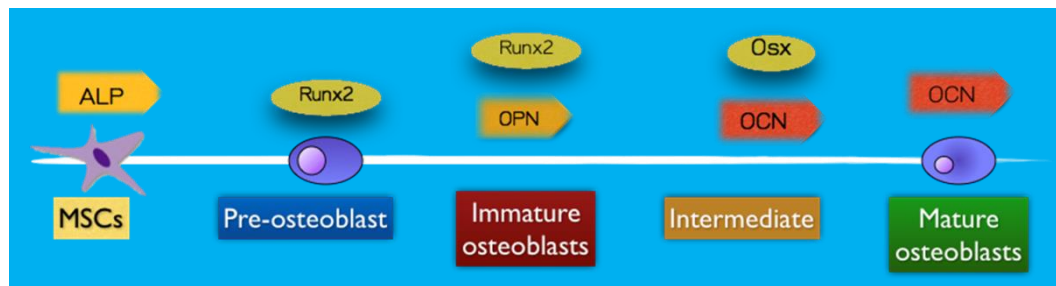


Figure 13 Regulation of gene expression in osteoblasts

Comparison of gene expression at 1 and 3 months was performed. Several genes in the control group had decreased expression at 3 months (statistically significant difference was found in Runx2 and Osx). While both Bio-Oss[®] and DFDBA had increased gene expression at 3 months. This implies that the use of bone graft materials can prolong specific bone marker genes in the *in vivo* mouse model.

In clinical studies, Bio-Oss[®] and DFDBA showed efficiency in decreased pocket depths and gains in clinical attachment levels in intrabony defects in humans [60]. However, from our micro-CT results, Bio-Oss[®] had superior bone volume to DFDBA and control groups at both periods. Nowadays, microCT has gained recognition in the use of studying small osseous and soft tissue structures of animals. This technique provides three-dimensional images of bone without destroying its structure and allows for the accurate visualization of the anatomy and morphology of tissues. Furthermore, the process is much faster compared to the processing time required in conventional histological procedures [65]. Therefore, microCT was selected for the examination of the amount and pattern of bone formation in this study. In previous histological studies, Mokbel 2008 found that DFDBA had a significantly greater mean bone formation than Bio-Oss[®] in rat calvarial bone defect models [8]. In another comparative study between Bio-Oss[®] and DFDBA in rabbit calvarias, it was found that DFDBA had a high resorption rate but this did not affect the new bone formation [66]. From our study, micro-CT was used to provide quantitative data of bone volume. However, a histological analysis would be beneficial, as it could provide qualitative data (discriminate immature bone,

inflammatory cells, residual graft particles) and further information from histological analysis to confirm our results.

Although DFDBA had high rerorption rate in micro-CT, it showed high gene expression levels, especially of *Osx*, a late marker in the osteoblastic pathway. It may be concluded that DFDBA can promote bone regeneration faster than Bio-Oss[®]. This is probably due to the difference in their components. DFDBA removed the mineral contents and has no structural capability while Bio-Oss[®] removed the organic tissues and provided structure and porosity for new bone [67].

The limitation of this study was that it was performed in mouse models. Their small size and low vascularization leads to limitation in surgical precision. Therefore, the amount of bone formation observed in this experiment may be lower compared to the intra-oral situation.

CHAPTER VI CONCLUSION

This study comparatively studied two commercially available bone grafts in their physical and biological responses after grafting in bone defect models. It was found that both materials have the potential to increase the expression of osteoblast related genes *in vivo* compared to natural bone healing. Bio-oss[®] has slow graft degradation, resulting in its act as a bone matrix for bone formation. However, further investigation should be performed by histological analysis, to study osteoclast activity and inflammatory response.

REFERENCES

1. Araujo, M.G. , and Lindhe, J. Dimensional ridge alterations following tooth extraction. An experimental study in the dog. J Clin Periodontol 32 (2005): 212-218.
2. Atwood, D.A. Bone loss of edentulous alveolar ridges. J Periodontol 50 (1979): 11-21.
3. Tallgren, A. The continuing reduction of the residual alveolar ridges in complete denture wearers: a mixed-longitudinal study covering 25 years. J Prosthet Dent 27 (1972): 120-132.
4. Schropp, L., Wenzel, A., Kostopoulos, L. , and Karring, T. Bone healing and soft tissue contour changes following single-tooth extraction: a clinical and radiographic 12-month prospective study. Int J Periodontics Restorative Dent 23 (2003): 313-323.
5. Albrektsson, T. , and Johansson, C. Osteoinduction, osteoconduction and osseointegration. Eur Spine J 10 Suppl 2 (2001): S96-101.
6. Gazdag, A.R., Lane, J.M., Glaser, D. , and Forster, R.A. Alternatives to Autogenous Bone Graft: Efficacy and Indications. J Am Acad Orthop Surg 3 (1995): 1-8.
7. Jensen, S.S., Broggini, N., Hjorting-Hansen, E., Schenk, R. , and Buser, D. Bone healing and graft resorption of autograft, anorganic bovine bone and beta-tricalcium phosphate. A histologic and histomorphometric study in the mandibles of minipigs. Clin Oral Implants Res 17 (2006): 237-243.
8. Mokbel, N., Bou Serhal, C., Matni, G. , and Naaman, N. Healing patterns of critical size bony defects in rat following bone graft. Oral Maxillofac Surg 12 (2008): 73-78.
9. Becker, W. Treatment of small defects adjacent to oral implants with various biomaterials. Periodontol 2000 33 (2003): 26-35.

10. Hansson, S. , and Halldin, A. Alveolar ridge resorption after tooth extraction: A consequence of a fundamental principle of bone physiology. Journal of Dental Biomechanics 3 (2012): 1758736012456543.
11. Van der Weijden, F., Dell'Acqua, F. , and Slot, D.E. Alveolar bone dimensional changes of post-extraction sockets in humans: a systematic review. J Clin Periodontol 36 (2009): 1048-1058.
12. Pietrokovski, J. , and Massler, M. Alveolar ridge resorption following tooth extraction. J Prosthet Dent 17 (1967): 21-27.
13. Nevins, M., et al. A study of the fate of the buccal wall of extraction sockets of teeth with prominent roots. Int J Periodontics Restorative Dent 26 (2006): 19-29.
14. Calori, G.M., Mazza, E., Colombo, M. , and Ripamonti, C. The use of bone-graft substitutes in large bone defects: any specific needs? Injury 42 Suppl 2 (2011): S56-63.
15. Crespi, R., Cappare, P. , and Gherlone, E. Dental implants placed in extraction sites grafted with different bone substitutes: radiographic evaluation at 24 months. J Periodontol 80 (2009): 1616-1621.
16. Urist, M.R. , and Strates, B.S. Bone morphogenetic protein. J Dent Res 50 (1971): 1392-1406.
17. Piattelli, A., Scarano, A., Corigliano, M. , and Piattelli, M. Comparison of bone regeneration with the use of mineralized and demineralized freeze-dried bone allografts: a histological and histochemical study in man. Biomaterials 17 (1996): 1127-1131.
18. Wood, R.A. , and Mealey, B.L. Histologic comparison of healing after tooth extraction with ridge preservation using mineralized versus demineralized freeze-dried bone allograft. J Periodontol 83 (2012): 329-336.
19. Crespi, R., Cappare, P., Romanos, G.E., Mariani, E., Benasciutti, E. , and Gherlone, E. Corticocancellous porcine bone in the healing of human extraction sockets: combining histomorphometry with osteoblast gene expression profiles in vivo. Int J Oral Maxillofac Implants 26 (2011): 866-872.

20. Tapety, F.I., Amizuka, N., Uoshima, K., Nomura, S. , and Maeda, T. A histological evaluation of the involvement of Bio-Oss in osteoblastic differentiation and matrix synthesis. Clin Oral Implants Res 15 (2004): 315-324.
21. Camelo, M., et al. Clinical, radiographic, and histologic evaluation of human periodontal defects treated with Bio-Oss and Bio-Gide. Int J Periodontics Restorative Dent 18 (1998): 321-331.
22. Caubet, J., Ramis, J.M., Ramos-Murguialday, M., Morey, M.A. , and Monjo, M. Gene expression and morphometric parameters of human bone biopsies after maxillary sinus floor elevation with autologous bone combined with Bio-Oss(R) or BoneCeramic(R). Clin Oral Implants Res 26 (2015): 727-735.
23. Develioglu, H., Unver Saraydin, S. , and Kartal, U. The bone-healing effect of a xenograft in a rat calvarial defect model. Dent Mater J 28 (2009): 396-400.
24. Kolerman, R., Samorodnitzky-Naveh, G.R., Barnea, E. , and Tal, H. Histomorphometric analysis of newly formed bone after bilateral maxillary sinus augmentation using two different osteoconductive materials and internal collagen membrane. Int J Periodontics Restorative Dent 32 (2012): e21-28.
25. Lindgren, C., Mordenfeld, A., Johansson, C.B. , and Hallman, M. A 3-year clinical follow-up of implants placed in two different biomaterials used for sinus augmentation. Int J Oral Maxillofac Implants 27 (2012): 1151-1162.
26. Farina, R. , and Trombelli, L. Wound healing of extraction sockets. Endodontic Topics 25 (2011): 16-43.
27. Mizuno, M. , and Kuboki, Y. Osteoblast-related gene expression of bone marrow cells during the osteoblastic differentiation induced by type I collagen. J Biochem 129 (2001): 133-138.
28. Boskey, A.L., Gadaleta, S., Gundberg, C., Doty, S.B., Ducky, P. , and Karsenty, G. Fourier transform infrared microspectroscopic analysis of bones of osteocalcin-deficient mice provides insight into the function of osteocalcin. Bone 23 (1998): 187-196.

29. Shimizu, T. Participation of Runx2 in mandibular condylar cartilage development. Eur J Med Res 11 (2006): 455-461.
30. Tsai, M.-T., Lin, Y.-S., Chen, W.-C. , and Ho, C.-H. Runx2 and Osterix Gene Expression in Human Bone Marrow Stromal Cells Are Mediated by Far-Infrared Radiation. Lecture Notes in Engineering and Computer Science (2011):
31. Komori, T. Regulation of osteoblast differentiation by Runx2. Adv Exp Med Biol 658 (2010): 43-49.
32. Gilbert, L., et al. Expression of the osteoblast differentiation factor RUNX2 (Cbfa1/AML3/Pebp2alpha A) is inhibited by tumor necrosis factor-alpha. J Biol Chem 277 (2002): 2695-2701.
33. Nakashima, K., et al. The novel zinc finger-containing transcription factor osterix is required for osteoblast differentiation and bone formation. Cell 108 (2002): 17-29.
34. Tu, Q., Valverde, P., Li, S., Zhang, J., Yang, P. , and Chen, J. Osterix overexpression in mesenchymal stem cells stimulates healing of critical-sized defects in murine calvarial bone. Tissue Eng 13 (2007): 2431-2440.
35. Sollazzo, V., et al. Bio-Oss(R)acts on Stem cells derived from Peripheral Blood. Oman Med J 25 (2010): 26-31.
36. Vaziri, S., Vahabi, S., Torshabi, M. , and Hematzadeh, S. In vitro assay for osteoinductive activity of different demineralized freeze-dried bone allograft. J Periodontal Implant Sci 42 (2012): 224-230.
37. van Houdt, C.I., et al. Bone regeneration and gene expression in bone defects under healthy and osteoporotic bone conditions using two commercially available bone graft substitutes. Biomed Mater 10 (2015): 035003.
38. Virolainen, P., Vuorio, E. , and Aro, H.T. Gene expression at graft-host interfaces of cortical bone allografts and autografts. Clin Orthop Relat Res (1993): 144-149.
39. Gomes, P.S. , and Fernandes, M.H. Rodent models in bone-related research: the relevance of calvarial defects in the assessment of bone regeneration strategies. Lab Anim 45 (2011): 14-24.

40. Spicer, P.P., Kretlow, J.D., Young, S., Jansen, J.A., Kasper, F.K. , and Mikos, A.G. Evaluation of bone regeneration using the rat critical size calvarial defect. Nat Protoc 7 (2012): 1918-1929.
41. Szpalski, C., Barr, J., Wetterau, M., Saadeh, P.B. , and Warren, S.M. Cranial bone defects: current and future strategies. Neurosurg Focus 29 (2010): E8.
42. O'Loughlin, P.F., Morr, S., Bogunovic, L., Kim, A.D., Park, B. , and Lane, J.M. Selection and development of preclinical models in fracture-healing research. J Bone Joint Surg Am 90 Suppl 1 (2008): 79-84.
43. Vieira, A.E., et al. Intramembranous Bone Healing Process Subsequent to Tooth Extraction in Mice: Micro-Computed Tomography, Histomorphometric and Molecular Characterization. PLoS ONE 10 (2015): e0128021.
44. Cowan, C.M., et al. Adipose-derived adult stromal cells heal critical-size mouse calvarial defects. Nat Biotechnol 22 (2004): 560-567.
45. Inoda, H., Yamamoto, G. , and Hattori, T. rh-BMP2-induced ectopic bone for grafting critical size defects: a preliminary histological evaluation in rat calvariae. Int J Oral Maxillofac Surg 36 (2007): 39-44.
46. Wu, X., Downes, S. , and Watts, D.C. Evaluation of critical size defects of mouse calvarial bone: An organ culture study. Microsc Res Tech 73 (2010): 540-547.
47. Zong, C., et al. Reconstruction of rat calvarial defects with human mesenchymal stem cells and osteoblast-like cells in poly-lactic-co-glycolic acid scaffolds. Eur Cell Mater 20 (2010): 109-120.
48. Byzova, B.A.K.a.T.V., MicroCT: An Essential Tool in Bone Metastasis Research. Computed Tomography - Clinical Applications. ed. InTech: 2012.
49. Postnov, A., et al. High resolution micro-CT scanning as an innovative tool for evaluation of the surgical positioning of cochlear implant electrodes. Acta Otolaryngol 126 (2006): 467-474.
50. Ireland, D. Analysis of gene expression in bone by quantitative RT-PCR. Methods Mol Med 80 (2003): 433-440.

51. Jozefczuk, J. , and Adjaye, J. Quantitative real-time PCR-based analysis of gene expression. Methods Enzymol 500 (2011): 99-109.
52. Machida, A., Okuhara, S., Harada, K. , and Iseki, S. Difference in apical and basal growth of the frontal bone primordium in Foxc1ch/ch mice. Congenit Anom (Kyoto) 54 (2014): 172-177.
53. Carter, L.E., Kilroy, G., Gimble, J.M. , and Floyd, Z.E. An improved method for isolation of RNA from bone. BMC Biotechnol 12 (2012): 5.
54. Stephens, A.S., Stephens, S.R. , and Morrison, N.A. Internal control genes for quantitative RT-PCR expression analysis in mouse osteoblasts, osteoclasts and macrophages. BMC Res Notes 4 (2011): 410.
55. Livak, K.J. , and Schmittgen, T.D. Analysis of relative gene expression data using real-time quantitative PCR and the 2(-Delta Delta C(T)) Method. Methods 25 (2001): 402-408.
56. Pfaffl, M.W. A new mathematical model for relative quantification in real-time RT-PCR. Nucleic Acids Res 29 (2001): e45.
57. Yuan, J.S., Reed, A., Chen, F. , and Stewart, N.C. Statistical analysis of real-time PCR data. BMC Bioinformatics 7 (2006): 1-12.
58. McAllister, B.S., Margolin, M.D., Cogan, A.G., Buck, D., Hollinger, J.O. , and Lynch, S.E. Eighteen-month radiographic and histologic evaluation of sinus grafting with anorganic bovine bone in the chimpanzee. Int J Oral Maxillofac Implants 14 (1999): 361-368.
59. Iezzi, G., Scarano, A., Mangano, C., Cirotti, B. , and Piattelli, A. Histologic results from a human implant retrieved due to fracture 5 years after insertion in a sinus augmented with anorganic bovine bone. J Periodontol 79 (2008): 192-198.
60. Richardson, C.R., Mellonig, J.T., Brunsvold, M.A., McDonnell, H.T. , and Cochran, D.L. Clinical evaluation of Bio-Oss: a bovine-derived xenograft for the treatment of periodontal osseous defects in humans. J Clin Periodontol 26 (1999): 421-428.

61. Skoglund, A., Hising, P. , and Young, C. A clinical and histologic examination in humans of the osseous response to implanted natural bone mineral. Int J Oral Maxillofac Implants 12 (1997): 194-199.
62. Artzi, Z., Tal, H. , and Dayan, D. Porous bovine bone mineral in healing of human extraction sockets: 2. Histochemical observations at 9 months. J Periodontol 72 (2001): 152-159.
63. Monjo, M., Ramis, J.M., Ronold, H.J., Taxt-Lamolle, S.F., Ellingsen, J.E. , and Lyngstadaas, S.P. Correlation between molecular signals and bone bonding to titanium implants. Clin Oral Implants Res 24 (2013): 1035-1043.
64. Shapses, S.A., et al. Osteopontin facilitates bone resorption, decreasing bone mineral crystallinity and content during calcium deficiency. Calcif Tissue Int 73 (2003): 86-92.
65. Cowan, C.M., et al. MicroCT evaluation of three-dimensional mineralization in response to BMP-2 doses in vitro and in critical sized rat calvarial defects. Tissue Eng 13 (2007): 501-512.
66. Ghanavati, F., et al. Bone augmentation potential in rabbit calvaria and ex vivo cytotoxicity of four bone substituting materials. Journal of Periodontology & Implant Dentistry 3 (2011): 1-7.
67. Desterro, F.d.P.d., Sader, M.S., Soares, G.D.d.A. , and Vidigal Jr, G.M. Can Inorganic Bovine Bone Grafts Present Distinct Properties? Brazilian Dental Journal 25 (2014): 282-288.

APPENDIX

Nucleic acid concentration and purity

The total RNA concentration and 260/280 ratio (sample x_1, x_2 refer as C = control, B= Bio-Oss, D= DFDBA; x_1 = month after bone grafted, x_2 = number of mice)

Sample	Average RNA concentration(ng/ μ l)	A260	A280	260/280
C11	6.06	0.152	0.077	1.98
C12	20.9	0.522	0.274	1.91
C15 (left)	22	0.55	0.289	1.90
C15 (right)	13.4	0.335	0.172	1.95
C16	44.36	1.11	0.578	1.92
C17	34.83	0.871	0.455	1.91
B11	62.6	1.57	0.78	2.0
B13	17.4	0.43	0.24	1.82
B14	95.73	2.393	1.232	1.94
B16	109.96	2.749	1.4	1.96
B18	20.43	0.511	0.26	1.96
B19	36.86	0.921	0.45	2.04
D12	41	1.023	0.526	1.95
D13	24.1	0.603	0.318	1.9
D14	35.6	0.891	0.451	1.98
D17	48.7	1.22	0.611	2.0
D18	42.03	1.051	0.532	1.98
D19	46.1	1.15	0.576	2.0
C31	17.56	0.439	0.263	1.67
C32	14.7	0.368	0.213	1.73
C35 (left)	10.6	0.265	0.146	1.82
C35 (right)	12.6	0.315	0.19	1.67
C36	13.1	0.327	0.183	1.79
C37	11.16	0.279	0.158	1.77
B31	10.8	0.27	0.141	1.91
B33	12.23	0.31	0.16	1.94
B34	15.76	0.394	0.22	1.8
B36	16.46	0.411	0.227	1.81
B38	17.83	0.446	0.258	1.73
B39	12.1	0.303	0.187	1.62
D32	13.4	0.34	0.17	2
D33	17.5	0.437	0.26	1.69
D34	10	0.25	0.145	1.72
D37	12.73	0.319	0.176	1.81
D38	11.83	0.296	0.147	2
D39	10.76	0.269	0.145	1.86

Average C_t value in qRT-PCR

The C_t value are shown in the table below (sample x_1x_2 refer as C = control, B= Bio-Oss, D= DFDBA; x_1 = month after bone grafted, x_2 = number of mice)

Sample	Runx2	Osx	ALP	OCN	OPN	18S
C11	29.89	31.33	29.94	34.43	30.87	23.36
C13	26.83	29.22	29.54	33.43	25.84	20.34
C15 (left)	25.64	27.97	27.23	30.72	22.7	19.52
C15 (right)	25.92	27.52	27.08	30.92	23.34	18.66
C16	25.64	26.6	26.96	30.69	24.24	18.19
C17	25.62	27.37	26.69	29.95	22.82	18.74
B11	27.19	30.43	29.92	34.43	25.59	21.29
B13	28.72	30.48	30.44	33.43	27.72	22.59
B14	29.89	25.86	26.35	30.1	25.51	18.05
B16	25.53	26.36	26.47	31.39	26.02	18.26
B18	25.99	28.62	28.35	32.41	23.76	19.09
B19	26.61	28.73	29.69	32.68	24.81	19.76
D12	27.37	29.37	29.12	32.79	29.53	20.76
D13	28.69	32.54	32.82	33.28	26.28	24.22
D14	27.2	28.46	28.36	33.77	27.56	19.33
D17	27.36	29.76	27.77	31.84	24.71	19.63
D18	25.97	26.39	26.55	33.15	27.17	18.05
D19	26.45	27.46	27.02	31.58	29.29	19.07
C31	30.82	31.81	30.72	32.83	27.47	21.08
C32	29.4	31.56	28.38	32.16	24.49	19.56
C35 (left)	29.15	29.75	28.55	32.49	24.67	20.16
C35 (right)	29.77	32.04	31.09	35.23	24.35	21.19
C36	30.43	31.08	29.92	32.84	27.06	20.46
C37	29.54	30.99	29.89	34.09	24.94	21.63
B31	27.7	29.53	29.38	34.7	23.24	21.78
B33	28.57	29.55	29.38	33.54	25.73	21.86
B34	29.19	30.45	30.52	33.98	24.99	22.71
B36	28.13	29.51	28.97	34.71	25.09	21.69
B38	28.95	30.11	29.35	32.82	24.29	21.18
B39	29.67	31.28	30.6	35.61	26.39	23.11
D32	28.16	30.62	30.27	34.05	23.54	21.95
D33	29.27	31.51	31.52	34.44	24.26	23.25
D34	29.23	30.59	31.4	36.18	25.59	23.52
D37	26.88	29.22	29.66	34.67	22.96	22.13
D38	28.02	29.56	30.01	35.06	24.36	21.26
C31	30.82	31.81	30.72	32.83	27.47	21.08

Statistics test

MicroCT 1 month (1= control, 2= Bio-Oss, 3= DFDBA)

Descriptives

	N	Mean	Std. Deviation	Std. Error	95% Confidence Interval for Mean		Minimum	Maximum
					Lower Bound	Upper Bound		
1	6	.247583	.0808391	.0330024	.162748	.332419	.1530	.3548
2	5	2.006700	.4556135	.2037565	1.440981	2.572419	1.6195	2.6390
3	5	.500260	.1221725	.0546372	.348563	.651957	.3556	.6586
Total	16	.876269	.8322849	.2080712	.432775	1.319762	.1530	2.6390

ANOVA

	Sum of Squares	df	Mean Square	F	Sig.
Between Groups	9.468	2	4.734	66.695	.000
Within Groups	.923	13	.071		
Total	10.390	15			

Multiple Comparisons

Dependent Variable: Bone volume

(I) Group	(J) Group	Mean Difference (I-J)	Std. Error	Sig.	95% Confidence Interval		
					Lower Bound	Upper Bound	
Tukey HSD	1	2	-1.7591167	.1613235	.000	-2.185081	-1.333152
		3	-.2526767	.1613235	.294	-.678641	.173288
	2	1	1.7591167	.1613235	.000	1.333152	2.185081
		3	1.5064400	.1684969	.000	1.061535	1.951345
	3	1	.2526767	.1613235	.294	-.173288	.678641
		2	-1.5064400	.1684969	.000	-1.951345	-1.061535
Dunnnett T3	1	2	-1.7591167	.2064119	.002	-2.513366	-1.004867
		3	-.2526767	.0638309	.016	-.449735	-.055618
	2	1	1.7591167	.2064119	.002	1.004867	2.513366
		3	1.5064400	.2109549	.003	.763191	2.249689
	3	1	.2526767	.0638309	.016	.055618	.449735
		2	-1.5064400	.2109549	.003	-2.249689	-.763191

*. The mean difference is significant at the 0.05 level.

MicroCT 3 month

Descriptives

	N	Mean	Std. Deviation	Std. Error	95% Confidence Interval for Mean		Minimum	Maximum
					Lower Bound	Upper Bound		
Control	6	.330683	.1254397	.0512105	.199042	.462324	.1705	.4628
Bio-oss	6	1.062167	.6923651	.2826569	.335574	1.788759	.4505	2.3364
DFDBA	6	.484600	.2088870	.0852777	.265387	.703813	.3038	.8701
Total	18	.625817	.5132580	.1209761	.370579	.881054	.1705	2.3364

ANOVA

	Sum of Squares	df	Mean Square	F	Sig.
Between Groups	1.785	2	.892	4.969	.022
Within Groups	2.694	15	.180		
Total	4.478	17			

Multiple Comparisons

Dependent Variable: Bone volume

(I) Group	(J) Group	Mean Difference (I-J)	Std. Error	Sig.	95% Confidence Interval		
					Lower Bound	Upper Bound	
Tukey HSD	1	2	-.7314833	.2446626	.023	-1.366987	-.095979
		3	-.1539167	.2446626	.807	-.789421	.481587
	2	1	.7314833	.2446626	.023	.095979	1.366987
		3	.5775667	.2446626	.078	-.057937	1.213071
	3	1	.1539167	.2446626	.807	-.481587	.789421
		2	-.5775667	.2446626	.078	-1.213071	.057937
Dunnnett t (2-sided) ^a	1	3	-.1539167	.2446626	.758	-.750696	.442862
	2	3	.5775667	.2446626	.058	-.019212	1.174346

*. The mean difference is significant at the 0.05 level.

a. Dunnnett t-tests treat one group as a control, and compare all other groups against it.

One-way ANOVA and Post hoc Tukey's HSD of the gene expression among groups

PCR 1 month Runx2 (1= control, 2= Bio-Oss, 3= DFDBA)

Descriptives

gene

	N	Mean	Std. Deviation	Std. Error	95% Confidence Interval for Mean		Minimum	Maximum
					Lower Bound	Upper Bound		
1	6	1.05234362	.358076313	.146184043	.67656558	1.42812167	.632878	1.591073
2	6	1.00987835	.645993397	.263725700	.33194985	1.68780684	.030151	1.851036
3	6	1.12856483	1.201606809	.490553925	-.13244418	2.38957384	.456388	3.526735
Total	18	1.06359560	.766593845	.180687902	.68237745	1.44481375	.030151	3.526735

ANOVA

gene

	Sum of Squares	df	Mean Square	F	Sig.
Between Groups	.043	2	.022	.033	.968
Within Groups	9.947	15	.663		
Total	9.990	17			

Multiple Comparisons

Dependent Variable: gene

	(I) Group	(J) Group	Mean Difference (I-J)	Std. Error	Sig.	95% Confidence Interval
						Lower Bound
Tukey HSD	1	2	.042465276	.470151869	.996	-1.17874022
		3	-.076221223	.470151869	.986	-1.29742672
	2	1	-.042465276	.470151869	.996	-1.26367077
		3	-.118686499	.470151869	.966	-1.33989199
	3	1	.076221223	.470151869	.986	-1.14498427
		2	.118686499	.470151869	.966	-1.10251899
Dunnett T3	1	2	.042465276	.301531125	.998	-.85444329
		3	-.076221223	.511871981	.998	-1.72070383
	2	1	-.042465276	.301531125	.998	-.93937384
		3	-.118686499	.556950981	.995	-1.78237268
	3	1	.076221223	.511871981	.998	-1.56826138
		2	.118686499	.556950981	.995	-1.54499968

PCR 1 month Osx

Descriptives

gene

	N	Mean	Std. Deviation	Std. Error	95% Confidence Interval for Mean		Minimum	Maximum
					Lower Bound	Upper Bound		
1	6	1.02897023	.256934081	.104892899	.75933445	1.29860601	.790041	1.484524
2	6	1.07666410	.502381768	.205096498	.54944677	1.60388143	.501157	1.650992
3	6	.89123104	.332066252	.135565480	.54274888	1.23971320	.330640	1.159364
Total	18	.99895512	.364176525	.085837230	.81785440	1.18005585	.330640	1.650992

ANOVA

gene

	Sum of Squares	df	Mean Square	F	Sig.
Between Groups	.111	2	.056	.389	.684
Within Groups	2.143	15	.143		
Total	2.255	17			

Multiple Comparisons

Dependent Variable: gene

	(I) Group	(J) Group	Mean Difference (I-J)	Std. Error	Sig.	95% Confidence Interval
						Lower Bound
Tukey HSD	1	2	-.047693865	.218243131	.974	-.61457391
		3	.137739162	.218243131	.806	-.42914088
	2	1	.047693865	.218243131	.974	-.51918617
		3	.185433027	.218243131	.679	-.38144701
	3	1	-.137739162	.218243131	.806	-.70461920
		2	-.185433027	.218243131	.679	-.75231307
Dunnett T3	1	2	-.047693865	.230362961	.995	-.74062595
		3	.137739162	.171407476	.807	-.35259487
	2	1	.047693865	.230362961	.995	-.64523822
		3	.185433027	.245850719	.834	-.52930654
	3	1	-.137739162	.171407476	.807	-.62807320
		2	-.185433027	.245850719	.834	-.90017260

PCR 1 month ALP

Descriptives

gene

	N	Mean	Std. Deviation	Std. Error	95% Confidence Interval for Mean		Minimum	Maximum
					Lower Bound	Upper Bound		
1	6	1.20565581	.880840934	.359601806	.28126994	2.13004168	.469761	2.887858
2	6	.73716333	.333330774	.136081719	.38735414	1.08697252	.282241	1.193336
3	6	.82069377	.206173905	.084170144	.60432753	1.03706002	.526681	1.113422
Total	18	.92117097	.563435147	.132802938	.64098126	1.20136068	.282241	2.887858

ANOVA

gene

	Sum of Squares	df	Mean Square	F	Sig.
Between Groups	.749	2	.375	1.209	.326
Within Groups	4.647	15	.310		
Total	5.397	17			

Multiple Comparisons

Dependent Variable: gene

	(I) Group	(J) Group	Mean Difference (I-J)	Std. Error	Sig.	95% Confidence Interval
						Lower Bound
Tukey HSD	1	2	.468492482	.321368187	.338	-.36625182
		3	.384960464	.321368187	.472	-.44978384
	2	1	-.468492482	.321368187	.338	-1.30323679
		3	-.083532018	.321368187	.964	-.91827632
	3	1	-.384960464	.321368187	.472	-1.21970477
		2	.083532018	.321368187	.964	-.75121229
Dunnett T3	1	2	.468492482	.384488872	.567	-.73538242
		3	.384960464	.369321044	.673	-.82456072
	2	1	-.468492482	.384488872	.567	-1.67236739
		3	-.083532018	.160008778	.934	-.55255164
	3	1	-.384960464	.369321044	.673	-1.59448165
		2	.083532018	.160008778	.934	-.38548760

PCR 1 month OCN

Descriptives

gene

	N	Mean	Std. Deviation	Std. Error	95% Confidence Interval for Mean		Minimum	Maximum
					Lower Bound	Upper Bound		
1	6	1.14084729	.582148643	.237661189	.52991976	1.75177483	.435275	1.765406
2	6	.77747078	.660535926	.269662663	.08428084	1.47066072	.370702	2.068139
3	6	1.27621407	1.864172872	.761045388	-.68011538	3.23254352	.107942	5.022248
Total	18	1.06484405	1.138883594	.268437437	.49849056	1.63119753	.107942	5.022248

ANOVA

gene

	Sum of Squares	df	Mean Square	F	Sig.
Between Groups	.798	2	.399	.282	.758
Within Groups	21.252	15	1.417		
Total	22.050	17			

Multiple Comparisons

Dependent Variable: gene

(I) Group	(J) Group	Mean Difference (I-J)	Std. Error	Sig.	95% Confidence Interval		
					Lower Bound	Upper Bound	
Tukey HSD	1	2	.363376509	.687212179	.859	-1.42163668	
		3	-.135366791	.687212179	.979	-1.92037998	
	2	1	-.363376509	.687212179	.859	-2.14838970	
		3	-.498743300	.687212179	.752	-2.28375649	
	3	1	.135366791	.687212179	.979	-1.64964640	
		2	.498743300	.687212179	.752	-1.28626989	
Dunnett T3	1	2	.363376509	.359445117	.684	-.65628648	
		3	-.135366791	.797290986	.997	-2.68528737	
	2	1	-.363376509	.359445117	.684	-1.38303950	
		3	-.498743300	.807408217	.897	-3.04646994	
	3	1	.135366791	.797290986	.997	-2.41455379	
		2	.498743300	.807408217	.897	-2.04898334	

PCR 1 month OPN

Descriptives

gene

	N	Mean	Std. Deviation	Std. Error	95% Confidence Interval for Mean		Minimum	Maximum
					Lower Bound	Upper Bound		
1	6	1.50699491	1.387419118	.566411483	.05098784	2.96300198	.197510	3.972370
2	6	.95234480	.658898279	.268994096	.26087347	1.64381614	.165702	1.823445
3	6	1.36037563	2.355837776	.961766745	-1.11192450	3.83267575	.030116	6.090947
Total	18	1.27323845	1.544182596	.363967328	.50533451	2.04114239	.030116	6.090947

ANOVA

gene

	Sum of Squares	df	Mean Square	F	Sig.
Between Groups	.923	2	.462	.170	.845
Within Groups	40.800	15	2.720		
Total	41.723	17			

Multiple Comparisons

Dependent Variable: gene

	(I) Group	(J) Group	Mean Difference (I-J)	Std. Error	Sig.	95% Confidence Interval
						Lower Bound
Tukey HSD	1	2	.554650107	.952188363	.831	-1.91863084
		3	.265421231	.952188363	.958	-2.20785972
	2	1	-.554650107	.952188363	.831	-3.02793105
		3	-.289228876	.952188363	.951	-2.76250982
	3	1	-.265421231	.952188363	.958	-2.73870218
		2	.289228876	.952188363	.951	-2.18405207
Dunnett T3	1	2	.554650107	.627040503	.763	-1.35105906
		3	.265421231	1.134740584	.993	-3.09217552
	2	1	-.554650107	.627040503	.763	-2.46035927
		3	-.289228876	1.019397886	.988	-3.58908884
	3	1	-.265421231	1.134740584	.993	-3.62301798
		2	.289228876	1.019397886	.988	-3.01063109

PCR 3 month Runx2

Descriptives

gene

	N	Mean	Std. Deviation	Std. Error	95% Confidence Interval for Mean		Minimum	Maximum
					Lower Bound	Upper Bound		
1	6	1.15159345	.708049015	.289059800	.40854158	1.89464532	.574349	2.394957
2	6	6.14835998	2.211133178	.902691340	3.82791802	8.46880194	2.642066	9.524654
3	6	1.85818642	.973276477	.397338458	.83679539	2.87957744	.924450	3.723519
Total	18	3.05271328	2.650567412	.624744730	1.73461712	4.37080945	.574349	9.524654

ANOVA

gene

	Sum of Squares	df	Mean Square	F	Sig.
Between Groups	87.745	2	43.873	20.767	.000
Within Groups	31.689	15	2.113		
Total	119.434	17			

Multiple Comparisons

Dependent Variable: gene

	(I) Group	(J) Group	Mean Difference (I-J)	Std. Error	Sig.	95% Confidence Interval
						Lower Bound
Tukey HSD	1	2	-4.731542183 [*]	1.230328902	.004	-7.92728491
		3	-5.952045201 [*]	1.230328902	.001	-9.14778793
	2	1	4.731542183 [*]	1.230328902	.004	1.53579946
		3	-1.220503019	1.230328902	.593	-4.41624574
	3	1	5.952045201 [*]	1.230328902	.001	2.75630248
		2	1.220503019	1.230328902	.593	-1.97523971
Dunnett T3	1	2	-4.731542183 [*]	.715252397	.001	-6.91644511
		3	-5.952045201 [*]	1.359255429	.015	-10.41560851
	2	1	4.731542183 [*]	.715252397	.001	2.54663925
		3	-1.220503019	1.477148032	.795	-5.68991758
	3	1	5.952045201 [*]	1.359255429	.015	1.48848189
		2	1.220503019	1.477148032	.795	-3.24891154

PCR 3 month O₂

Descriptives

gene

	N	Mean	Std. Deviation	Std. Error	95% Confidence Interval for Mean		Minimum	Maximum
					Lower Bound	Upper Bound		
1	6	1.19012845	.729098768	.297653326	.42498622	1.95527068	.360982	2.250117
2	6	5.92167063	1.593088489	.650375652	4.24982679	7.59351447	3.020945	7.135428
3	6	7.14217365	3.248671561	1.326264611	3.73290193	10.55144537	3.617518	10.966262
Total	18	4.75132424	3.314183748	.781160601	3.10321944	6.39942905	.360982	10.966262

ANOVA

gene

	Sum of Squares	df	Mean Square	F	Sig.
Between Groups	118.608	2	59.304	13.059	.001
Within Groups	68.117	15	4.541		
Total	186.725	17			

Multiple Comparisons

Dependent Variable: gene

(I) Group	(J) Group	Mean Difference (I-J)	Std. Error	Sig.	95% Confidence Interval	
					Lower Bound	
Tukey HSD	1	2	-4.731542183 [*]	1.230328902	.004	-7.92728491
		3	-5.952045201 [*]	1.230328902	.001	-9.14778793
	2	1	4.731542183 [*]	1.230328902	.004	1.53579946
		3	-1.220503019	1.230328902	.593	-4.41624574
	3	1	5.952045201 [*]	1.230328902	.001	2.75630248
		2	1.220503019	1.230328902	.593	-1.97523971
Dunnett T3	1	2	-4.731542183 [*]	.715252397	.001	-6.91644511
		3	-5.952045201 [*]	1.359255429	.015	-10.41560851
	2	1	4.731542183 [*]	.715252397	.001	2.54663925
		3	-1.220503019	1.477148032	.795	-5.68991758
	3	1	5.952045201 [*]	1.359255429	.015	1.48848189
		2	1.220503019	1.477148032	.795	-3.24891154

PCR 3 month ALP

Descriptives

gene

	N	Mean	Std. Deviation	Std. Error	95% Confidence Interval for Mean		Minimum	Maximum
					Lower Bound	Upper Bound		
1	6	1.09822499	.507573678	.207216087	.56555908	1.63089089	.566442	1.765406
2	6	2.75038457	.550352636	.224680523	2.17282490	3.32794424	1.876876	3.478182
3	6	2.10152927	.643347818	.262645647	1.42637714	2.77668139	1.255562	2.924791
Total	18	1.98337961	.880728488	.207589695	1.54540363	2.42135558	.566442	3.478182

ANOVA

gene

	Sum of Squares	df	Mean Square	F	Sig.
Between Groups	8.315	2	4.157	12.799	.001
Within Groups	4.872	15	.325		
Total	13.187	17			

Multiple Comparisons

Dependent Variable: gene

	(I) Group	(J) Group	Mean Difference (I-J)	Std. Error	Sig.	95% Confidence Interval
						Lower Bound
Tukey HSD	1	2	-1.652159587 [*]	.329041618	.000	-2.50683540
		3	-1.003304279 [*]	.329041618	.021	-1.85798009
	2	1	1.652159587 [*]	.329041618	.000	.79748377
		3	.648855308	.329041618	.153	-.20582051
	3	1	1.003304279 [*]	.329041618	.021	.14862846
		2	-.648855308	.329041618	.153	-1.50353112
Dunnett T3	1	2	-1.652159587 [*]	.305646600	.001	-2.51778711
		3	-1.003304279 [*]	.334546323	.040	-1.95881239
	2	1	1.652159587 [*]	.305646600	.001	.78653207
		3	.648855308	.345635752	.233	-.33305776
	3	1	1.003304279 [*]	.334546323	.040	.04779617
		2	-.648855308	.345635752	.233	-1.63076837

PCR 3 month OCN

Descriptives

gene

	N	Mean	Std. Deviation	Std. Error	95% Confidence Interval for Mean		Minimum	Maximum
					Lower Bound	Upper Bound		
1	6	1.09960411	.455866259	.186106621	.62120181	1.57800641	.366021	1.790050
2	6	1.48839290	.720324281	.294071156	.73245893	2.24432687	.743979	2.502436
3	6	1.03725433	.857377877	.350023053	.13749143	1.93701723	.135216	2.434007
Total	18	1.20841711	.687109468	.161953255	.86672561	1.55010861	.135216	2.502436

ANOVA

gene

	Sum of Squares	df	Mean Square	F	Sig.
Between Groups	.714	2	.357	.733	.497
Within Groups	7.302	15	.487		
Total	8.016	17			

Multiple Comparisons

Dependent Variable: gene

	(I) Group	(J) Group	Mean Difference (I-J)	Std. Error	Sig.	95% Confidence Interval
						Lower Bound
Tukey HSD	1	2	-.388788791	.402815154	.609	-1.43508917
		3	.060849779	.402815154	.988	-.98545060
	2	1	.388788791	.402815154	.609	-.65751159
		3	.449638569	.402815154	.519	-.59666181
	3	1	-.060849779	.402815154	.988	-1.10715016
		2	-.449638569	.402815154	.519	-1.49593895
Dunnett T3	1	2	-.388788791	.348013677	.621	-1.40592690
		3	.060849779	.396121481	.998	-1.12407699
	2	1	.388788791	.348013677	.621	-.62834932
		3	.449638569	.456896485	.701	-.84960194
	3	1	-.060849779	.396121481	.998	-1.24577655
		2	-.449638569	.456896485	.701	-1.74887908

PCR 3 month OPN

Descriptives

gene

	N	Mean	Std. Deviation	Std. Error	95% Confidence Interval for Mean		Minimum	Maximum
					Lower Bound	Upper Bound		
1	6	1.46709220	1.247223428	.509176832	.15821148	2.77597291	.291183	3.160165
2	6	4.46809429	3.121935807	1.274524956	1.19182359	7.74436499	1.927414	10.243712
3	6	9.66674382	4.631998646	1.891005529	4.80575936	14.52772828	3.286761	15.852810
Total	18	5.20064344	4.667281732	1.100088854	2.87965883	7.52162804	.291183	15.852810

ANOVA

gene

	Sum of Squares	df	Mean Square	F	Sig.
Between Groups	206.533	2	103.266	9.457	.002
Within Groups	163.787	15	10.919		
Total	370.320	17			

Multiple Comparisons

Dependent Variable: gene

	(I) Group	(J) Group	Mean Difference (I-J)	Std. Error	Sig.	95% Confidence Interval
						Lower Bound
Tukey HSD	1	2	-3.001002091	1.907804466	.287	-7.95646744
		3	-8.199651621 [*]	1.907804466	.002	-13.15511697
	2	1	3.001002091	1.907804466	.287	-1.95446326
		3	-5.198649530 [*]	1.907804466	.039	-10.15411488
	3	1	8.199651621 [*]	1.907804466	.002	3.24418627
		2	5.198649530 [*]	1.907804466	.039	.24318418
Dunnett T3	1	2	-3.001002091	1.372470368	.172	-7.26955915
		3	-8.199651621 [*]	1.958357208	.017	-14.54729339
	2	1	3.001002091	1.372470368	.172	-1.26755497
		3	-5.198649530	2.280420087	.131	-11.81320273
	3	1	8.199651621 [*]	1.958357208	.017	1.85200985
		2	5.198649530	2.280420087	.131	-1.41590367

Independent T-test of the gene expression between 1 and 3 month

Control

Group Statistics

	Month	N	Mean	Std. Deviation	Std. Error Mean
Runx2	1	6	1.05234362	.358076313	.146184043
	3	6	.22097649	.135865821	.055466989
Osx	1	6	1.02897023	.256934081	.104892899
	3	6	.29811074	.182766693	.074614190
ALP	1	6	1.20565581	.880840934	.359601806
	3	6	.55871081	.258222955	.105419080
OCN	1	6	1.14084729	.582148643	.237661189
	3	6	.67610421	.280294603	.114429792
OPN	1	6	1.50699491	1.387419118	.566411483
	3	6	1.86558256	1.585993216	.647479019

Independent Samples Test

Runx2	Levene's Test for Equality of Variances		t-test for Equality of Means						
								95% Confidence Interval of the Difference	
	F	Sig.	t	df	Sig. (2-tailed)	Mean Difference	Std. Error Difference	Lower	Upper
Equal variances assumed	5.905	.035	5.317	10	.000	.831367127	.156353322	.482990216	1.179744038
Equal variances not assumed			5.317	6.410	.001	.831367127	.156353322	.454644611	1.208089644

Independent Samples Test

Osx	Levene's Test for Equality of Variances		t-test for Equality of Means						
								95% Confidence Interval of the Difference	
	F	Sig.	t	df	Sig. (2-tailed)	Mean Difference	Std. Error Difference	Lower	Upper
Equal variances assumed	.248	.629	5.678	10	.000	.730859488	.128723726	.444045153	1.017673823
Equal variances not assumed			5.678	9.029	.000	.730859488	.128723726	.439806482	1.021912494

Independent Samples Test

ALP	Levene's Test for Equality of Variances		t-test for Equality of Means						
								95% Confidence Interval of the Difference	
	F	Sig.	t	df	Sig. (2-tailed)	Mean Difference	Std. Error Difference	Lower	Upper
Equal variances assumed	2.453	.148	1.726	10	.115	.646945002	.374735428	-.188017565	1.481907568
Equal variances not assumed			1.726	5.853	.136	.646945002	.374735428	-.275607117	1.569497120

Independent Samples Test

OCN	Levene's Test for Equality of Variances		t-test for Equality of Means						
								95% Confidence Interval of the Difference	
	F	Sig.	t	df	Sig. (2-tailed)	Mean Difference	Std. Error Difference	Lower	Upper
Equal variances assumed	12.467	.005	1.762	10	.109	.464743081	.263774559	-.122983262	1.052469424
Equal variances not assumed			1.762	7.200	.120	.464743081	.263774559	-.155489157	1.084975319

Independent Samples Test

OPN	Levene's Test for Equality of Variances		t-test for Equality of Means						
								95% Confidence Interval of the Difference	
	F	Sig.	t	df	Sig. (2-tailed)	Mean Difference	Std. Error Difference	Lower	Upper
Equal variances assumed	.398	.542	-.417	10	.686	-.358587647	.860262198	-2.275371273	1.558195978
Equal variances not assumed			-.417	9.826	.686	-.358587647	.860262198	-2.279975288	1.562799993

Bio-Oss

Group Statistics

	Month	N	Mean	Std. Deviation	Std. Error Mean
Runx2	1	6	1.63110333	1.043375158	.425956125
	3	6	1.90554230	.685289707	.279768351
Osx	1	6	1.10437864	.515313638	.210375912
	3	6	1.53085494	.411841106	.168133428
ALP	1	6	1.11346500	.503486996	.205547706
	3	6	2.11105870	.422423369	.172453618
OCN	1	6	1.24705678	1.059494384	.432536771
	3	6	1.46113426	.707132158	.288685495
OPN	1	6	1.40726033	.973640439	.397487045
	3	6	8.40545722	5.873040307	2.397658665

Independent Samples Test

Runx2	Levene's Test for Equality of Variances		t-test for Equality of Means						
								95% Confidence Interval of the Difference	
	F	Sig.	t	df	Sig. (2-tailed)	Mean Difference	Std. Error Difference	Lower	Upper
Equal variances assumed	.996	.342	-.539	10	.602	-.274438974	.509616474	-1.409935239	.861057291
Equal variances not assumed			-.539	8.637	.604	-.274438974	.509616474	-1.434698921	.885820973

Independent Samples Test

Osx	Levene's Test for Equality of Variances		t-test for Equality of Means						
								95% Confidence Interval of the Difference	
	F	Sig.	t	df	Sig. (2-tailed)	Mean Difference	Std. Error Difference	Lower	Upper
Equal variances assumed	1.764	.214	-1.584	10	.144	-.426476300	.269308139	-1.026532228	.173579627
Equal variances not assumed			-1.584	9.537	.146	-.426476300	.269308139	-1.030508947	.177556347

Independent Samples Test

ALP	Levene's Test for Equality of Variances		t-test for Equality of Means						
								95% Confidence Interval of the Difference	
	F	Sig.	t	df	Sig. (2-tailed)	Mean Difference	Std. Error Difference	Lower	Upper
Equal variances assumed	.333	.576	-3.718	10	.004	-.997593694	.268309727	-1.595425022	-.399762366
Equal variances not assumed			-3.718	9.707	.004	-.997593694	.268309727	-1.597880974	-.397306414

Independent Samples Test

OCN	Levene's Test for Equality of Variances		t-test for Equality of Means						
								95% Confidence Interval of the Difference	
	F	Sig.	t	df	Sig. (2-tailed)	Mean Difference	Std. Error Difference	Lower	Upper
Equal variances assumed	.251	.627	-.412	10	.689	-.214077477	.520026320	-1.372768324	.944613370
Equal variances not assumed			-.412	8.717	.691	-.214077477	.520026320	-1.396306577	.968151623

Independent Samples Test

OPN	Levene's Test for Equality of Variances		t-test for Equality of Means						
								95% Confidence Interval of the Difference	
	F	Sig.	t	df	Sig. (2-tailed)	Mean Difference	Std. Error Difference	Lower	Upper
Equal variances assumed	7.545	.021	-2.879	10	.016	-6.998196891	2.430383308	-1.241342837E1	-1.582965417
Equal variances not assumed			-2.879	5.275	.033	-6.998196891	2.430383308	-1.314911539E1	-.847278388

DFDBA

Group Statistics

	Month	N	Mean	Std. Deviation	Std. Error Mean
Runx2	1	6	1.38142380	1.470831061	.600464266
	3	6	2.50920193	1.314263838	.536545965
Osx	1	6	1.08714027	.405060638	.165365313
	3	6	2.19065639	.996436584	.406793532
ALP	1	6	1.01884433	.243112779	.099250376
	3	6	1.34081130	.410466815	.167572376
OCN	1	5	.79971696	.555679622	.248507482
	3	6	1.64663541	1.357787553	.554314447
OPN	1	5	1.16749313	1.903235149	.851152634
	3	6	1.06918178E2	5.123181736E1	2.091530186E1

Independent Samples Test

Runx2	Levene's Test for Equality of Variances		t-test for Equality of Means						
								95% Confidence Interval of the Difference	
	F	Sig.	t	df	Sig. (2-tailed)	Mean Difference	Std. Error Difference	Lower	Upper
Equal variances assumed	.043	.840	-1.401	10	.192	-1.127778130	.805257044	-2.922002636	.666446377
Equal variances not assumed			-1.401	9.876	.192	-1.127778130	.805257044	-2.925062343	.669506084

Independent Samples Test

Osx	Levene's Test for Equality of Variances		t-test for Equality of Means						
								95% Confidence Interval of the Difference	
	F	Sig.	t	df	Sig. (2-tailed)	Mean Difference	Std. Error Difference	Lower	Upper
Equal variances assumed	10.330	.009	-2.513	10	.031	-1.103516118	.439120330	-2.081937186	-.125095050
Equal variances not assumed			-2.513	6.609	.042	-1.103516118	.439120330	-2.154469370	-.052562866

Independent Samples Test

ALP	Levene's Test for Equality of Variances		t-test for Equality of Means						
								95% Confidence Interval of the Difference	
	F	Sig.	t	df	Sig. (2-tailed)	Mean Difference	Std. Error Difference	Lower	Upper
Equal variances assumed	3.166	.106	-1.653	10	.129	-.321966974	.194759180	-7.755917470	.111983522
Equal variances not assumed			-1.653	8.124	.136	-.321966974	.194759180	-7.769895744	.125961797

Independent Samples Test

OCN	Levene's Test for Equality of Variances		t-test for Equality of Means						
								95% Confidence Interval of the Difference	
	F	Sig.	t	df	Sig. (2-tailed)	Mean Difference	Std. Error Difference	Lower	Upper
Equal variances assumed	3.667	.088	-1.298	9	.227	-.846918449	.652583470	-2.323164821	.629327923
Equal variances not assumed			-1.394	6.865	.207	-.846918449	.607470555	-2.289096059	.595259161

Independent Samples Test

OPN	Levene's Test for Equality of Variances		t-test for Equality of Means						
								95% Confidence Interval of the Difference	
	F	Sig.	t	df	Sig. (2-tailed)	Mean Difference	Std. Error Difference	Lower	Upper
Equal variances assumed	8.342	.018	-4.571	9	.001	-1.057506845E2	2.313549721E1	-1.580868152E2	-5.341455375E1
Equal variances not assumed			-5.052	5.017	.004	-1.057506845E2	2.093261361E1	-1.595063064E2	-5.199506252E1

SCANCO MEDICAL

Control_Month 1_Mouse 1



VOI	x	y	z	Mean/Density [mg HA/ccm]
Position [p]	360	500	15	of TV (Apparent) - 6.6958
Dimension [p]	164	160	100	of BV (Material) 658.4879
Element size [mm]	0.0200	0.0200	0.0200	

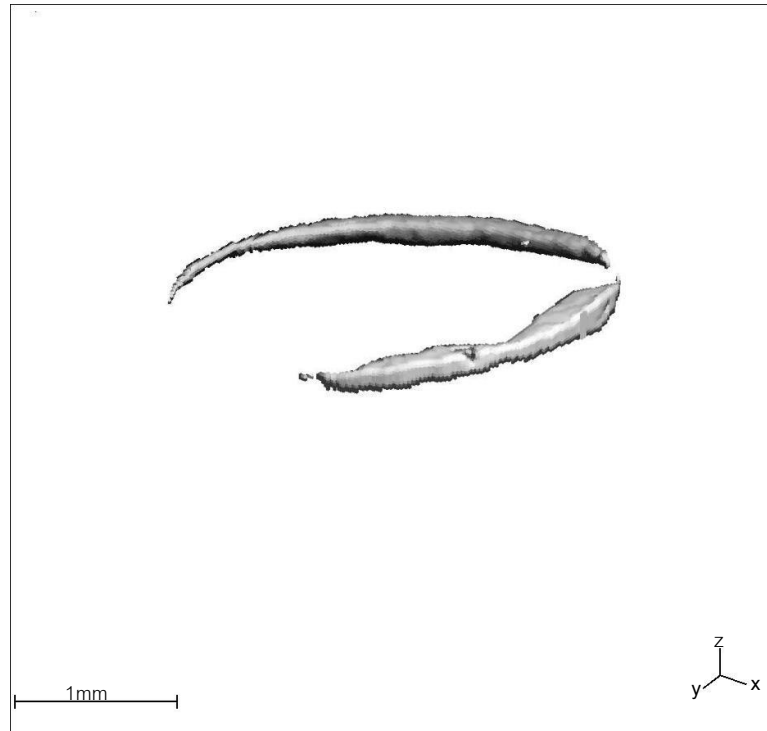
Direct (No model)		TRI(Plate model)		Anisotropy	
TV [mm ³]	15.7536	TV [mm ³]	-	H1 [mm]	-
BV [mm ³]	0.2149	BV [mm ³]	-	H2 [mm]	-
BV/TV [1]	0.0136	BV/TV [1]	-	H3 [mm]	-
Conn.D. [1/mm ³]	-	BS [mm ²]	-	DA [1]	
SMI [1]	-	BS/TV [1/mm]	-		
Tb.N* [1/mm]	-	Tb.N [1/mm]	-	Segmentation	: 0.8 / 1 / 220
Tb.Th* [mm]	-	Tb.Th [mm]	-		
Tb.Sp* [1/mm]	-	Tb.Sp [1/mm]	-		

μCT 35

SCANCO MEDICAL

SCANCO MEDICAL

Control_Month1_Mouse 2



VOI	x	y	z	Mean/Density [mg HA/ccm]
Position [p]	362	512	10	of TV (Apparent) - 11.6720
Dimension [p]	164	160	105	of BV (Material) 646.9069
Element size [mm]	0.0200	0.0200	0.0200	

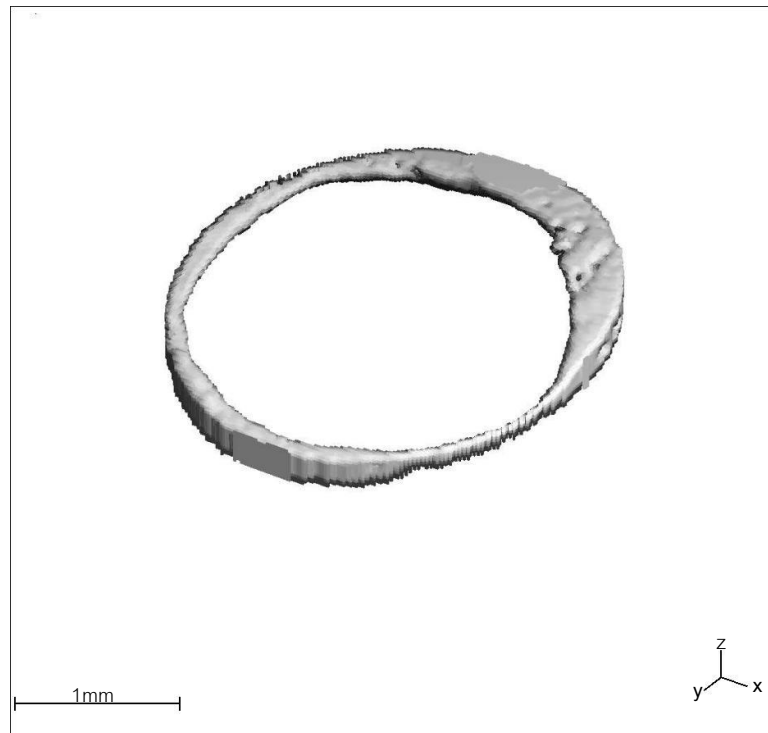
Direct (No model)		TRI(Plate model)		Anisotropy	
TV [mm ³]	16.5413	TV [mm ³]	-	H1 [mm]	-
BV [mm ³]	0.1530	BV [mm ³]	-	H2 [mm]	-
BV/TV [1]	0.0092	BV/TV [1]	-	H3 [mm]	-
Conn.D. [1/mm ³]	-	BS [mm ²]	-	DA [1]	
SMI [1]	-	BS/TV [1/mm]	-		
Tb.N* [1/mm]	-	Tb.N [1/mm]	-	Segmentation : 0.8 / 1 / 220	
Tb.Th* [mm]	-	Tb.Th [mm]	-		
Tb.Sp* [1/mm]	-	Tb.Sp [1/mm]	-		

μCT 35

SCANCO MEDICAL

SCANCO MEDICAL

Control_Month1_Mouse 5 (left)



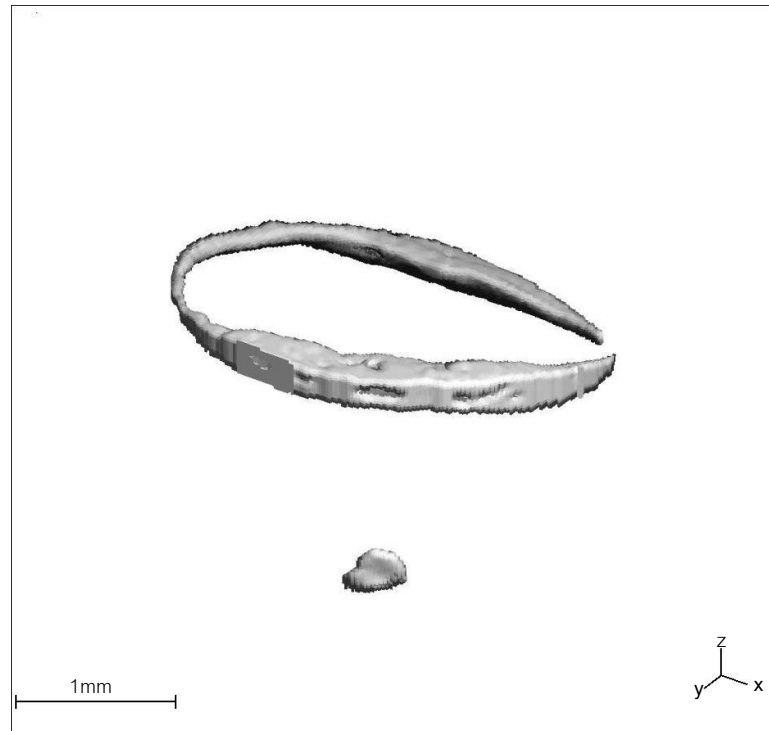
VOI	x	y	z	Mean/Density [mg HA/ccm]
Position [p]	362	512	10	of TV (Apparent) 0.9947
Dimension [p]	164	160	105	of BV (Material) 633.9688
Element size [mm]	0.0200	0.0200	0.0200	

Direct (No model)		TRI(Plate model)		Anisotropy	
TV [mm ³]	15.2810	TV [mm ³]	-	H1 [mm]	-
BV [mm ³]	0.3079	BV [mm ³]	-	H2 [mm]	-
BV/TV [1]	0.0201	BV/TV [1]	-	H3 [mm]	-
Conn.D. [1/mm ³]	-	BS [mm ²]	-	DA [1]	
SMI [1]	-	BS/TV [1/mm]	-		
Tb.N* [1/mm]	-	Tb.N [1/mm]	-	Segmentation : 0.8 / 1 / 220	
Tb.Th* [mm]	-	Tb.Th [mm]	-		
Tb.Sp* [1/mm]	-	Tb.Sp [1/mm]	-		

μCT 35
SCANCO MEDICAL

SCANCO MEDICAL

Control_Month1_Mouse 5 (right)



VOI	x	y	z	Mean/Density [mg HA/ccm]
Position [p]	450	218	2	of TV (Apparent) -21.8958
Dimension [p]	164	160	114	of BV (Material) 655.7736
Element size [mm]	0.0200	0.0200	0.0200	

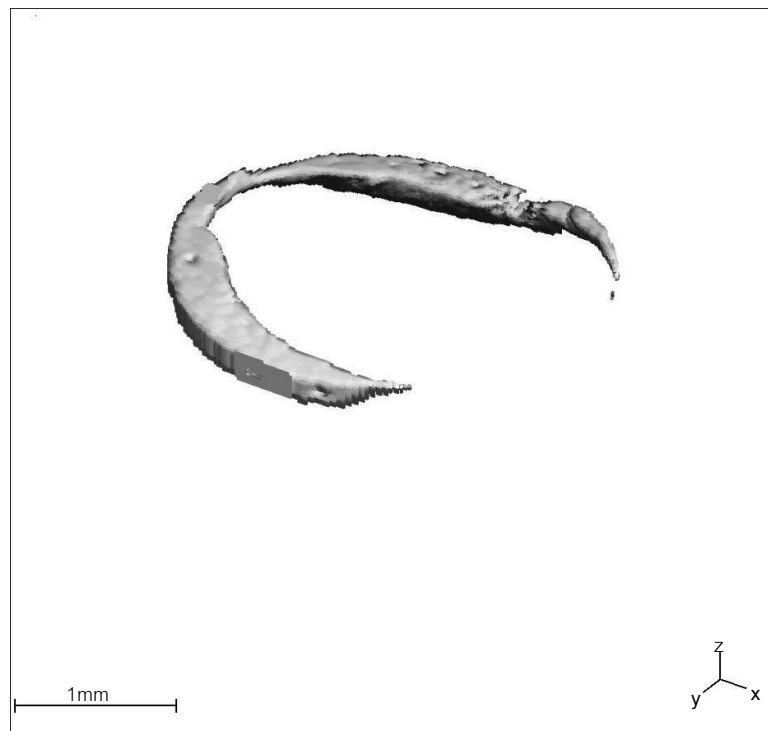
Direct (No model)		TRI(Plate model)		Anisotropy	
TV [mm ³]	17.5951	TV [mm ³]	-	H1 [mm]	-
BV [mm ³]	0.3548	BV [mm ³]	-	H2 [mm]	-
BV/TV [1]	0.0198	BV/TV [1]	-	H3 [mm]	-
Conn.D. [1/mm ³]	-	BS [mm ²]	-	DA [1]	
SMI [1]	-	BS/TV [1/mm]	-		
Tb.N* [1/mm]	-	Tb.N [1/mm]	-	Segmentation : 0.8 / 1 / 220	
Tb.Th* [mm]	-	Tb.Th [mm]	-		
Tb.Sp* [1/mm]	-	Tb.Sp [1/mm]	-		

μCT 35

SCANCO MEDICAL

SCANCO MEDICAL

Control_Month1_Mouse 6



VOI	x	y	z	Mean/Density [mg HA/ccm]
Position [p]	416	512	6	of TV (Apparent) 10.1329
Dimension [p]	164	160	109	of BV (Material) 655.8641
Element size [mm]	0.0200	0.0200	0.0200	

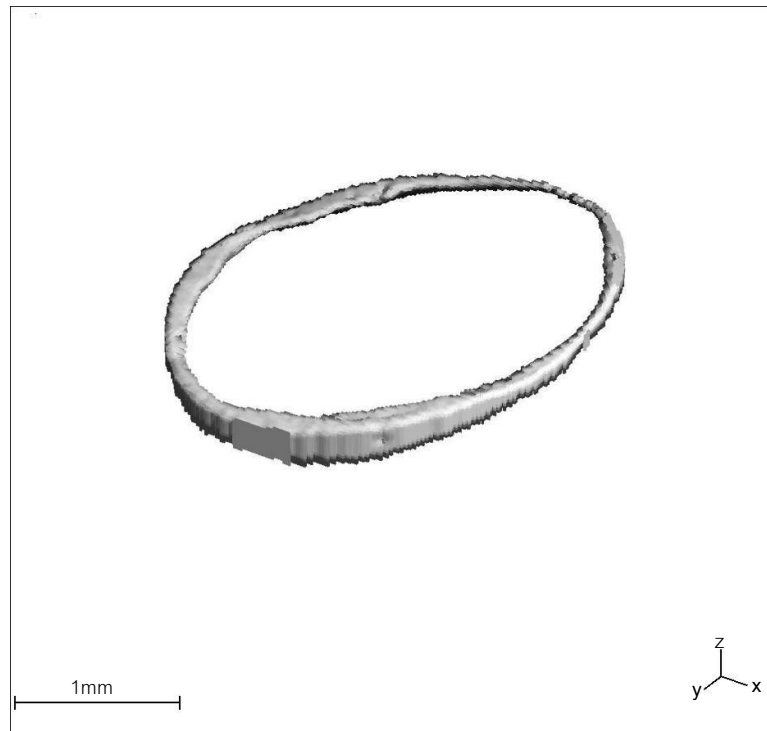
Direct (No model)		TRI(Plate model)		Anisotropy	
TV [mm ³]	17.1714	TV [mm ³]	-	H1 [mm]	-
BV [mm ³]	0.2854	BV [mm ³]	-	H2 [mm]	-
BV/TV [1]	0.0166	BV/TV [1]	-	H3 [mm]	-
Conn.D. [1/mm ³]	-	BS [mm ²]	-	DA [1]	
SMI [1]	-	BS/TV [1/mm]	-		
Tb.N* [1/mm]	-	Tb.N [1/mm]	-	Segmentation : 0.8 / 1 / 220	
Tb.Th* [mm]	-	Tb.Th [mm]	-		
Tb.Sp* [1/mm]	-	Tb.Sp [1/mm]	-		

μCT 35

SCANCO MEDICAL

SCANCO MEDICAL

Control_Month1_Mouse 7



VOI	x	y	z	Mean/Density [mg HA/ccm]
Position [p]	382	624	20	of TV (Apparent) - 16.1958
Dimension [p]	164	160	96	of BV (Material) 641.6593
Element size [mm]	0.0200	0.0200	0.0200	

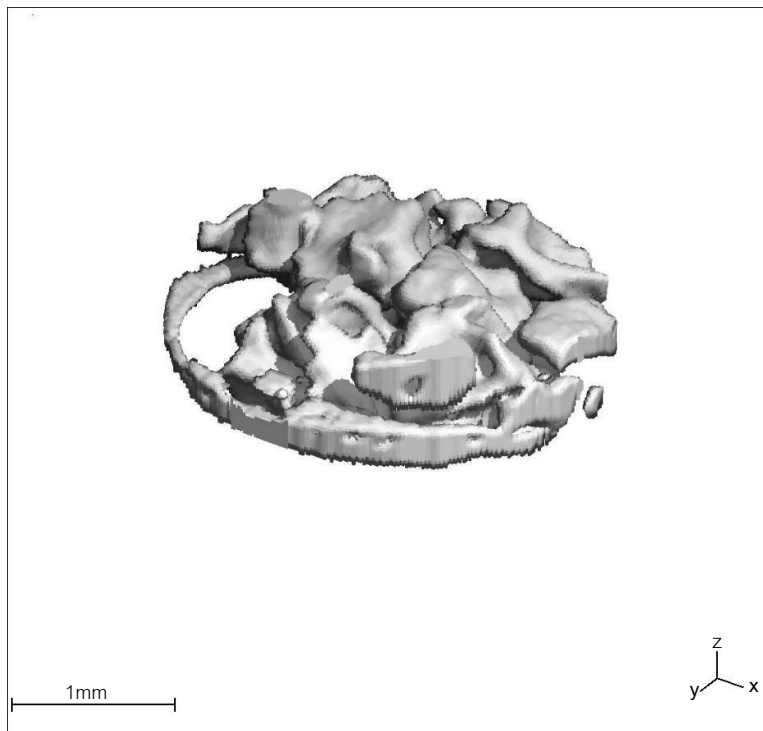
Direct (No model)		TRI(Plate mdel)		Anisotropy	
TV [mm ³]	15.1234	TV [mm ³]	-	H1 [mm]	-
BV [mm ³]	0.1695	BV [mm ³]	-	H2 [mm]	-
BV/TV [1]	0.0112	BV/TV [1]	-	H3 [mm]	-
Conn.D. [1/mm ³]	-	BS [mm ²]	-	DA [1]	
SMI [1]	-	BS/TV [1/mm]	-		
Tb.N* [1/mm]	-	Tb.N [1/mm]	-	Segmentation : 0.8 / 1 / 220	
Tb.Th* [mm]	-	Tb.Th [mm]	-		
Tb.Sp* [1/mm]	-	Tb.Sp [1/mm]	-		

μCT 35

SCANCO MEDICAL

SCANCO MEDICAL

Bio-Oss_Month1_Mouse 1



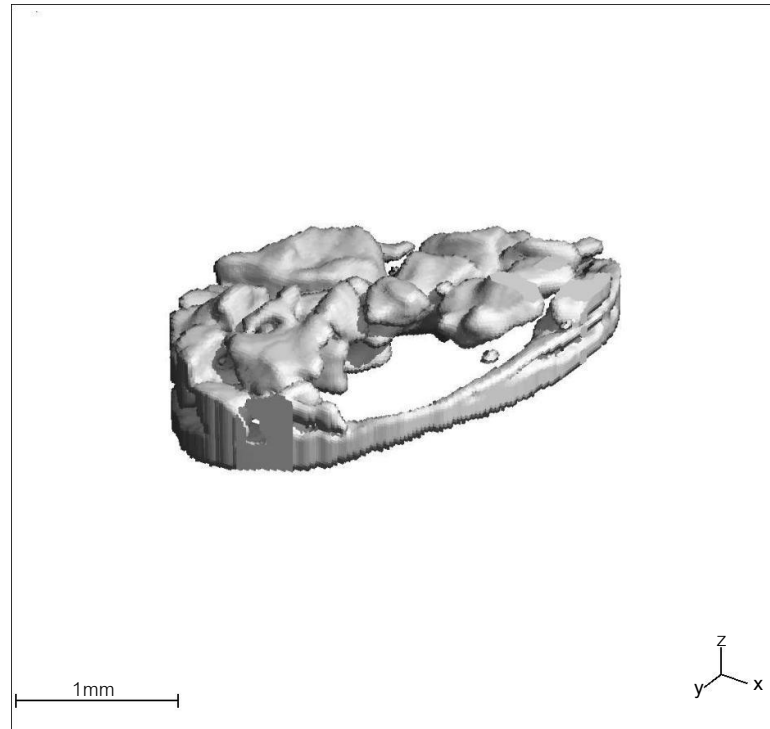
VOI	x	y	z	Mean/Density [mg HA/ccm]
Position [p]	452	360	13	of TV (Apparent) 180.4098
Dimension [p]	164	160	103	of BV (Material) 1119.3755
Element size [mm]	0.0200	0.0200	0.0200	

Direct (No model)		TRI(Plate model)		Anisotropy	
TV [mm ³]	16.2262	TV [mm ³]	-	H1 [mm]	-
BV [mm ³]	2.6309	BV [mm ³]	-	H2 [mm]	-
BV/TV [1]	0.1626	BV/TV [1]	-	H3 [mm]	-
Conn.D. [1/mm ³]	-	BS [mm ²]	-	DA [1]	
SMI [1]	-	BS/TV [1/mm]	-		
Tb.N* [1/mm]	-	Tb.N [1/mm]	-	Segmentation : 0.8 / 1 / 220	
Tb.Th* [mm]	-	Tb.Th [mm]	-		
Tb.Sp* [1/mm]	-	Tb.Sp [1/mm]	-		

μCT 35
SCANCO MEDICAL

SCANCO MEDICAL

Bio-Oss_Month1_Mouse 3



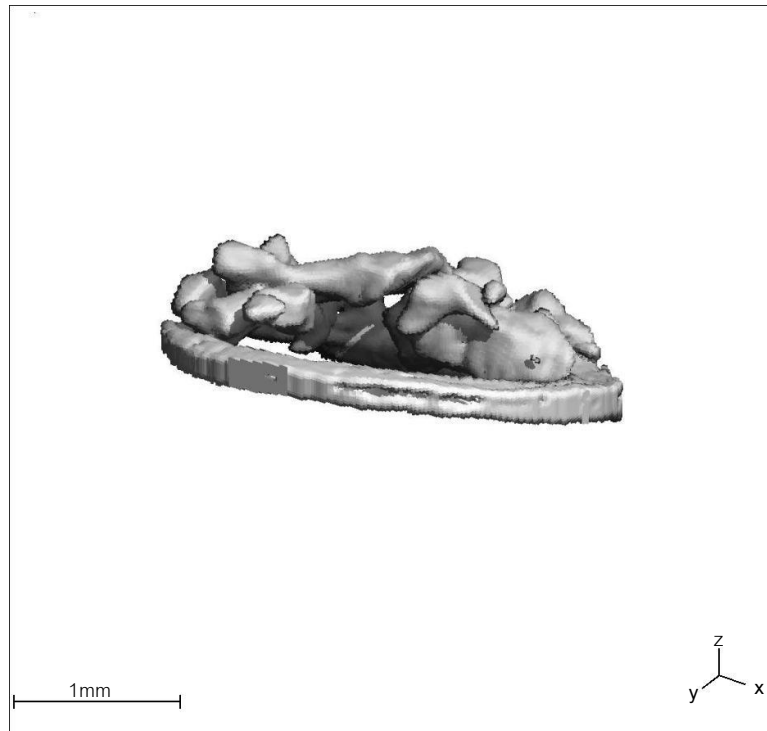
VOI	x	y	z	Mean/Density [mg HA/ccm]
Position [p]	378	502	8	of TV (Apparent) 90.6570
Dimension [p]	164	160	107	of BV (Material) 1077.7563
Element size [mm]	0.0200	0.0200	0.0200	

Direct (No model)		TRI(Plate mdel)		Anisotropy	
TV [mm ³]	16.8563	TV [mm ³]	-	H1 [mm]	-
BV [mm ³]	1.7870	BV [mm ³]	-	H2 [mm]	-
BV/TV [1]	0.1060	BV/TV [1]	-	H3 [mm]	-
Conn.D. [1/mm ³]	-	BS [mm ²]	-	DA [1]	
SMI [1]	-	BS/TV [1/mm]	-		
Tb.N* [1/mm]	-	Tb.N [1/mm]	-	Segmentation : 0.8 / 1 / 220	
Tb.Th* [mm]	-	Tb.Th [mm]	-		
Tb.Sp* [1/mm]	-	Tb.Sp [1/mm]	-		

μCT 35
SCANCO MEDICAL

SCANCO MEDICAL

Bio-oss_Month1_Mouse 6



VOI	x	y	z	Mean/Density [mg HA/ccm]
Position [p]	350	300	26	of TV (Apparent) 90.2951
Dimension [p]	164	160	89	of BV (Material) 998.6798
Element size [mm]	0.0200	0.0200	0.0200	

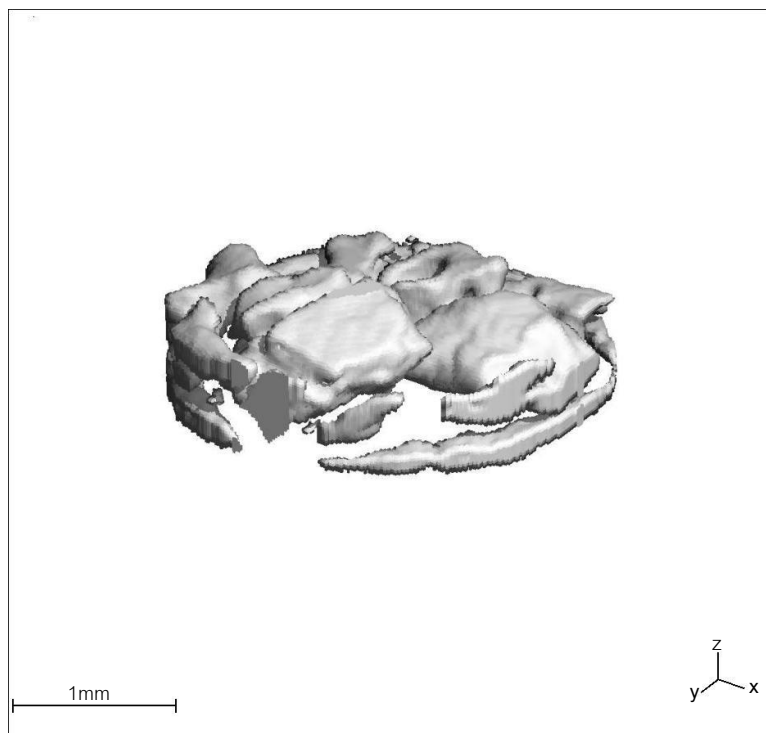
Direct (No model)		TRI(Plate model)		Anisotropy	
TV [mm ³]	14.0207	TV [mm ³]	-	H1 [mm]	-
BV [mm ³]	1.6534	BV [mm ³]	-	H2 [mm]	-
BV/TV [1]	0.1179	BV/TV [1]	-	H3 [mm]	-
Conn.D. [1/mm ³]	-	BS [mm ²]	-	DA [1]	
SMI [1]	-	BS/TV [1/mm]	-		
Tb.N* [1/mm]	-	Tb.N [1/mm]	-	Segmentation : 0.8 / 1 / 220	
Tb.Th* [mm]	-	Tb.Th [mm]	-		
Tb.Sp* [1/mm]	-	Tb.Sp [1/mm]	-		

μCT 35

SCANCO MEDICAL

SCANCO MEDICAL

Bio-oss_Month1_Mouse 8



VOI	x	y	z	Mean/Density [mg HA/ccm]
Position [p]	318	418	12	of TV (Apparent) 91.9237
Dimension [p]	164	160	104	of BV (Material) 1079.3849
Element size [mm]	0.0200	0.0200	0.0200	

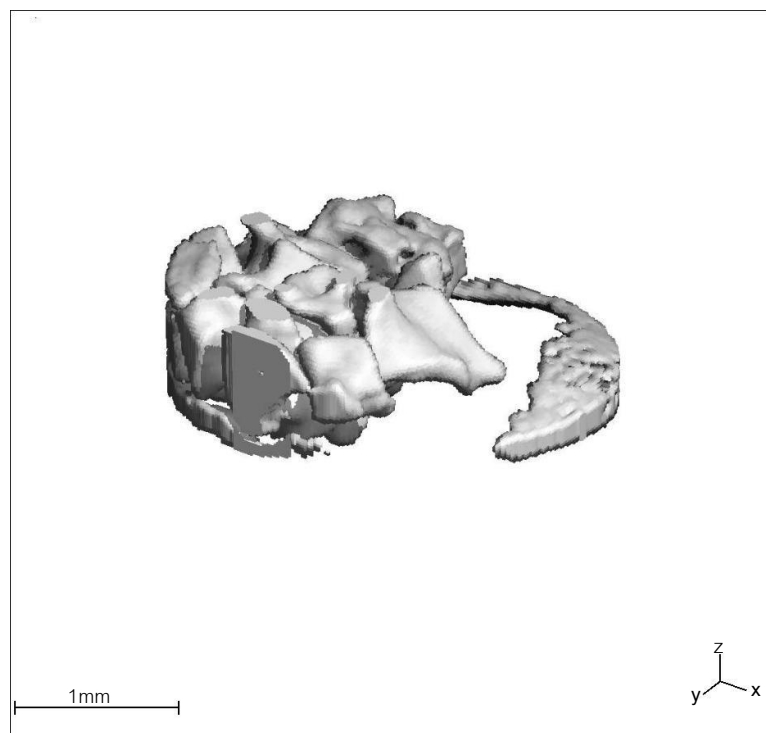
Direct (No model)		TRI(Plate model)		Anisotropy	
TV [mm ³]	16.3837	TV [mm ³]	-	H1 [mm]	-
BV [mm ³]	1.6195	BV [mm ³]	-	H2 [mm]	-
BV/TV [1]	0.0988	BV/TV [1]	-	H3 [mm]	-
Conn.D. [1/mm ³]	-	BS [mm ²]	-	DA [1]	
SMI [1]	-	BS/TV [1/mm]	-		
Tb.N* [1/mm]	-	Tb.N [1/mm]	-	Segmentation : 0.8 / 1 / 220	
Tb.Th* [mm]	-	Tb.Th [mm]	-		
Tb.Sp* [1/mm]	-	Tb.Sp [1/mm]	-		

μCT 35

SCANCO MEDICAL

SCANCO MEDICAL

Bio-Oss_Month1_Mouse 9

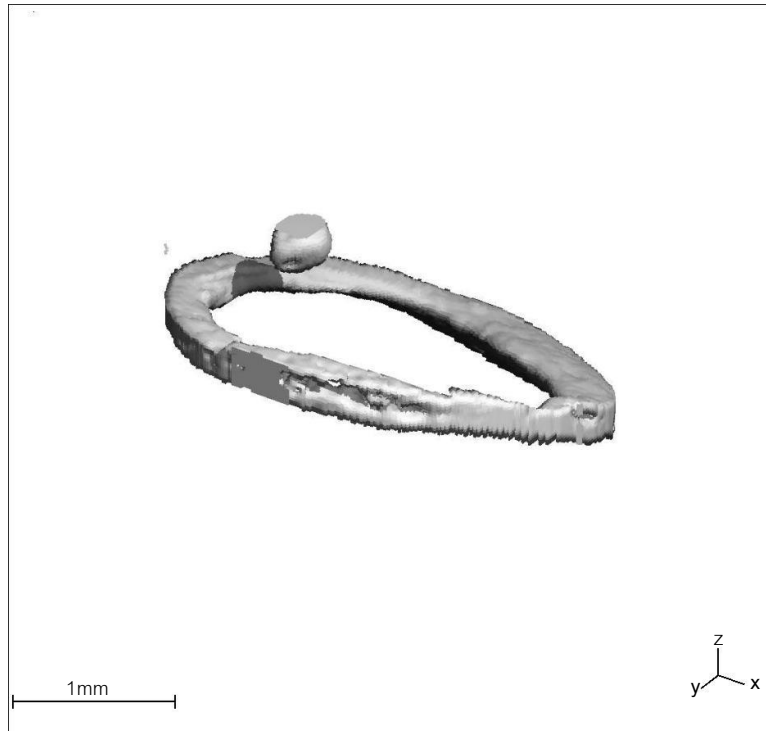


VOI	x	y	z	Mean/Density [mg HA/ccm]
Position [p]	370	380	11	of TV (Apparent) 148.0191
Dimension [p]	164	160	101	of BV (Material) 1136.7471
Element size [mm]	0.0200	0.0200	0.0200	

Direct (No model)		TRI(Plate model)		Anisotropy	
TV [mm ³]	15.9111	TV [mm ³]	-	H1 [mm]	-
BV [mm ³]	2.3346	BV [mm ³]	-	H2 [mm]	-
BV/TV [1]	0.1467	BV/TV [1]	-	H3 [mm]	-
Conn.D. [1/mm ³]	-	BS [mm ²]	-	DA [1]	
SMI [1]	-	BS/TV [1/mm]	-		
Tb.N* [1/mm]	-	Tb.N [1/mm]	-	Segmentation : 0.8 / 1 / 220	
Tb.Th* [mm]	-	Tb.Th [mm]	-		
Tb.Sp* [1/mm]	-	Tb.Sp [1/mm]	-		

μCT 35
SCANCO MEDICAL

DFDBA_Month1_Mouse 2



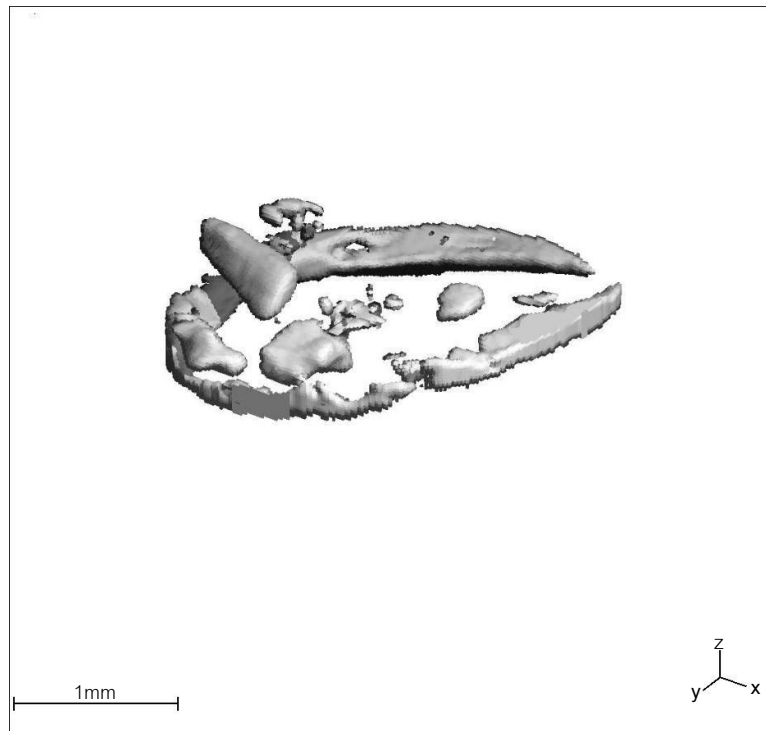
VOI	x	y	z	Mean/Density [mg HA/ccm]
Position [p]	394	354	10	of TV (Apparent) -0.3624
Dimension [p]	164	160	105	of BV (Material) 702.5500
Element size [mm]	0.0200	0.0200	0.0200	

Direct (No model)		TRI(Plate model)		Anisotropy	
TV [mm ³]	16.5413	TV [mm ³]	-	H1 [mm]	-
BV [mm ³]	0.6586	BV [mm ³]	-	H2 [mm]	-
BV/TV [1]	0.0398	BV/TV [1]	-	H3 [mm]	-
Conn.D. [1/mm ³]	-	BS [mm ²]	-	DA [1]	
SMI [1]	-	BS/TV [1/mm]	-		
Tb.N* [1/mm]	-	Tb.N [1/mm]	-	Segmentation : 0.8 / 1 / 220	
Tb.Th* [mm]	-	Tb.Th [mm]	-		
Tb.Sp* [1/mm]	-	Tb.Sp [1/mm]	-		

μCT 35

SCANCO MEDICAL

DFDBA_Month1_Mouse 3



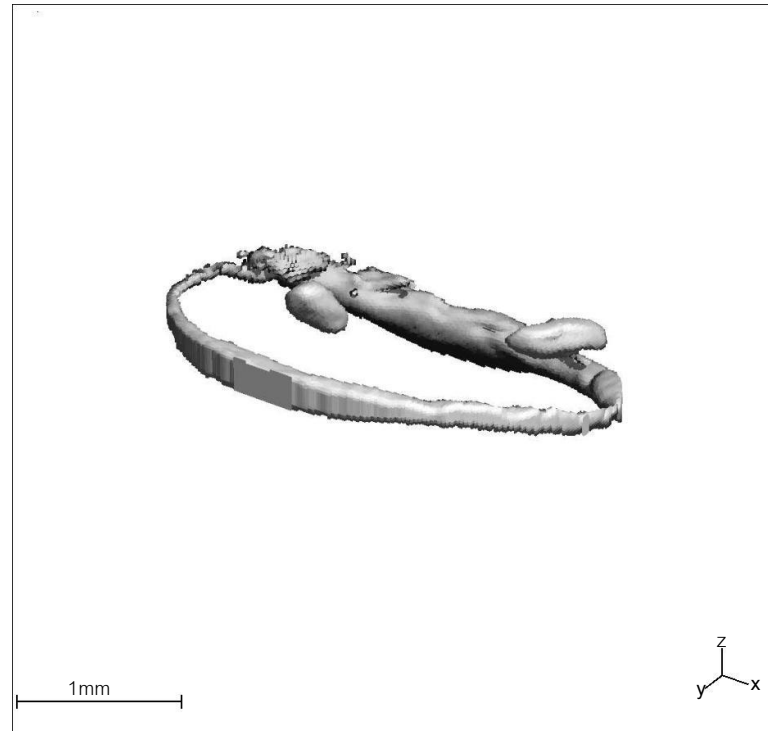
VOI	x	y	z	Mean/Density [mg HA/ccm]
Position [p]	422	324	15	of TV (Apparent) 23.6139
Dimension [p]	164	160	101	of BV (Material) 757.7407
Element size [mm]	0.0200	0.0200	0.0200	

Direct (No model)		TRI(Plate model)		Anisotropy	
TV [mm ³]	15.9111	TV [mm ³]	-	H1 [mm]	-
BV [mm ³]	0.5122	BV [mm ³]	-	H2 [mm]	-
BV/TV [1]	0.0322	BV/TV [1]	-	H3 [mm]	-
Conn.D. [1/mm ³]	-	BS [mm ²]	-	DA [1]	
SMI [1]	-	BS/TV [1/mm]	-		
Tb.N* [1/mm]	-	Tb.N [1/mm]	-	Segmentation : 0.8 / 1 / 220	
Tb.Th* [mm]	-	Tb.Th [mm]	-		
Tb.Sp* [1/mm]	-	Tb.Sp [1/mm]	-		

μCT 35

SCANCO MEDICAL

DFDBA_Month1_Mouse 7



VOI	x	y	z	Mean/Density [mg HA/ccm]
Position [p]	410	304	18	of TV (Apparent) -3.5291
Dimension [p]	164	160	98	of BV (Material) 697.3928
Element size [mm]	0.0200	0.0200	0.0200	

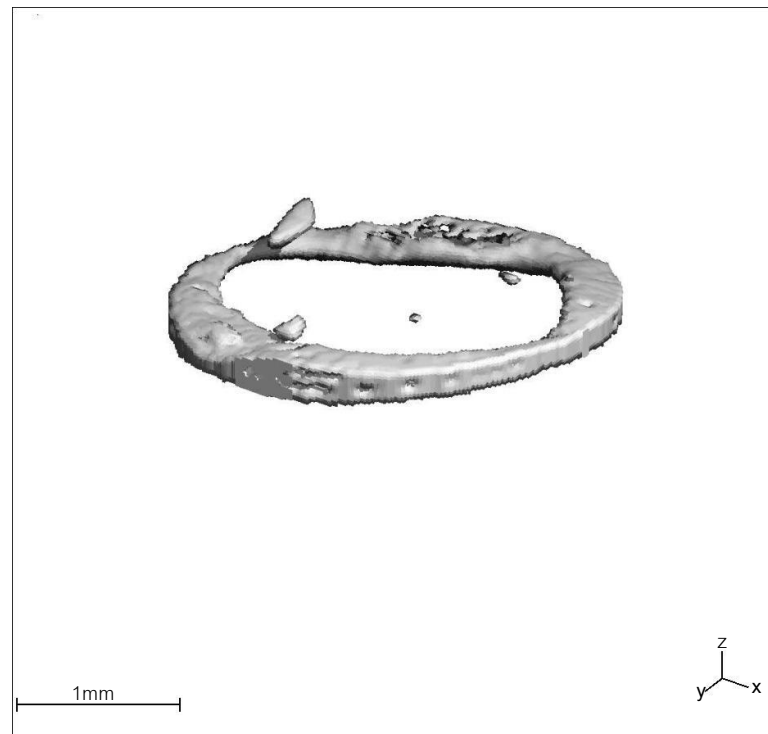
Direct (No model)		TRI(Plate mdel)		Anisotropy	
TV [mm ³]	15.4385	TV [mm ³]	-	H1 [mm]	-
BV [mm ³]	0.4061	BV [mm ³]	-	H2 [mm]	-
BV/TV [1]	0.0263	BV/TV [1]	-	H3 [mm]	-
Conn.D. [1/mm ³]	-	BS [mm ²]	-	DA [1]	
SMI [1]	-	BS/TV [1/mm]	-		
Tb.N* [1/mm]	-	Tb.N [1/mm]	-	Segmentation : 0.8 / 1 / 220	
Tb.Th* [mm]	-	Tb.Th [mm]	-		
Tb.Sp* [1/mm]	-	Tb.Sp [1/mm]	-		

μCT 35

SCANCO MEDICAL

SCANCO MEDICAL

DFDBA_Month1_Mouse 8



VOI	x	y	z	Mean/Density [mg HA/ccm]	
Position [p]	300	318	13	of TV (Apparent)	30.3996
Dimension [p]	164	160	103	of BV (Material)	690.2452
Element size [mm]	0.0200	0.0200	0.0200		

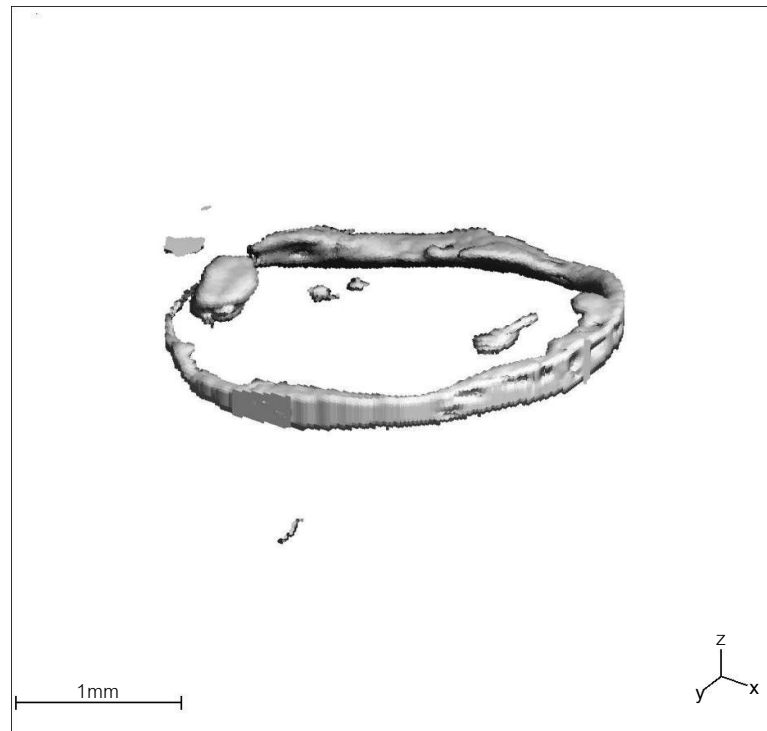
Direct (No model)		TRI(Plate model)		Anisotropy	
TV [mm ³]	16.2262	TV [mm ³]	-	H1 [mm]	-
BV [mm ³]	0.5688	BV [mm ³]	-	H2 [mm]	-
BV/TV [1]	0.0351	BV/TV [1]	-	H3 [mm]	-
Conn.D. [1/mm ³]	-	BS [mm ²]	-	DA [1]	
SMI [1]	-	BS/TV [1/mm]	-	Segmentation : 0.8 / 1 / 220	
Tb.N* [1/mm]	-	Tb.N [1/mm]	-		
Tb.Th* [mm]	-	Tb.Th [mm]	-		
Tb.Sp* [1/mm]	-	Tb.Sp [1/mm]	-		

μCT 35

SCANCO MEDICAL

SCANCO MEDICAL

DFDBA_Month1_Mouse 9



VOI	x	y	z	Mean/Density [mg HA/ccm]
Position [p]	288	310	21	of TV (Apparent) 10.9472
Dimension [p]	164	160	95	of BV (Material) 749.7788
Element size [mm]	0.0200	0.0200	0.0200	

Direct (No model)		TRI(Plate mdl)		Anisotropy	
TV [mm ³]	14.9659	TV [mm ³]	-	H1 [mm]	-
BV [mm ³]	0.3556	BV [mm ³]	-	H2 [mm]	-
BV/TV [1]	0.0238	BV/TV [1]	-	H3 [mm]	-
Conn.D. [1/mm ³]	-	BS [mm ²]	-	DA [1]	
SMI [1]	-	BS/TV [1/mm]	-		
Tb.N* [1/mm]	-	Tb.N [1/mm]	-	Segmentation : 0.8 / 1 / 220	
Tb.Th* [mm]	-	Tb.Th [mm]	-		
Tb.Sp* [1/mm]	-	Tb.Sp [1/mm]	-		

μCT 35

SCANCO MEDICAL

SCANCO MEDICAL

Control_Month3_Mouse 1



VOI	x	y	z	Mean/Density [mg HA/ccm]
Position [p]	356	513	2	of TV (Apparent) -43.0673
Dimension [p]	164	160	95	of BV (Material) 662.2880
Element size [mm]	0.0200	0.0200	0.0200	

Direct (No model)		TRI(Plate model)		Anisotropy	
TV [mm ³]	17.7988	TV [mm ³]	-	H1 [mm]	-
BV [mm ³]	0.1705	BV [mm ³]	-	H2 [mm]	-
BV/TV [1]	0.0096	BV/TV [1]	-	H3 [mm]	-
Conn.D. [1/mm ³]	-	BS [mm ²]	-	DA [1]	
SMI [1]	-	BS/TV [1/mm]	-		
Tb.N* [1/mm]	-	Tb.N [1/mm]	-	Segmentation : 0.8 / 1 / 220	
Tb.Th* [mm]	-	Tb.Th [mm]	-		
Tb.Sp* [1/mm]	-	Tb.Sp [1/mm]	-		

μCT 35

SCANCO MEDICAL

Control_Month3_Mouse 2



VOI	x	y	z	Mean/Density [mg HA/ccm]
Position [p]	450	579	2	of TV (Apparent) -30.4911
Dimension [p]	164	160	113	of BV (Material) 668.4404
Element size [mm]	0.0200	0.0200	0.0200	

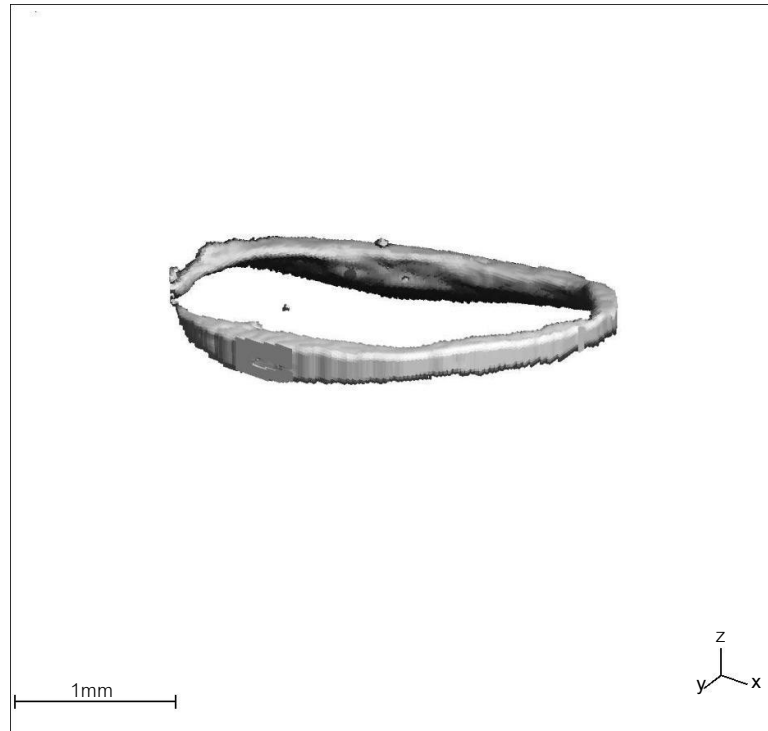
Direct (No model)		TRI(Plate model)		Anisotropy	
TV [mm ³]	17.7988	TV [mm ³]	-	H1 [mm]	-
BV [mm ³]	0.1872	BV [mm ³]	-	H2 [mm]	-
BV/TV [1]	0.0105	BV/TV [1]	-	H3 [mm]	-
Conn.D. [1/mm ³]	-	BS [mm ²]	-	DA [1]	
SMI [1]	-	BS/TV [1/mm]	-		
Tb.N* [1/mm]	-	Tb.N [1/mm]	-	Segmentation : 0.8 / 1 / 220	
Tb.Th* [mm]	-	Tb.Th [mm]	-		
Tb.Sp* [1/mm]	-	Tb.Sp [1/mm]	-		

μCT 35

SCANCO MEDICAL

SCANCO MEDICAL

Control_Month3_Mouse 5 (Left)



VOI	x	y	z	Mean/Density [mg HA/ccm]
Position [p]	371	295	2	of TV (Apparent) -3.4386
Dimension [p]	164	160	113	of BV (Material) 699.3834
Element size [mm]	0.0200	0.0200	0.0200	

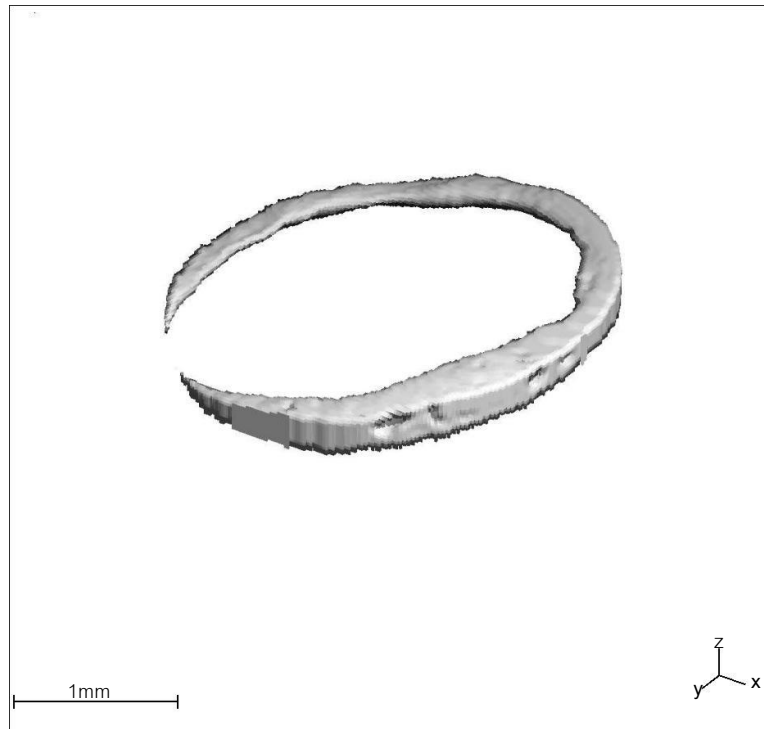
Direct (No model)		TRI(Plate mdl)		Anisotropy	
TV [mm ³]	17.8016	TV [mm ³]	-	H1 [mm]	-
BV [mm ³]	0.4449	BV [mm ³]	-	H2 [mm]	-
BV/TV [1]	0.0250	BV/TV [1]	-	H3 [mm]	-
Conn.D. [1/mm ³]	-	BS [mm ²]	-	DA [1]	
SMI [1]	-	BS/TV [1/mm]	-		
Tb.N* [1/mm]	-	Tb.N [1/mm]	-	Segmentation : 0.8 / 1 / 220	
Tb.Th* [mm]	-	Tb.Th [mm]	-		
Tb.Sp* [1/mm]	-	Tb.Sp [1/mm]	-		

μCT 35

SCANCO MEDICAL

SCANCO MEDICAL

Control_Month3_Mouse 5 (Right)



VOI	x	y	z	Mean/Density [mg HA/ccm]
Position [p]	415	499	11	of TV (Apparent) -1.1767
Dimension [p]	164	160	99	of BV (Material) 693.1404
Element size [mm]	0.0200	0.0200	0.0200	

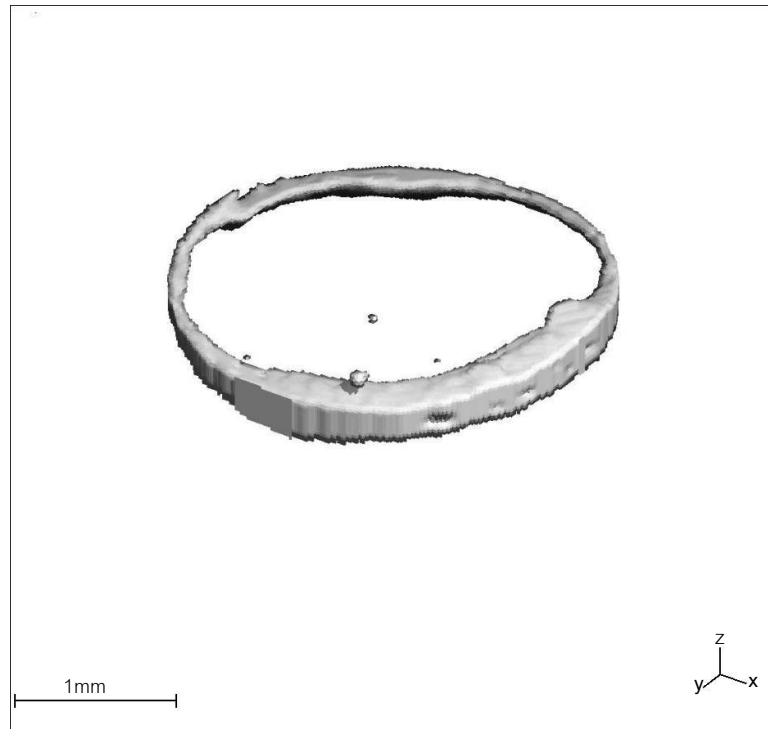
Direct (No model)		TRI(Plate model)		Anisotropy	
TV [mm ³]	15.5961	TV [mm ³]	-	H1 [mm]	-
BV [mm ³]	0.3474	BV [mm ³]	-	H2 [mm]	-
BV/TV [1]	0.0223	BV/TV [1]	-	H3 [mm]	-
Conn.D. [1/mm ³]	-	BS [mm ²]	-	DA [1]	
SMI [1]	-	BS/TV [1/mm]	-		
Tb.N* [1/mm]	-	Tb.N [1/mm]	-	Segmentation : 0.8 / 1 / 220	
Tb.Th* [mm]	-	Tb.Th [mm]	-		
Tb.Sp* [1/mm]	-	Tb.Sp [1/mm]	-		

μCT 35

SCANCO MEDICAL

SCANCO MEDICAL

Control_Month3_Mouse 6



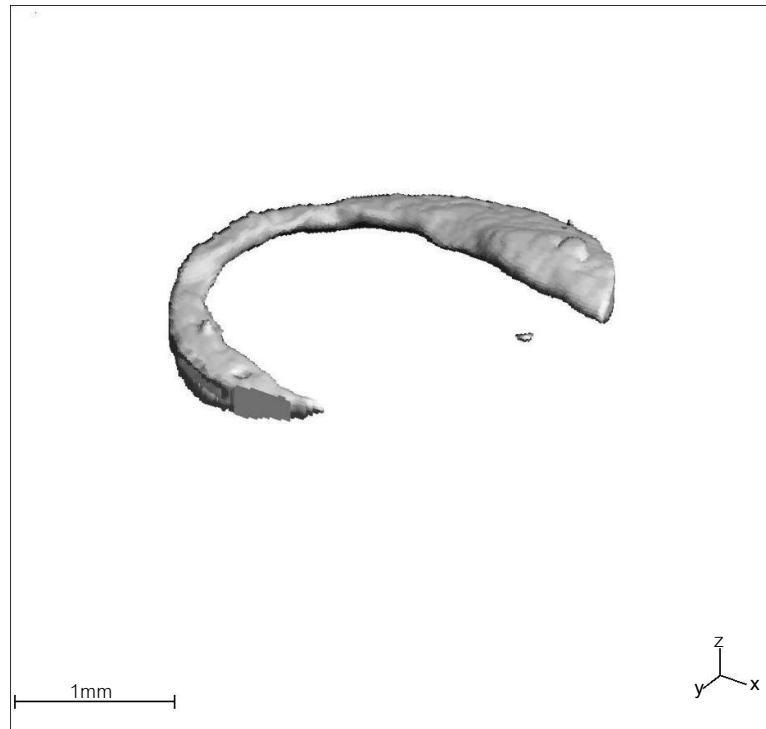
VOI	x	y	z	Mean/Density [mg HA/ccm]
Position [p]	469	591	2	of TV (Apparent) 9.2281
Dimension [p]	164	160	108	of BV (Material) 706.1691
Element size [mm]	0.0200	0.0200	0.0200	

Direct (No model)		TRI(Plate mdel)		Anisotropy	
TV [mm ³]	17.0139	TV [mm ³]	-	H1 [mm]	-
BV [mm ³]	0.3713	BV [mm ³]	-	H2 [mm]	-
BV/TV [1]	0.0218	BV/TV [1]	-	H3 [mm]	-
Conn.D. [1/mm ³]	-	BS [mm ²]	-	DA [1]	
SMI [1]	-	BS/TV [1/mm]	-		
Tb.N* [1/mm]	-	Tb.N [1/mm]	-	Segmentation : 0.8 / 1 / 220	
Tb.Th* [mm]	-	Tb.Th [mm]	-		
Tb.Sp* [1/mm]	-	Tb.Sp [1/mm]	-		

μCT 35

SCANCO MEDICAL

Control_Month3_Mouse 7



VOI	x	y	z	Mean/Density [mg HA/ccm]
Position [p]	412	529	2	of TV (Apparent) -5.7910
Dimension [p]	164	160	114	of BV (Material) 703.3643
Element size [mm]	0.0200	0.0200	0.0200	

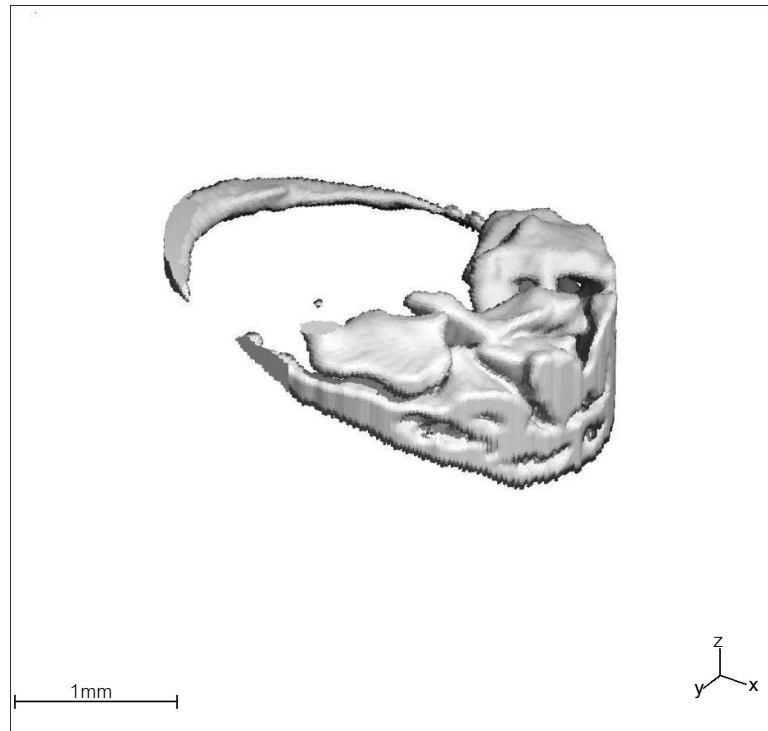
Direct (No model)		TRI(Plate model)		Anisotropy	
TV [mm ³]	17.9564	TV [mm ³]	-	H1 [mm]	-
BV [mm ³]	0.4628	BV [mm ³]	-	H2 [mm]	-
BV/TV [1]	0.0258	BV/TV [1]	-	H3 [mm]	-
Conn.D. [1/mm ³]	-	BS [mm ²]	-	DA [1]	
SMI [1]	-	BS/TV [1/mm]	-		
Tb.N* [1/mm]	-	Tb.N [1/mm]	-	Segmentation : 0.8 / 1 / 220	
Tb.Th* [mm]	-	Tb.Th [mm]	-		
Tb.Sp* [1/mm]	-	Tb.Sp [1/mm]	-		

μCT 35

SCANCO MEDICAL

SCANCO MEDICAL

Bio-Oss_Month3_Mouse 1



VOI	x	y	z	Mean/Density [mg HA/ccm]
Position [p]	568	449	9	of TV (Apparent) 72.0188
Dimension [p]	164	160	114	of BV (Material) 1064.5468
Element size [mm]	0.0200	0.0200	0.0200	

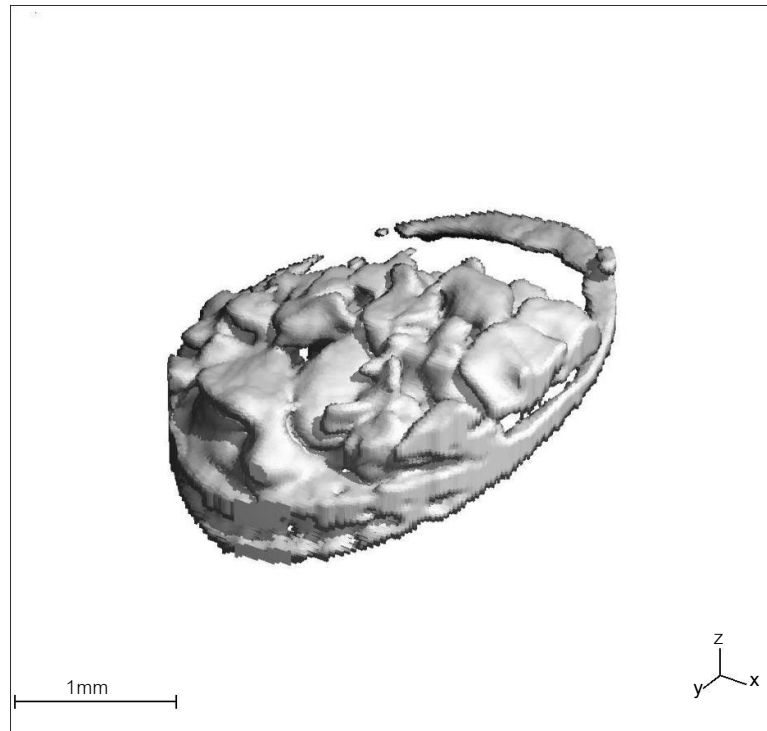
Direct (No model)		TRI(Plate mdel)		Anisotropy	
TV [mm ³]	16.6963	TV [mm ³]	-	H1 [mm]	-
BV [mm ³]	1.1890	BV [mm ³]	-	H2 [mm]	-
BV/TV [1]	0.0712	BV/TV [1]	-	H3 [mm]	-
Conn.D. [1/mm ³]	-	BS [mm ²]	-	DA [1]	
SMI [1]	-	BS/TV [1/mm]	-		
Tb.N* [1/mm]	-	Tb.N [1/mm]	-	Segmentation : 0.8 / 1 / 220	
Tb.Th* [mm]	-	Tb.Th [mm]	-		
Tb.Sp* [1/mm]	-	Tb.Sp [1/mm]	-		

μCT 35

SCANCO MEDICAL

SCANCO MEDICAL

Bio-Oss_Month3_Mouse 3



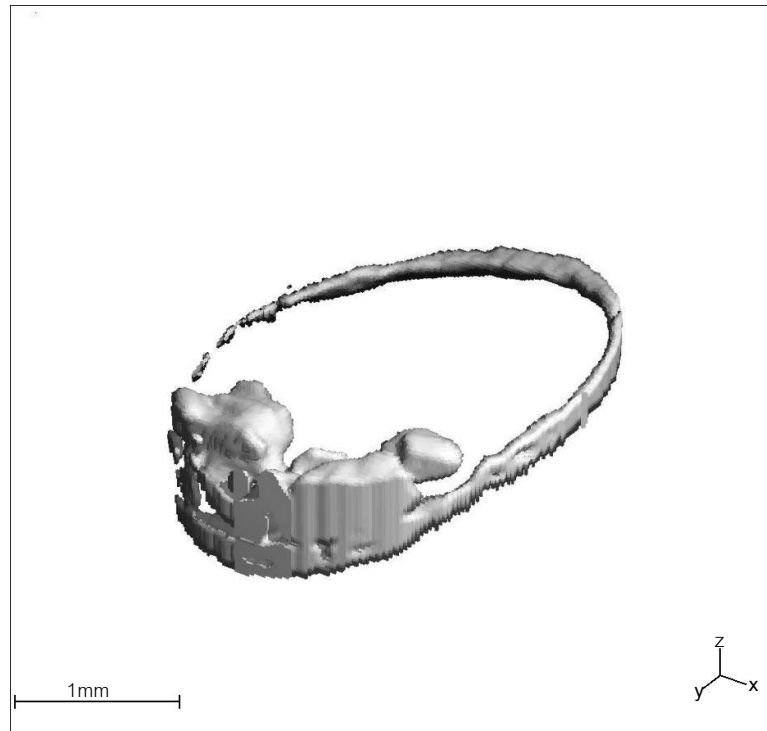
VOI	x	y	z	Mean/Density [mg HA/ccm]
Position [p]	376	605	2	of TV (Apparent) 106.5809
Dimension [p]	164	160	103	of BV (Material) 1056.0420
Element size [mm]	0.0200	0.0200	0.0200	

Direct (No model)		TRI(Plate model)		Anisotropy	
TV [mm ³]	17.0113	TV [mm ³]	-	H1 [mm]	-
BV [mm ³]	2.3364	BV [mm ³]	-	H2 [mm]	-
BV/TV [1]	0.1373	BV/TV [1]	-	H3 [mm]	-
Conn.D. [1/mm ³]	-	BS [mm ²]	-	DA [1]	
SMI [1]	-	BS/TV [1/mm]	-		
Tb.N* [1/mm]	-	Tb.N [1/mm]	-	Segmentation : 0.8 / 1 / 220	
Tb.Th* [mm]	-	Tb.Th [mm]	-		
Tb.Sp* [1/mm]	-	Tb.Sp [1/mm]	-		

μCT 35

SCANCO MEDICAL

Bio-Oss_Month3_Mouse 4



VOI	x	y	z	Mean/Density [mg HA/ccm]
Position [p]	405	577	2	of TV (Apparent) -104.5009
Dimension [p]	164	160	97	of BV (Material) 1024.2230
Element size [mm]	0.0200	0.0200	0.0200	

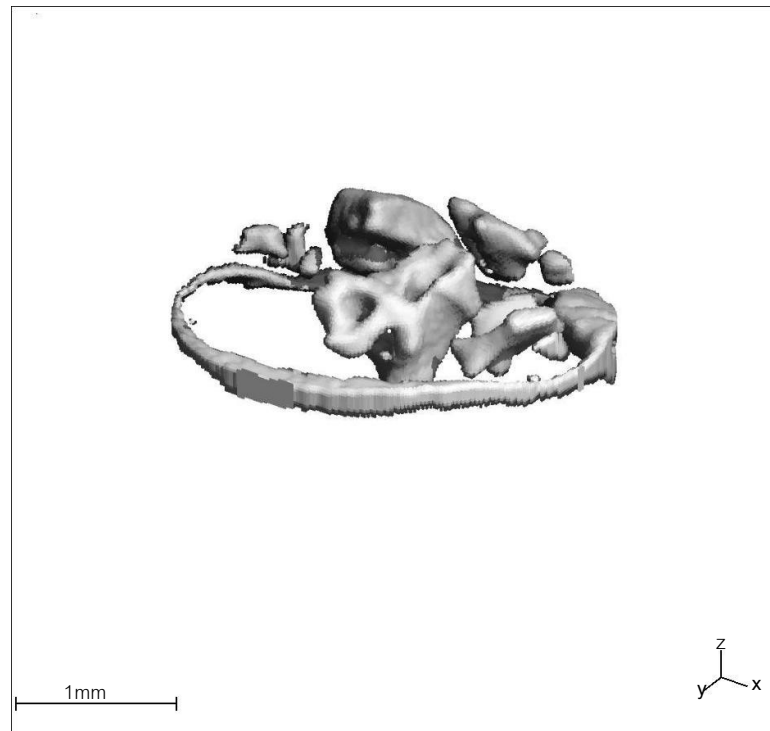
Direct (No model)		TRI(Plate model)		Anisotropy	
TV [mm ³]	15.2810	TV [mm ³]	-	H1 [mm]	-
BV [mm ³]	0.6057	BV [mm ³]	-	H2 [mm]	-
BV/TV [1]	0.0396	BV/TV [1]	-	H3 [mm]	-
Conn.D. [1/mm ³]	-	BS [mm ²]	-	DA [1]	
SMI [1]	-	BS/TV [1/mm]	-		
Tb.N* [1/mm]	-	Tb.N [1/mm]	-	Segmentation : 0.8 / 1 / 220	
Tb.Th* [mm]	-	Tb.Th [mm]	-		
Tb.Sp* [1/mm]	-	Tb.Sp [1/mm]	-		

μCT 35

SCANCO MEDICAL

SCANCO MEDICAL

Bio-Oss_Month3_Mouse 6

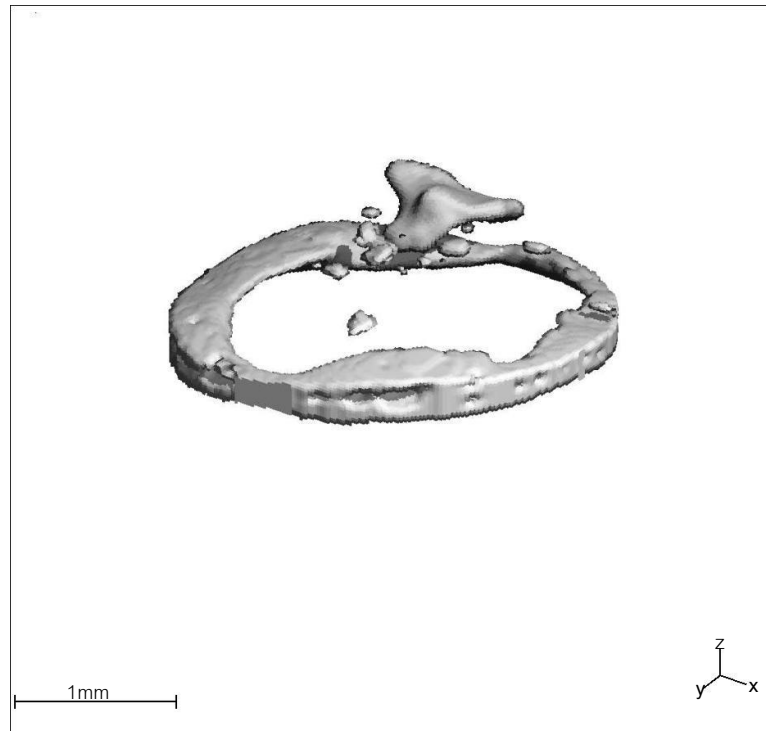


VOI	x	y	z	Mean/Density [mg HA/ccm]
Position [p]	459	525	2	of TV (Apparent) 60.6188
Dimension [p]	164	160	113	of BV (Material) 1195.3759
Element size [mm]	0.0200	0.0200	0.0200	

Direct (No model)		TRI(Plate model)		Anisotropy	
TV [mm ³]	17.8016	TV [mm ³]	-	H1 [mm]	-
BV [mm ³]	1.1388	BV [mm ³]	-	H2 [mm]	-
BV/TV [1]	0.0640	BV/TV [1]	-	H3 [mm]	-
Conn.D. [1/mm ³]	-	BS [mm ²]	-	DA [1]	
SMI [1]	-	BS/TV [1/mm]	-		
Tb.N* [1/mm]	-	Tb.N [1/mm]	-	Segmentation : 0.8 / 1 / 220	
Tb.Th* [mm]	-	Tb.Th [mm]	-		
Tb.Sp* [1/mm]	-	Tb.Sp [1/mm]	-		

μCT 35
SCANCO MEDICAL

Bio-Oss_Month3_Mouse 8



VOI	x	y	z	Mean/Density [mg HA/ccm]
Position [p]	356	481	2	of TV (Apparent) 6.3329
Dimension [p]	164	160	108	of BV (Material) 777.6456
Element size [mm]	0.0200	0.0200	0.0200	

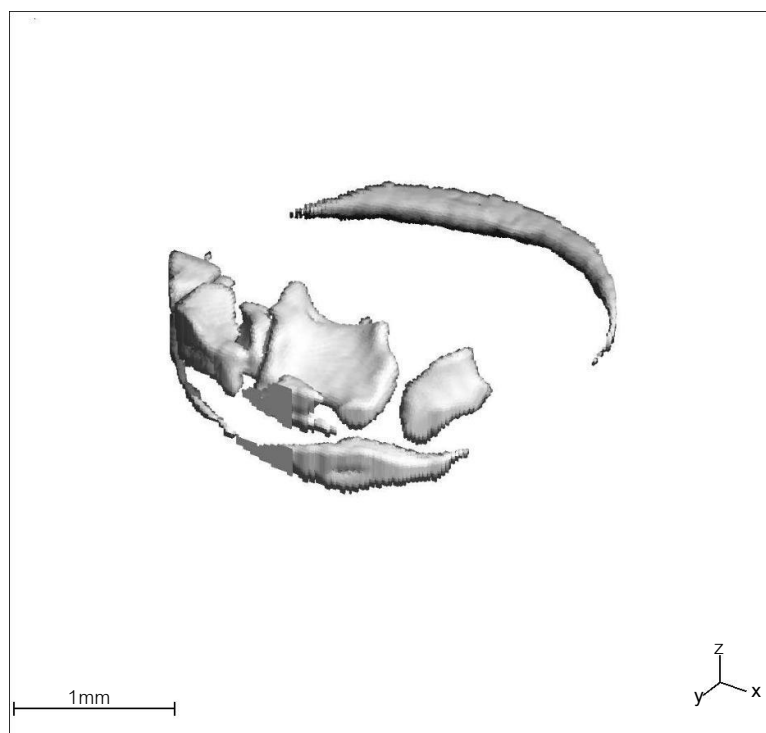
Direct (No model)		TRI(Plate model)		Anisotropy	
TV [mm ³]	17.0139	TV [mm ³]	-	H1 [mm]	-
BV [mm ³]	0.6516	BV [mm ³]	-	H2 [mm]	-
BV/TV [1]	0.0383	BV/TV [1]	-	H3 [mm]	-
Conn.D. [1/mm ³]	-	BS [mm ²]	-	DA [1]	
SMI [1]	-	BS/TV [1/mm]	-		
Tb.N* [1/mm]	-	Tb.N [1/mm]	-	Segmentation : 0.8 / 1 / 220	
Tb.Th* [mm]	-	Tb.Th [mm]	-		
Tb.Sp* [1/mm]	-	Tb.Sp [1/mm]	-		

μCT 35

SCANCO MEDICAL

SCANCO MEDICAL

Bio-Oss_Month3_Mouse 9



VOI	x	y	z	Mean/Density [mg HA/ccm]
Position [p]	500	509	2	of TV (Apparent) 11.2186
Dimension [p]	164	160	108	of BV (Material) 1060.4753
Element size [mm]	0.0200	0.0200	0.0200	

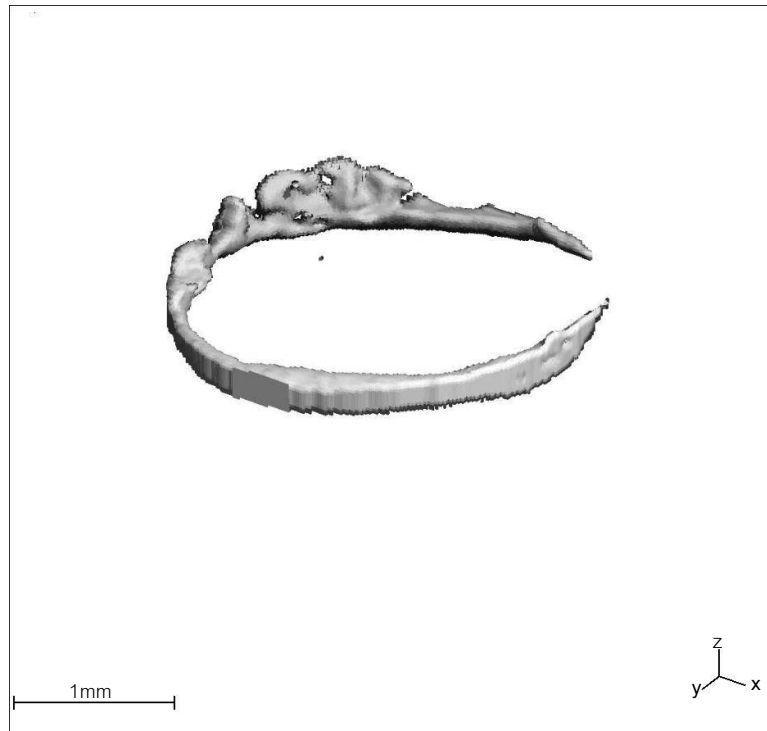
Direct (No model)		TRI(Plate mdl)		Anisotropy	
TV [mm ³]	17.8016	TV [mm ³]	-	H1 [mm]	-
BV [mm ³]	0.4505	BV [mm ³]	-	H2 [mm]	-
BV/TV [1]	0.0253	BV/TV [1]	-	H3 [mm]	-
Conn.D. [1/mm ³]	-	BS [mm ²]	-	DA [1]	
SMI [1]	-	BS/TV [1/mm]	-		
Tb.N* [1/mm]	-	Tb.N [1/mm]	-	Segmentation : 0.8 / 1 / 220	
Tb.Th* [mm]	-	Tb.Th [mm]	-		
Tb.Sp* [1/mm]	-	Tb.Sp [1/mm]	-		

μCT 35

SCANCO MEDICAL

SCANCO MEDICAL

DFDBA_Month3_Mouse 2



VOI	x	y	z	Mean/Density [mg HA/ccm]
Position [p]	414	455	2	of TV (Apparent) 5.8805
Dimension [p]	164	160	113	of BV (Material) 719.4691
Element size [mm]	0.0200	0.0200	0.0200	

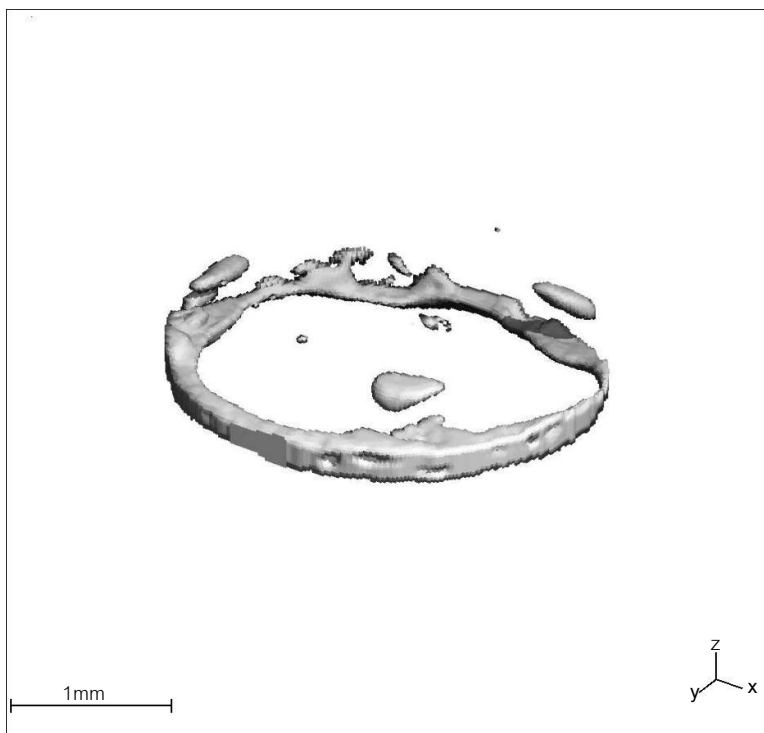
Direct (No model)		TRI(Plate mdl)		Anisotropy	
TV [mm ³]	17.7988	TV [mm ³]	-	H1 [mm]	-
BV [mm ³]	0.3038	BV [mm ³]	-	H2 [mm]	-
BV/TV [1]	0.0171	BV/TV [1]	-	H3 [mm]	-
Conn.D. [1/mm ³]	-	BS [mm ²]	-	DA [1]	
SMI [1]	-	BS/TV [1/mm]	-		
Tb.N* [1/mm]	-	Tb.N [1/mm]	-	Segmentation : 0.8 / 1 / 220	
Tb.Th* [mm]	-	Tb.Th [mm]	-		
Tb.Sp* [1/mm]	-	Tb.Sp [1/mm]	-		

μCT 35

SCANCO MEDICAL

SCANCO MEDICAL

DFDBA_Month3_Mouse 3

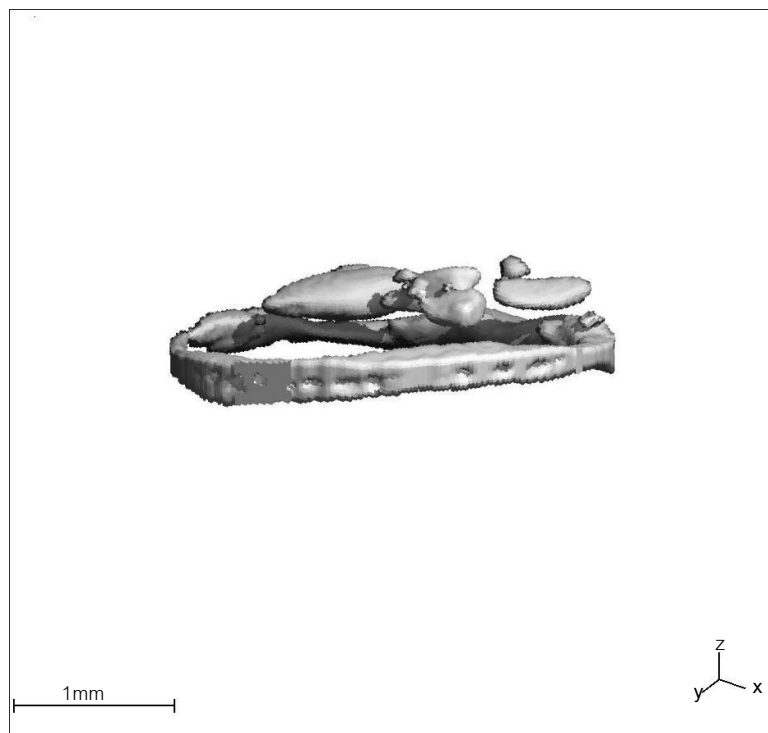


VOI	x	y	z	Mean/Density [mg HA/ccm]
Position [p]	474	349	2	of TV (Apparent) -27.0530
Dimension [p]	164	160	113	of BV (Material) 705.6262
Element size [mm]	0.0200	0.0200	0.0200	

Direct (No model)		TRI(Plate mdl)		Anisotropy	
TV [mm ³]	17.7988	TV [mm ³]	-	H1 [mm]	-
BV [mm ³]	0.3564	BV [mm ³]	-	H2 [mm]	-
BV/TV [1]	0.0200	BV/TV [1]	-	H3 [mm]	-
Conn.D. [1/mm ³]	-	BS [mm ²]	-	DA [1]	
SMI [1]	-	BS/TV [1/mm]	-		
Tb.N* [1/mm]	-	Tb.N [1/mm]	-	Segmentation : 0.8 / 1 / 220	
Tb.Th* [mm]	-	Tb.Th [mm]	-		
Tb.Sp* [1/mm]	-	Tb.Sp [1/mm]	-		

SCANCO MEDICAL

DFDBA_Month3_Mouse 4



VOI	x	y	z	Mean/Density [mg HA/ccm]
Position [p]	439	301	2	of TV (Apparent) -104.8628
Dimension [p]	164	160	113	of BV (Material) 759.7312
Element size [mm]	0.0200	0.0200	0.0200	

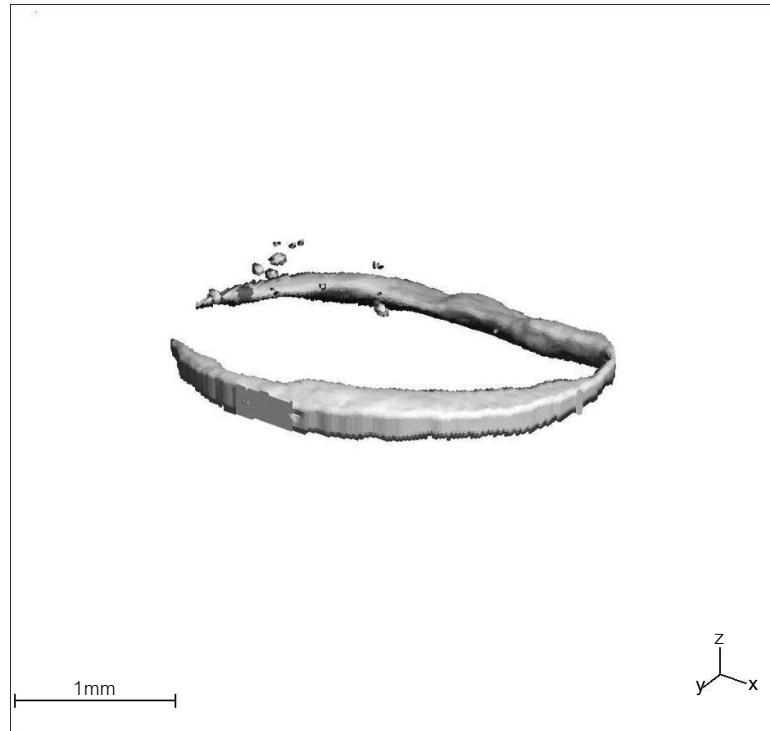
Direct (No model)		TRI(Plate mdl)		Anisotropy	
TV [mm ³]	17.8016	TV [mm ³]	-	H1 [mm]	-
BV [mm ³]	0.8101	BV [mm ³]	-	H2 [mm]	-
BV/TV [1]	0.0455	BV/TV [1]	-	H3 [mm]	-
Conn.D. [1/mm ³]	-	BS [mm ²]	-	DA [1]	
SMI [1]	-	BS/TV [1/mm]	-		
Tb.N* [1/mm]	-	Tb.N [1/mm]	-	Segmentation : 0.8 / 1 / 220	
Tb.Th* [mm]	-	Tb.Th [mm]	-		
Tb.Sp* [1/mm]	-	Tb.Sp [1/mm]	-		

μCT 35

SCANCO MEDICAL

SCANCO MEDICAL

DFDBA_Month3_Mouse 7



VOI	x	y	z	Mean/Density [mg HA/ccm]
Position [p]	422	337	2	of TV (Apparent) -24.1577
Dimension [p]	164	160	113	of BV (Material) 721.3691
Element size [mm]	0.0200	0.0200	0.0200	

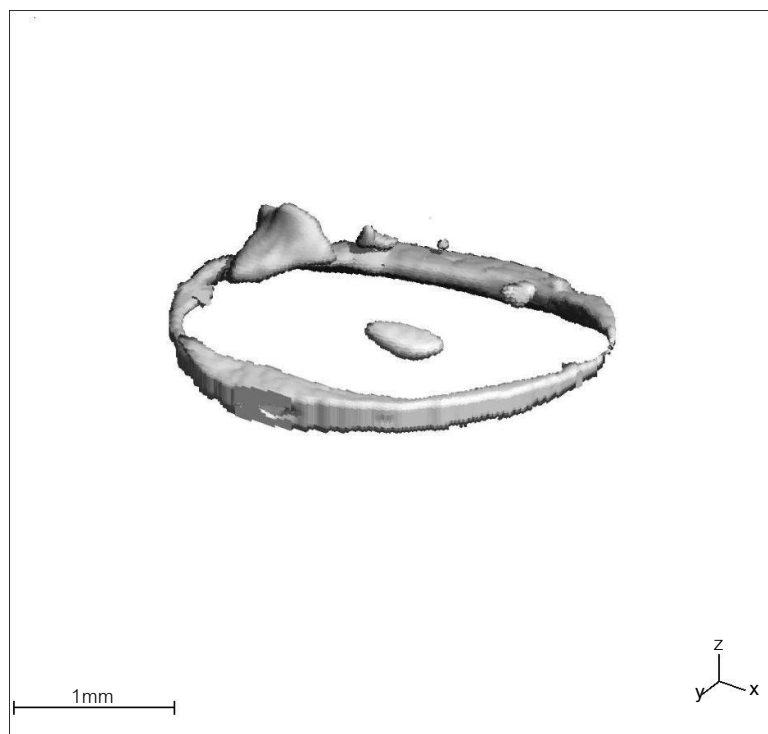
Direct (No model)		TRI(Plate mdl)		Anisotropy	
TV [mm ³]	17.8016	TV [mm ³]	-	H1 [mm]	-
BV [mm ³]	0.3711	BV [mm ³]	-	H2 [mm]	-
BV/TV [1]	0.0208	BV/TV [1]	-	H3 [mm]	-
Conn.D. [1/mm ³]	-	BS [mm ²]	-	DA [1]	
SMI [1]	-	BS/TV [1/mm]	-		
Tb.N* [1/mm]	-	Tb.N [1/mm]	-	Segmentation : 0.8 / 1 / 220	
Tb.Th* [mm]	-	Tb.Th [mm]	-		
Tb.Sp* [1/mm]	-	Tb.Sp [1/mm]	-		

μCT 35

SCANCO MEDICAL

SCANCO MEDICAL

DFDBA_Month3_Mouse 8



VOI	x	y	z	Mean/Density [mg HA/ccm]
Position [p]	440	399	4	of TV (Apparent) 8.9567
Dimension [p]	164	160	112	of BV (Material) 849.0316
Element size [mm]	0.0200	0.0200	0.0200	

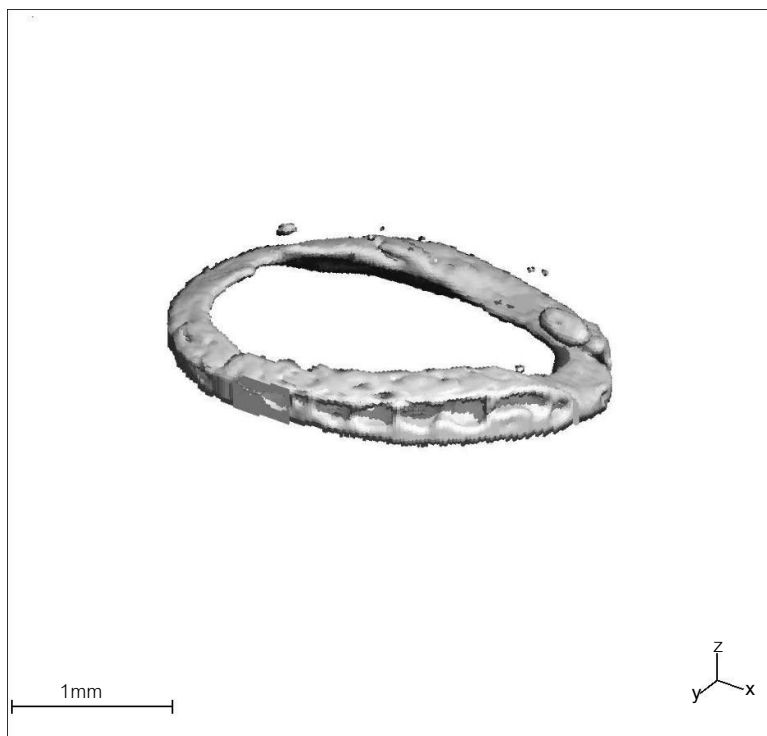
Direct (No model)		TRI(Plate mdl)		Anisotropy	
TV [mm ³]	17.6440	TV [mm ³]	-	H1 [mm]	-
BV [mm ³]	0.4445	BV [mm ³]	-	H2 [mm]	-
BV/TV [1]	0.0252	BV/TV [1]	-	H3 [mm]	-
Conn.D. [1/mm ³]	-	BS [mm ²]	-	DA [1]	
SMI [1]	-	BS/TV [1/mm]	-		
Tb.N* [1/mm]	-	Tb.N [1/mm]	-	Segmentation : 0.8 / 1 / 220	
Tb.Th* [mm]	-	Tb.Th [mm]	-		
Tb.Sp* [1/mm]	-	Tb.Sp [1/mm]	-		

μCT 35

SCANCO MEDICAL

SCANCO MEDICAL

DFDBA_Month3_Mouse 9



VOI	x	y	z	Mean/Density [mg HA/ccm]
Position [p]	425	427	2	of TV (Apparent) -6.3339
Dimension [p]	164	160	113	of BV (Material) 698.6595
Element size [mm]	0.0200	0.0200	0.0200	

Direct (No model)		TRI(Plate mdl)		Anisotropy	
TV [mm ³]	17.8016	TV [mm ³]	-	H1 [mm]	-
BV [mm ³]	0.5617	BV [mm ³]	-	H2 [mm]	-
BV/TV [1]	0.0316	BV/TV [1]	-	H3 [mm]	-
Conn.D. [1/mm ³]	-	BS [mm ²]	-	DA [1]	
SMI [1]	-	BS/TV [1/mm]	-		
Tb.N* [1/mm]	-	Tb.N [1/mm]	-	Segmentation : 0.8 / 1 / 220	
Tb.Th* [mm]	-	Tb.Th [mm]	-		
Tb.Sp* [1/mm]	-	Tb.Sp [1/mm]	-		



Animal care

Husbandry consideration:

1 Housing Place: building Preclinical building, Faculty of Dentistry, Chulalongkorn University Animal located on 7th floor

2 Experimental Place: building Preclinical building, Faculty of Dentistry, Chulalongkorn University Animal located on 7th floor

3 Housing System:

- Conventional Strictly hygienic conventional
 Barrier Containment
 Others, please specify.....

4 Caging:

- Solid bottom, open top Static filtered top cages
 Metabolic cages Individual ventilated cage (IVC)
 Environmental chamber Isolator
 Others, please specify.....

5 Caging materials:

- Plastic Stainless steel Others, please specify.....

5.1. Cage size (W x L x H) 36x22x15 cm³.

5.2 Number of animals / cage 3

5.3 Environmental requirements:

Temperature 25 ± 2 °C

Humidity.....

Light: Standard fluorescent
 Others, please specify.....

Light cycle: Standard 12 :12
 Others, please specify.....

5.4 Food:

Type of food: Standard diet

Source/Vendor: National Laboratory Animal Center of Salaya Campus, Mahidol University

Feeding schedule:

- Ad libitum
 Others, please specify.....meal(s)/day

5.5 Water (if needed):

- Type of water: Tap water
- Hyperchlorinated.....ppm
- Acidified, pH.....
- RO-UV
- Others, please specify.....

Water Provided:

- Ad libitum
- Others, please specify.....

5.6 Bedding/housing media:

- No
- Yes , please specify Wood shaving

All procedures will be performed under aseptic technique to prevent contamination. The surgeons will wear face mask, sterile gloves, and clean lab coats and follow the rodent surgery policy. The rodent survival surgery policy will be performed according to the guidelines of National Research Council, Institute of Laboratory Animal Resources, Commission on Life Sciences, USA.

VITA

Miss Thanyaporn Kangwannarongkul was born on September 7, 1985 in Bangkok, Thailand. She graduated with the Degree of Doctor surgery (D.D.S.) from the Faculty of Dentistry, Prince of Songkhla University in 2010. After graduation, she worked at Si Kao hospital, Trang from 2010-2012. She started her post-graduated study in 2012 for the Master of Science Program (M.Sc.) in Prosthodontics at the Department of Prosthodontics Faculty of Dentistry, Chulalongkorn University. At present, she works in the private dental clinic.

